UNIVERSITÉ DE BLIDA 1

Faculté de Technologie

Département de Génie Civil

Laboratoire de Géo matériaux et Génie Civil

THÈSE DE DOCTORAT

Spécialité: Structures et Matériaux du Génie civil

CONCEPTION D'UN SYSTÈME PERMETTANT LA MESURE DE LA RÉSISTANCE EN TRACTION DES MATÉRIAUX CIMENTAIRES – CORRÉLATION AVEC LES ESSAIS CLASSIQUES

Par

Oussama MERABET

Soutenue le: 18/02/2025, devant le jury composé de:

Mr. Belkacem MENADI	Prof.	Université de Blida 1	Président
Mr. Farih MESSAOUDI	M.C.A	Université de Blida 1	Examinateur
Mr. Farid DEBIEB	Prof.	Université de Médéa	Examinateur
Mr. Mohamed BENTCHIKOU	Prof.	Université de Médéa	Rapporteur
Mr. Nasreddine AMOURA	M.C.A	ENP ALGER	Co-Rapporteur

Blida, 2024

Acknowledgments

In the light of this work, I would first like to thank ALLAH All-Powerful for all the wonders he does in my life and for giving me the courage, strength, goodwill and especially the patience to complete this modest scientific contribution.

*I would like to express my deepest thanks to my respected supervisors, **Prof. Mohamed Bentchikou** and **Dr. Nasreddine Amoura**, for their invaluable guidance, support, and assistance throughout the years of this research. Their expertise, understanding, and patience have greatly enriched my research experience and have been a constant source of motivation throughout my thesis.*

*I would also like to express my deep gratitude to the jury members: **Prof. Belkacem Menadi, Dr. Farih Messaoudi and Prof. Farid Debieb,** for their valuable comments and suggestions on this thesis. It is a great honor for me to have my thesis reviewed by such distinguished and expert researchers in this field.*

I am thankful to the entire administrative staff of the Civil Engineering Department and the Faculty of Technology at the University of Blida 1 for their administrative facilitation and support.

*Special thanks go to **Mr. Sofiane Mouloud**, Head of the Science and Technology Laboratory at the University of Médéa, for his invaluable assistance in conducting the experimental program.*

*I would also like to extend my sincere gratitude to **Mr. Fouad Mokeddem** and **Mr. Imad Mokeddem** for their contributions in fabricating the components of the testing device.*

Special thanks to my beloved mother, whose unwavering love, guidance, and support have been the foundation of my journey.

I would like to thank all those who have helped me from near or far during these years of research and study.

I cannot conclude without a word of thanks to all my teachers and colleagues.

Mr. Oussama MERABET

ملخــص

تُعَدُّ قوة الشد من الخصائص الميكانيكية الأساسية للخرسانة. ومع ذلك، على عكس قوة الضغط، فإنّ تحديد قوة الشد الحقيقية للخرسانة تحت الشد أحادي المحور يُعد أمرًا صعبًا نظرًا للسلوك الهش للمادة. تُقدّم الطرق القياسية غير المباشرة المعتمدة، مثل اختبارات الثني والانشطار، نتائج مبالغ فيها وغير دقيقة على الرغم من استخدامها الواسع واعتماد نتائجها. يهدف هذا البحث إلى تطوير طريقة اختبار جديدة سهلة التنفيذ بحيث تعطي قيمًا لقوة الشد أقرب إلى تلك المستخلصة من اختبارات الشد المباشر. في هذا السياق، تم تصميم وتصنيع جهاز اختبار جديد إلى جانب تقنية جديدة لتحضير العينات الخرسانية. تم تنفيذ البرنامج التجريبي على ثلاثة أنواع من الخرسانة: الخرسانة العادية، الخرسانة المرصوصة ذاتيا، والخرسانة المسلحة بالألياف الحديدية. تمت مقارنة النتائج المُحصَّل عليها تجريبيا مع نتائج الطرق غير المباشرة والدراسات السابقة. أظهرت النتائج أن قوة الشد التي تم قياسها باستخدام الطريقة المقترحة كانت أقل بكثير من نتائج اختبار الثني وأقرب إلى النتائج المستخلصة من اختبار الانشطار. بالإضافة إلى ذلك، أظهرت جميع العينات المختبرة باستخدام الطريقة المقترحة حدوث كسر مفاجئ وواضح في الجزء الأوسط من العينة.

الكلمات المفتاحية: قوة الشد؛ اختبار الثني؛ اختبار الانشطار؛ اختبار الشد المباشر؛ جهاز الاختبار؛ الخرسانة.

Résumé

La résistance en traction est l'une des propriétés mécaniques clés du béton. Cependant, contrairement à la résistance en compression, il est difficile de déterminer la résistance réelle du béton sous tension uniaxiale en raison de son comportement fragile. Les méthodes indirectes normalisées, telles que les essais de flexion et de fendage, bien qu'elles soient largement utilisées et acceptées, tendent à fournir des résultats surestimés et moins précis. L'objectif de cette recherche est de développer une nouvelle méthode d'essai simple à réaliser, permettant d'obtenir des valeurs de résistance en traction plus proches de celles obtenues par des essais de traction directe. Dans ce contexte, un nouveau dispositif d'essai a été conçu et fabriqué, accompagné d'une nouvelle technique de préparation des échantillons. Le programme expérimental a été réalisé sur trois types de béton : le béton ordinaire, le béton autoplaçant et le béton renforcé de fibres métalliques. Les résultats ont été comparés à ceux des méthodes indirectes et des études antérieures. Les résultats montrent que la résistance en traction mesurée par la méthode proposée est nettement inférieure à celle obtenue par l'essai de flexion et plus proche des résultats obtenus par l'essai de fendage. De plus, tous les échantillons testés avec la méthode proposée ont présenté une rupture soudaine et distincte au milieu de l'échantillon.

Mots clés : Résistance en traction; Essai; Flexion; Fendage; Traction directe; Dispositif d'essai; Bétons.

Abstract

Tensile strength is one of the key mechanical properties of concrete. However, unlike compressive strength, determining the true tensile strength of concrete under uniaxial tension is challenging due to the material's brittle behavior. Indirect standard methods, such as flexural and splitting tests, although widely used and accepted, often provide overestimated and less accurate results. The objective of this research is to develop a new testing method that is straightforward to conduct and yields tensile strength values closer to those obtained from direct tension tests. In this context, a novel testing device was designed and fabricated, along with a new specimen preparation technique. The experimental program was carried out on three types of concrete: Ordinary Concrete, Self-Compacting Concrete, and Steel Fiber Reinforced Concrete. The results were compared with those from indirect methods and previous studies. The findings demonstrate that the tensile strength measured by the proposed method is significantly lower than the flexural test results and closer to the values obtained from the splitting test. Additionally, all specimens tested using the proposed method exhibited a sudden and distinct fracture in the middle portion of the specimen.

Keywords: Tensile strength; Flexural test; Splitting test; Direct tension test; Testing device; Concrete.

Table of Contents

Chapter IV: Experimental Results and Discussion

Annexes

List of Figures

List of Tables

General Introduction

General Introduction

Cementitious materials are the most widely used civil engineering materials globally [1]. They play a fundamental role in the construction of various concrete structures such as buildings, dams, bridges, tunnels, roads, etc. [2]. Among these materials, concrete stands out as the most prevalent for many centuries due to its exceptional compressive strength, low cost, and ease of production. However, as the concrete is a heterogeneous material, its tensile strength is significantly lower than its compressive strength. This weak tensile behavior can lead to durability and serviceability issues, such as cracking, deflections, and failure in structural elements. Therefore, it is crucial to accurately assess tensile strength during the design phase to ensure the integrity of concrete structures [3].

The assessment of tensile strength of quasi-brittle materials has been extensively investigated since the introduction of the first tensile test method in 1943 [4,5]. Tensile test methods are typically classified into two categories: (a) direct methods and (b) indirect methods. According to researchers, the uniaxial tension test is the most accurate method for measuring the tensile properties of materials [6,7]. Various techniques for direct tension testing have been developed, depending on the method used to secure the specimen to the testing machine. These include: (1) rings on truncated cones, (2) embedded steel bars, (3) lateral gripping, (4) gluing (adhesive bonding) [8]. However, due to the difficulties involved in applying a pure uniaxial load to test samples, these methods suffer from many technical problems, such as load eccentricity, non-uniform stress distribution, and stress concentrations at the specimen ends. Moreover, there are still no standardized procedures for determining the direct tensile strength of concrete.

Most recent studies have focused on evaluating the tensile strength of concrete using indirect tensile test methods due to their simplicity. The most commonly utilized indirect tensile tests are the splitting test, also known as the Brazilian test, and the flexural strength test, which can be conducted using either center-point or two-point loading configurations. Although these methods are widely accepted, they do not yield the true tensile strength of concrete. Furthermore, validation of indirect tensile tests often relies on several assumptions, such as the homogeneity of the sample, uniform distribution of tensile stress, and the simplification of linear elastic behavior. Consequently, significant discrepancies have been observed between the results obtained from indirect tensile methods and direct tensile tests, with the magnitudes derived from indirect tensile tests frequently being overestimated [9].

This introduction aims to clarify that achieving the true tensile strength of concrete is extremely challenging, if not impossible. In this context, the primary objective of this research is to develop a novel experimental method to investigate the tensile strength of concrete by designing and fabricating a new, simple, and reliable testing device for determining the direct tensile strength. The proposed device will be compatible with most existing compression testing machines, and it is designed to be durable, inexpensive, and easy to use. Additionally, this study introduces a novel technique for specimen preparation, specifically developed to overcome the challenges associated with previous research methodologies.

This thesis comprises a total of four chapters. These chapters are organized as follows:

- **Chapter I : Literature Review**

This chapter presents a detailed literature review, focusing on the behavior of concrete under various stress conditions, with a particular emphasis on tensile strength. The chapter covers different methods of determining tensile strength of concrete, including standard and non-standard test methods, and explores the key factors influencing mechanical properties of concrete. Relationships between compressive and tensile strength are discussed, along with failure modes and the importance of accurate testing methodologies.

- **Chapter II : Development and Analysis of a Tensile Testing Device**

In this chapter, the design and fabrication of a novel device for direct tensile testing of cylindrical concrete specimens are detailed. The chapter outlines the technical challenges, design process, and validation of the device through both analytical calculations and numerical simulations. Special emphasis is placed on ensuring the compatibility of the device with standard compression testing machines and its ability to provide accurate tensile strength measurements.

- **Chapter III : Experimental Procedure for Assessing the Proposed Testing Device**

This chapter describes the materials and methods used in the experimental study. The composition of the concrete mixes, including ordinary concrete (OC), self-compacting concrete (SCC), and steel fiber-reinforced concrete (SFRC), is outlined. Detailed procedures for specimen preparation and curing are provided. The chapter also introduces the test methods used for compressive, tensile, and flexural strength testing, along with a description of the novel specimen preparation technique used in the direct tensile tests.

- **Chapter IV : Experimental Results and Discussion**

This chapter presents the experimental results obtained from the tensile tests performed using the newly developed testing device. A comparison is made between the direct tensile strength measurements and those obtained from indirect methods such as the splitting tensile and flexural tests. The chapter discusses the observed failure modes of specimens and the influence of the testing method on the test results.

Based on the experimental investigations, general conclusions and future prospects are discussed at the end of the thesis.

Chapter I

Literature Review

Chapter I: Literature Review

I.1. Introduction

The compressive strength of concrete is the property most valued by designers and quality control engineers. However, the tensile strength, although significantly lower than the concrete compressive strength, plays a crucial role in the material's overall behavior, especially in complex stress states. The primary focus of this chapter is to explore the behavior of concrete under various stress conditions. A detailed review of the literature is provided, describing different test methods for determining the tensile strength of concrete, including standard tests and methods proposed by previous researchers. Additionally, various factors influencing concrete strength are examined in detail. Furthermore, the relationships between uniaxial compressive strength and tensile strength, as suggested by different international codes and published studies are presented.

I.2. Concrete strength

The strength of a material is defined as the ability to resist stress without failure. Failure is sometimes identified with the appearance of cracks. However, microstructural investigations of ordinary concrete show that unlike most structural materials concrete contains many fine cracks even before it is subjected to external stresses [10]. In concrete, therefore, strength is related to the stress required to cause failure and it is defined as the maximum stress the concrete sample can withstand. In tension testing, the fracture of the test piece usually signifies failure. In compression, the test piece is considered to have failed even when no signs of external fracture are visible; however, the internal cracking has reached such an advanced state that the specimen is unable to carry a higher load.

I.3. Significance of concrete strength

In concrete design and quality control, strength is the property generally specified. This is because, compared to most other properties, testing of strength is relatively easy. Furthermore, many properties of concrete, such as elastic modulus, impermeability, and resistance to weathering agents including aggressive waters, are believed to be dependent on the strength and may therefore be deduced from the strength data [11]. The compressive strength of concrete is several times greater than other types of strength, therefore a majority of concrete elements are designed to take advantage of the higher compressive strength of the material. Although in practice most concrete is subjected simultaneously to a combination of compressive, tensile, and shearing stresses in two

or more directions, the uniaxial compression tests are the easiest to conduct in the laboratory, and the 28-day compressive strength of concrete determined by a standard uniaxial compression test is accepted universally as a general index of the concrete strength.

Generally, strength tests of concrete specimens are used for three main purposes:

- For research;
- For quality control and quality assurance;
- For determining in-place concrete strength [12].

I.4.   Size levels for assessing the concrete behavior

Concrete is frequently modeled as a two- or three-phase material. These phases include the aggregate phase, the cement-matrix phase, and a substantial number of pores (air voids) within the concrete structure.

The ratio between the subsequent constituents will influence the deformational properties of the concrete mix and the final strength [13]. Next to these internal structure-related variables, a large number of external factors will influence the observed behavior too. For small-sized tests on cubical or cylindrical specimens, for example, used for the determination of the strength and deformational properties of the material, these other factors are loading rate, specimen size, moisture conditions, temperature, etc.

At this point, it is essential to define the different size levels. Based on the classifications provided by Mihashi [14] and Wittmann [15], three distinct groups can be identified:

I.4.1.   Macroscopic level

The characteristic length typically ranges around 100 mm or more. The properties under study pertain to a continuum, including average stress and strain, as well as the non-linearity of mechanical properties. It is desirable to present the corresponding engineering models in a format suitable for immediate application in numerical analysis.

I.4.2.   Meso-level

At the Meso-level, also known as the sub-macroscopic level, the characteristic length typically ranges from 1 to 10 mm. Typical phenomena studied at this level include crack formation and fracture mechanisms, which significantly influence the average stress-strain, and non-linearity of mechanical properties at the macroscopic level.

I.4.3. Microlevel

At the micro level, concrete behavior is analyzed at the smallest scale (in the order of 10^{-1} mm or less). This level of analysis focuses on the atomic and molecular structure of concrete constituents, such as cement paste, aggregates, and hydration products. Phenomena studied at this level include chemical reactions, crystalline structures, and interatomic bonding.

I.5. Failure Modes in Concrete

Failure of concrete occurs as a result of the development of a network of microcracks that grow in length with increasing load until the concrete can no longer support further stress. Under uniaxial tension, relatively less energy is needed for the initiation and growth of cracks in the matrix. Before external loads are applied, fine cracks already exist in the concrete at the interface between the coarse aggregate and the cement paste. These cracks are caused by differences in mechanical properties and the effects of shrinkage or thermal strains. These pre-existing microcracks are responsible for the low tensile strength of concrete. As external load is applied, existing microcracks are stable up to about 30 % of the ultimate load, at which point interfacial cracks begin to increase in length, width, and quantity. When 70–90 % of the ultimate strength is reached, cracks penetrate into the bulk paste leading to continuous larger cracks until the concrete cannot support additional load [10].

However, in compression, the failure mode is less brittle because considerably more energy is needed to form and extend cracks in the matrix. It is generally agreed that, in a uniaxial compression test on medium- or low-strength concrete, no cracks are initiated in the matrix up to about 50 percent of the failure stress; at this stage, a stable system of cracks, called shear-bond cracks, already exists in the vicinity of coarse aggregate. At higher stress levels, cracks are initiated within the matrix; their number and size increase progressively with increasing stress levels. The cracks in the matrix and the interfacial transition zone (shear-bond cracks) eventually join up, and generally, a failure surface develops at about 20° to 30° from the direction of the load, as shown in Figure I.1.
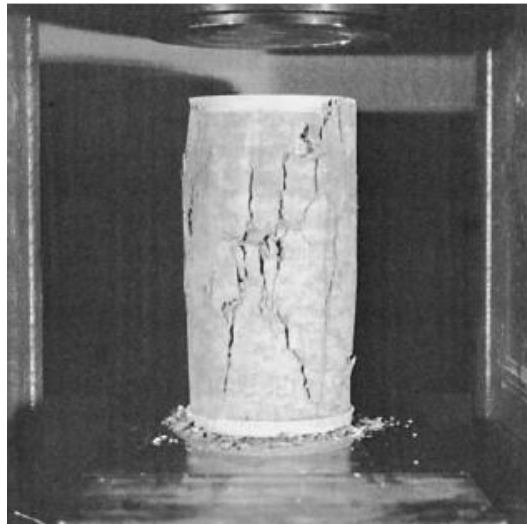
Figure I.1: The failure mode of concrete under compression [11].

I.6.   Behavior of concrete under various states of stress

Under practical conditions, concrete is rarely subjected to uniaxial stress (stress in one direction), since in most structural situations the concrete is stressed in multiple directions simultaneously. Nevertheless, an assumed uniaxial stress condition can be justified in many cases[16].

I.6.1.   Behavior of concrete under uniaxial compression

Compressive strength is one of the most important properties of concrete. Furthermore, it is commonly considered as a reference for many other properties, such as elastic modulus and tensile strength [10,17]. The assessment of concrete compressive strength is typically obtained from testing concrete specimens of either cubic or cylindrical shapes as suggested by different codes and standards.

Figure I.2 presents a typical stress-strain curve of a concrete specimen subjected to a uniaxial compression test. The curve shows a linear-elastic behavior up to about 30 percent of the ultimate strength f_{cu}. When existing interfacial microcracks begin to propagate, the curve shows a gradual deviation from linear behavior up to about 90% of ultimate strength; deviation from linearity increases as more interfacial cracks are formed. As ultimate strength is approached, interfacial and bulk paste microcracks join to form continuous cracks parallel to the direction of loading. At some point, the extent of cracking is so great that the concrete cannot support additional load, and subsequently, the stress required for additional strain decreases until the specimen is fractured [18].
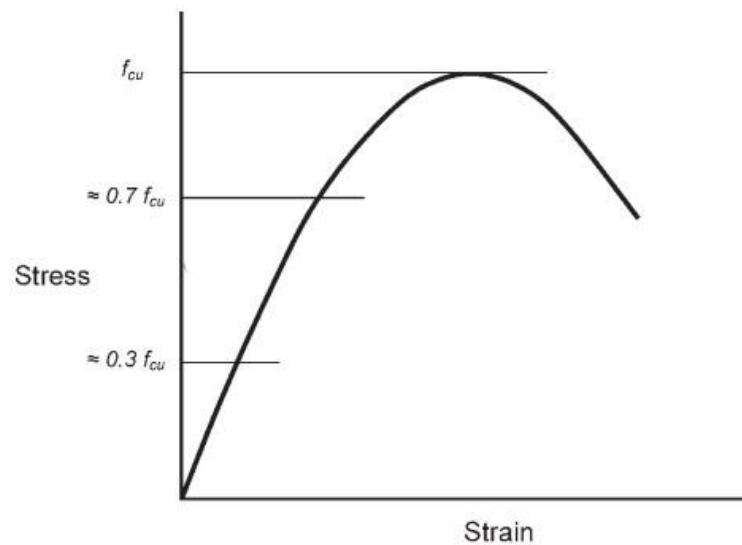
Figure I.2: Typical stress-strain curve of concrete in compression [18].

I.6.2. Behavior of concrete under uniaxial tension

Under uniaxial tension, the behavior of concrete differs significantly from its behavior under compression. Concrete tends to exhibit brittle fracture characteristics when subjected to tensile stress. Initially, the stress-strain curve shows linear behavior up to a certain limit. The propagation of existing microcracks within the concrete matrix leads to a rapid deviation from this linear behavior. Due to the nature of tensile stress, cracks are less frequently arrested compared to compressive stress, resulting in a shorter interval of stable crack propagation.

As the stress increases, these microcracks propagate and coalesce, reducing the effective load-carrying area and increasing the stress concentration at the crack tips. This process accelerates crack growth, making it difficult to observe the descending portion of the stress-strain curve in tensile tests. Consequently, concrete fails in a relatively brittle manner under uniaxial tension compared to the more ductile failure observed under uniaxial compression [19,20]

I.6.3. Behavior of concrete under shearing stress

Concrete under shearing stress exhibits a complex behavior due to its heterogeneous composition and the interaction between the aggregates and cement paste. The shear strength of concrete is influenced by factors such as the adhesion between cement paste and aggregates, frictional resistance, and the mechanical interlocking of the aggregate particles. These factors contribute to the mobilization of shear stress and displacement within the material. During shear stress application, microcracks can develop and propagate, leading to various failure modes that differ from those observed under uniaxial compression or tension [21].

I.6.4. Behavior of concrete under biaxial and multiaxial stresses

Concrete under biaxial and multiaxial stresses exhibits complex behavior significantly different from its uniaxial stress response. When subjected to biaxial stress, combinations of compression-compression, compression-tension, and tension-tension scenarios are considered. Research indicates that the strength of concrete in biaxial compression can be significantly higher than in uniaxial compression, often up to 1.5 to 2 times. However, the tensile strength is not significantly affected by the application of biaxial tensile stresses [10,22–24]. In multiaxial stress conditions, the presence of three-dimensional stress states further complicates the failure mechanisms, often leading to an increased compressive strength due to the confinement effect.

Biaxial stress tests typically involve concrete specimens subjected to in-plane loading using specialized platens to minimize restraint effects. These tests help understand the complex interplay between different stress components, providing critical insights for structural design and analysis under realistic loading conditions.

I.7.   Testing methods for tensile strength

I.7.1.   Historical overview

Galileo Galilei was perhaps the first to define the concept of stress [7]. Demonstrating methods to determine the maximum load of a material, such as the cantilevered beam test to which a weight was attached at the end (Figure I.3). He also identified the size effect, noting differences in load-carrying capacities of different bone sizes [25]. Determination of the uniaxial tensile strength is not straightforward, particularly in the days of Galilei, which posed significant challenges. Timoshenko [25] and Siviero [26] give historical overviews and describe tests on dog-bone-shaped specimens as a first attempt to measure the tensile capacity of concrete. The tensile strength of the material, defined as the maximum stress that the material specimen can carry, is simply calculated by dividing the maximum load by the net cross-section in the neck of the sample. However, Due to the difficulties in achieving pure axial tension and uncertainties from holding devices, direct tension tests are seldom used even for research purposes.
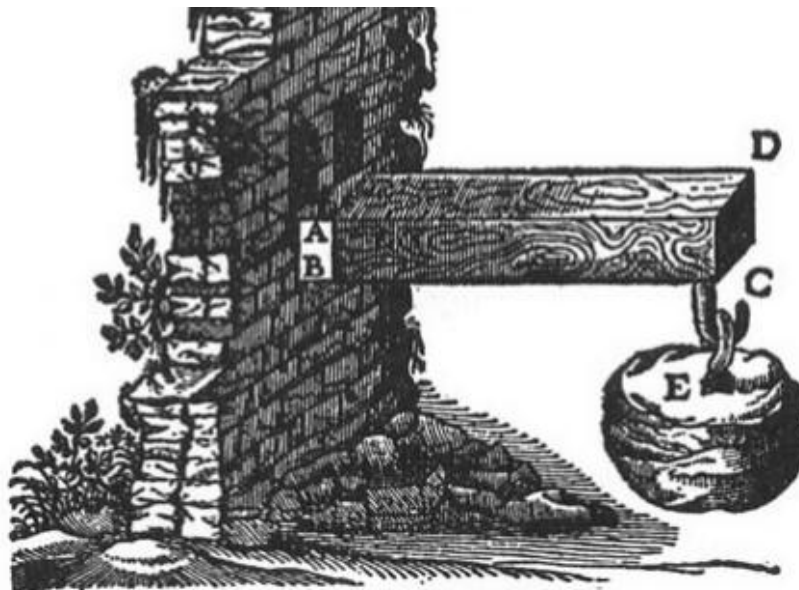
Figure I.3: Illustration of Galileo's Bending Test [25].

I.7.2.   Indirect tensile test methods

The tensile strength of quasi-brittle materials can be measured using direct and indirect tensile tests. Indirect tensile tests are frequently developed and adopted for determining tensile strength and the stress-strain relationship. The most commonly used indirect tensile tests for quasi-brittle materials include the splitting test (also known as the Brazilian test) [27], three-point bending test, and four-point bending test [28]. However, indirect tensile tests do not produce a

uniform and uniaxial tensile stress distribution across the fracture section. Additionally, these tests often require assumptions such as two-dimensional plane stress conditions, homogeneous sample characteristics, and linear elastic behavior simplifications for validating the testing method [29,30]. Consequently, significant discrepancies are observed between the results obtained through indirect tensile methods and direct uniaxial tensile tests, with the magnitudes determined by indirect tensile tests generally being overestimated [31–33].

I.7.2.1. Splitting test

a. Description of the test

One of the most commonly used indirect tensile tests for evaluating the tensile strength of concrete is the splitting test (NF EN 12390-6). This method was first proposed by Carneiro and Barcellos (1953) [34] in Brazil and independently developed by Akazawa (1953) in Japan [35]. In this test, a standard cylindrical specimen is placed horizontally between the loading platens of a testing machine and compressed along its vertical diameter. The experimental setup is depicted in Figure I.4.

During the test, a radial compressive load is applied to the surface of the specimen, causing a vertical crack to form along its diameter. As the radial compressive force increases, the tensile stress within the specimen also increases, ultimately causing it to split along the direction of the applied load (vertical diameter)
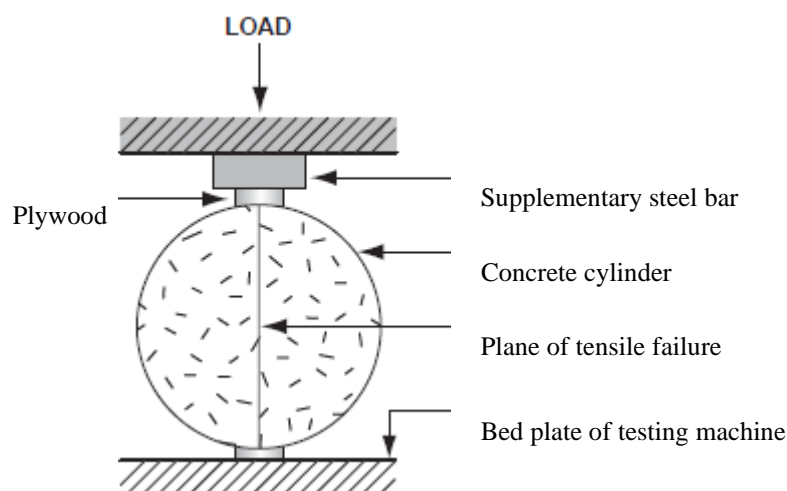
Figure I.4: Splitting tension test [36]

The loading rate recommended for this test is:

- $\dot{\sigma} \in [0.04; 0.06] MPa/s$ under imposed stress.

- $\dot{\varepsilon} = 1.65 \times 10^{-5} s^{-1}$ under imposed strain.

The cylindrical specimens used for this test must conform to the specifications outlined in the testing standards EN 12390-1 [37] and EN 12390-2 [38].

Cubes and prisms can also be subjected to the splitting test, with the load applied through loading pieces positioned on the center lines of two opposing faces of the cube (Figure I.5). This method covered by BS 1881: Part 117: 1983, and replaced by BS EN 12390-6: 2009, yields results comparable to those obtained from the splitting test on cylindrical specimens [39].
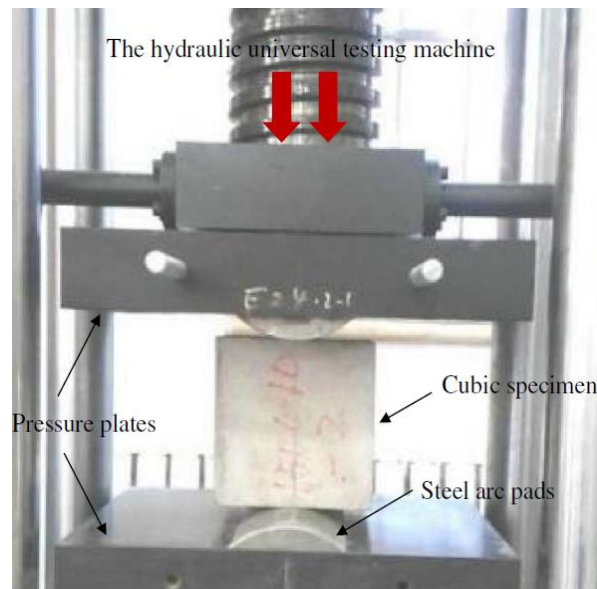
Figure I.5: Test setup of a cube subjected to the splitting test [40].

b. Expression of results

The calculation of the maximum principal stress in the splitting tensile test is based on elasticity theory. The two-dimensional stress field in the disc can be derived and simplified to focus only on the normal stress (σ_x) along the loading axis of two equal and opposed point loads, as illustrated in Figure I.6. The maximum principal stress (σ_x) in the specimen can be calculated using the following equation, as provided by Timoshenko and Goodier [41]:

$$\sigma_x = \frac{2F}{\pi dL} \tag{1}$$

Where:

σ_x: the horizontal normal stress, in MPa;

F: the maximum load, in N;

L: the length of the line of contact of the specimen, in mm;

d: the designated cross-sectional dimension, in mm.
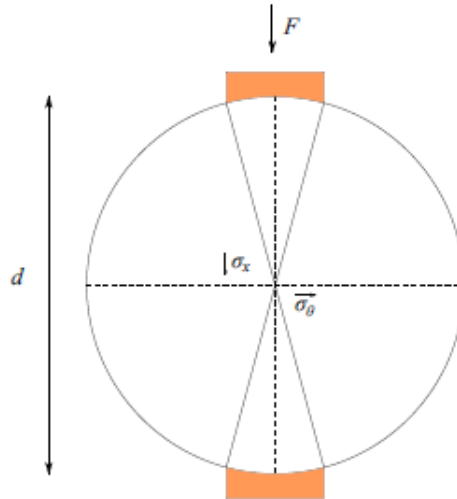
Figure I.6: Assumed load condition for splitting test [42].

As mentioned above, the splitting test methods use the Timoshenko and Goodier equation [41] to calculate the tensile strength of the material, assuming that the fracture mode initiates at the center of the specimen. The crack propagates in the direction of the highest stress, towards the loading strips. In their study on rupture mechanisms in the splitting test, Rocco et al. [43] identified that this primary mode of failure (schematically shown in Figure I.7.a) is followed by secondary cracking, as illustrated in Figure I.7.b. This observation suggests that, upon reaching the maximum tensile strength and the formation of a crack at the center along the loading axis, stress redistribution occurs, leading to the creation of new highly stressed regions.

By measuring transversal deformation during the test, Rocco et al. [43] found that both the formation of the principal crack and the secondary crack exhibited distinct peaks, as depicted in Figure I.7.c. The relative magnitudes of these peaks vary depending on the material type and specimen geometry. It is important to note that in the present test method, the tensile strength (f_t) is calculated based on the maximum load recorded during the test. In instances where the secondary peak load exceeds the principal peak load, the linear elastic solutions provided by both equations would become invalid.
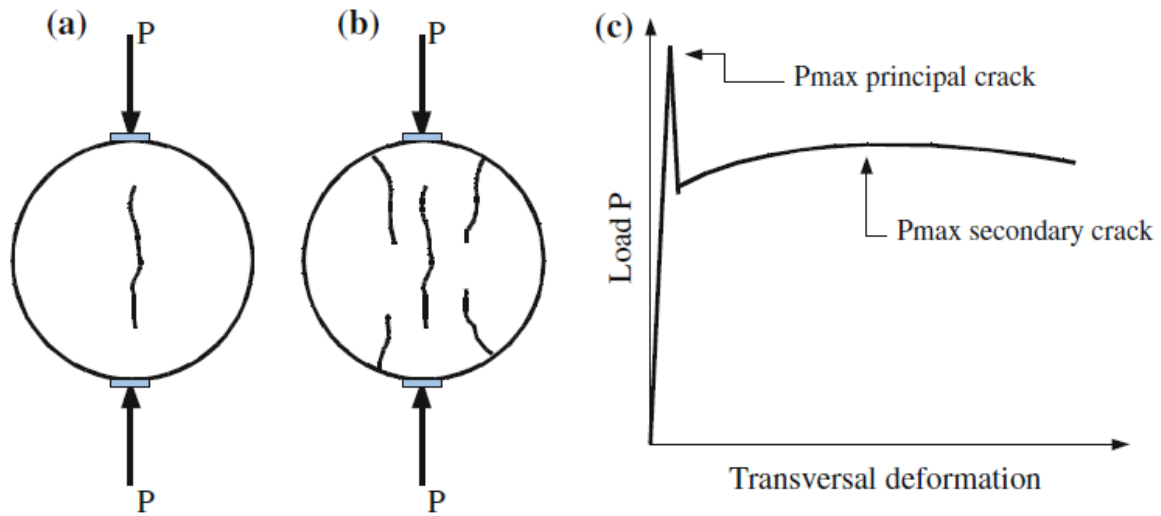
Figure I.7: a) Formation of principal crack; b) formation of secondary crack; c) Schematic representation of load-deformation curve [43].

c. Differences between the practical splitting test of concrete and theoretical analysis

The calculations outlined above provide an exact solution for the ideal case. However, the actual execution of the test deviates from these ideal conditions in the following respects:

1. **Material properties**

Theoretical analyses usually assume the concrete material to be perfectly elastic and isotropic. Practically, concrete exhibits heterogeneous and sometimes anisotropic properties, leading to variations throughout the specimen [44].

2. **Deviation from Hook's law**

The theoretical analysis of the stress field within the concrete cylinder assumes a linear elastic material behavior, where strain is proportional to stress. However, the elasticity theory is not applicable in the case of concrete [45]. The apparent decrease in elasticity modulus as stress increases indicates that the stress-strain curve redistributes stress from highly stressed regions on the top and bottom surfaces of the cylinder to areas of lower stress. As a result, this phenomenon tends to increase the load necessary to fracture the specimen, leading to a higher calculated value.

3. **Deviation from plane stress conditions**

In practical scenarios, elasticity theory assumes a state of plane stress, which may not always be achieved. While thin discs tend to approximate plane stress conditions, long cylinders

more closely resemble plane strain [45]. It is important to note that the theory has not been extended to accommodate the plane strain conditions.

4. Distribution of applied load

In splitting test methods, it is assumed that applying a point load on a thin plate generates a uniform tensile stress state along the generator of the cylinder during the test. However, as illustrated in Figure I.8.b, the actual loading conditions in the test setup differ from the simplified boundary conditions depicted in Figure I.8.a [46]. In practice, the loads are applied to the specimen using a loading strip with a certain width, rather than point loads.
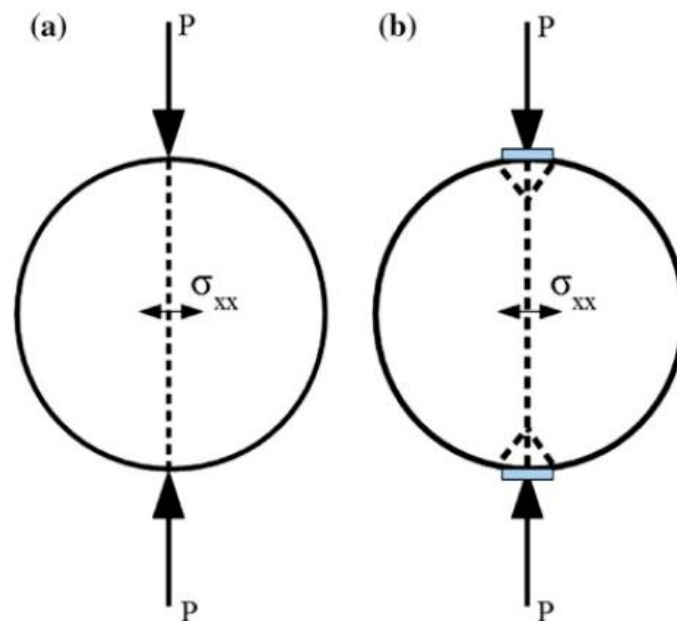
Figure I.8: Load conditions in splitting test: a) Assumed load; b) Actual load [46].

The stress distribution within a loaded cylinder, as illustrated in Figure I.9, reveals distinct patterns. Across approximately three-quarters of the vertical plane, the tensile stress remains relatively constant. However, at the top and bottom ends, there is a notable transition towards significantly higher compressive stress levels. Notably, the maximum compressive stress exceeds the maximum tensile stress by a factor of approximately 18 [45]. While this discrepancy might suggest a potential failure due to local compression along the loading lines, practical evidence refutes this assumption.
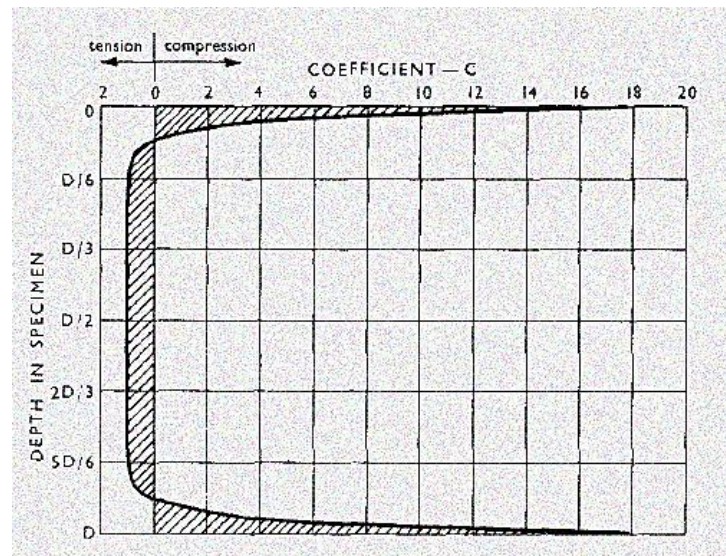
Figure I.9: Stress distribution in a loaded cylinder [45].

d. Parameters affecting the splitting tensile strength

1. Effect of specimen sizes

Like all brittle failures of concrete, split tensile failure exhibits a size effect, as demonstrated by various researchers. Malhotra [47] found that smaller concrete cylindrical specimens ($\Phi 102 \times 203$ mm) exhibited higher nominal strengths compared to larger ones ($\Phi 152 \times 305$ mm). Rocco et al. [48] also observed that the splitting tensile strength decreases with increasing specimen size in Brazilian tests. Similar findings were reported by Carmona [49], Wang et al. [50], and Zhang et al. [51].

Conversely, some researchers reported differing results. Zhou et al. [52] observed an increase in splitting tensile strength with larger specimen sizes. Additionally, Hasegawa et al. [53] and Bažant et al. [54] found that splitting tensile strength initially decreases and then slightly increases with the increase in structural size, concluding that the variability of splitting tensile strength decreases with increasing specimen size.

2. Effect of loading strips

In the Brazilian test, the load is applied to the concrete cylinder by means of loading strips with a certain width instead of concentrated loads. The loading strip causes an uneven distribution of the normal stress along the loading axis of the specimen, with compressive zones at the top and bottom of the tested specimen. Furthermore, the size of the compressive zone depends on the size (width) of the load strip. The deviation from the assumed simple boundary conditions leads to overestimating the tensile strength obtained [41]. Rocco et al. [43,55] investigated the influence

of the width of the loading strip on the results of the Brazilian test using international standards (BS 1881-117, ASTM C-469, ISO 4105). Their analysis shows that the split cylinder test can yield a true indication of the tensile strength as long as the width of the loading strip does not exceed 8% of the diameter of the specimen and the loading rate does not exceed 1.0 MPa/min.

3. Effect of specimen moisture condition

The moisture condition of concrete specimens plays a critical role in the outcomes of the splitting tensile strength test. Specimens in a saturated surface-dry condition generally show higher tensile strength due to the presence of internal moisture that helps distribute stress more evenly and prevents premature cracking. In contrast, dry specimens tend to exhibit lower strength because they are more brittle and prone to micro-cracking. Air-dried specimens typically have intermediate properties, with some retained moisture aiding in reducing brittleness [56,57].

4. Effect of loading rate

The loading rate significantly impacts the splitting tensile strength of concrete. Higher loading rates generally lead to increased tensile strength due to the rate-sensitive nature of concrete. This is attributed to the limited time available for microcrack development and the enhanced inertial resistance during rapid loading. In contrast, lower loading rates allow more time for microcracks to initiate and propagate, resulting in lower strength measurements [44,58].

I.7.2.2. Flexural strength test

a. Description of the test

The flexural strength test of concrete, also known as the modulus of rupture test, is an indirect method used to estimate the tensile strength of concrete. In this test, a standard unreinforced concrete beam (100 mm x 100 mm x 500 mm or 150 mm x 150 mm x 700 mm) is subjected to flexure until failure occurs. Typically, this is done using either a center-point or two-point loading setup. The center-point loading method involves applying the load at the midpoint of the span, while the two-point loading method applies the load at two points, each located at one-third of the span length from the support points, as shown in the Figure I.10. This loading configuration induces tensile stresses in the lower half of the beam and compressive stresses in the upper half, perpendicular to the direction of the applied load. The load is applied gradually without shock at a constant rate until failure occurs. The rate of loading typically ranges from 0.04 MPa/s to 0.06 MPa/s, depending on the specimen size.
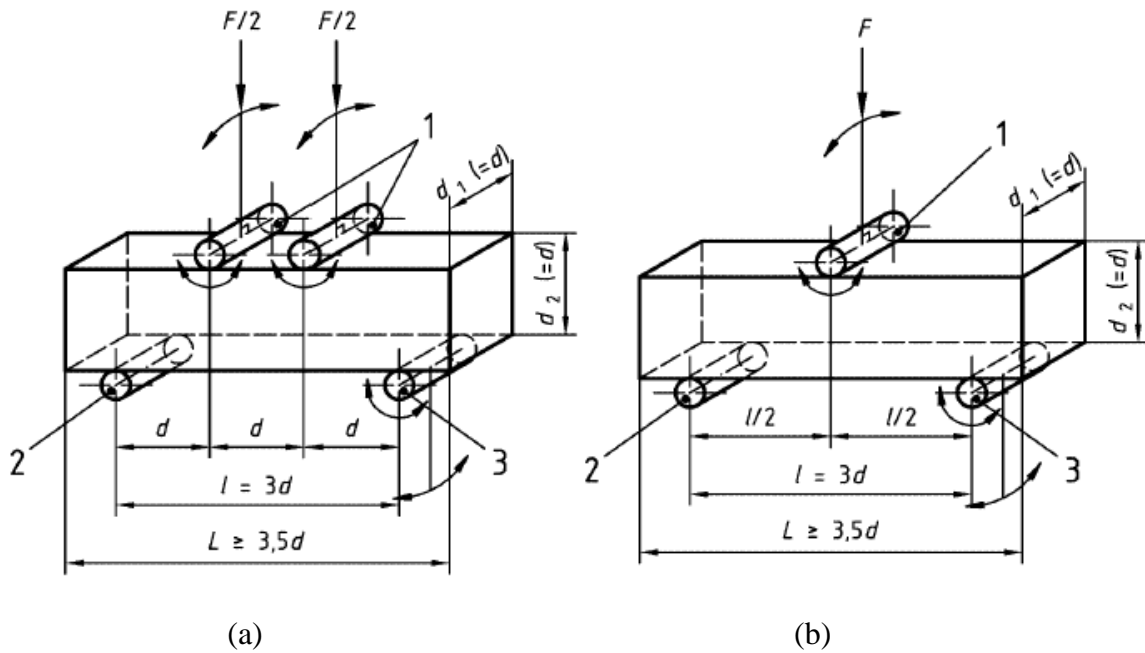
Figure I.10: Loading setup for the flexural test: a) two-point loading; b) center point loading [59].

b. Expression of results

The flexural strength (modulus of rupture) using center-point loading is calculated on the basis of elastic theory and is given by the equation:

$$f_{cf} = \frac{F \times l}{d_1 \times d_2^2} \qquad (2)$$

Where :

f_{cf} : the flexural strength, in MPa;

F : the maximum load, in N;

l : the distance between supporting rollers, in mm;

d_1 : the width of the beam, in mm;

d_2 : the depth of the beam, in mm.

If, however, the flexural strength of the beam is subjected to two-point loading, the modulus of rupture is given by:

$$f_{cf} = \frac{3 \times F \times l}{2 \times d_1 \times d_2^2} \qquad (3)$$

The flexural strength obtained using the center-point load test arrangement is higher than that obtained with the two-point load test configuration. A comparison conducted within the EC Measurement and Testing Programme, under contract MAT1-CT-94-0043, suggests that the modulus of rupture values from the center-point loading method can exceed those from the two-point loading method by up to 13%.

c. Differences between the practical test and the theoretical case

In the bending experiments, the equation for the flexural strength is based on the elastic beam theory, where the maximum tensile stress in the bottom fiber is determined by assuming the tensile stress within the beam varies proportionally with the distance from its neutral axis (the stress–strain relationship is assumed to be linear) [10], as shown in the Figure I.11. However, in the practical test, there is a progressive increase in strain as the stress surpasses approximately half of the tensile strength. Consequently, the stress block shape under loads nearing failure adopts a parabolic form rather than a triangular one.
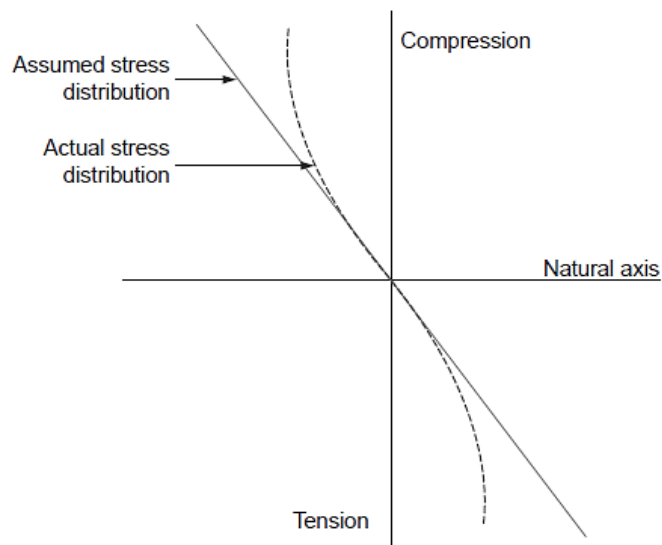
Figure I.11: Stress distribution across the depth of a concrete beam in the flexural test [60].

According to Wright [61], when the compressive stress distribution is linear and the tensile stress distribution follows a parabolic pattern, the maximum tensile stress is 0.735 times the conventional modulus of rupture value. Furthermore, Raphael [62] has demonstrated that the theoretical maximum tensile stress exceeds the correct value of the modulus of rupture by 25% (see Figure I.12). As expected, results from the flexural test tend to overestimate the tensile strength of concrete by 50% to 100% [60].
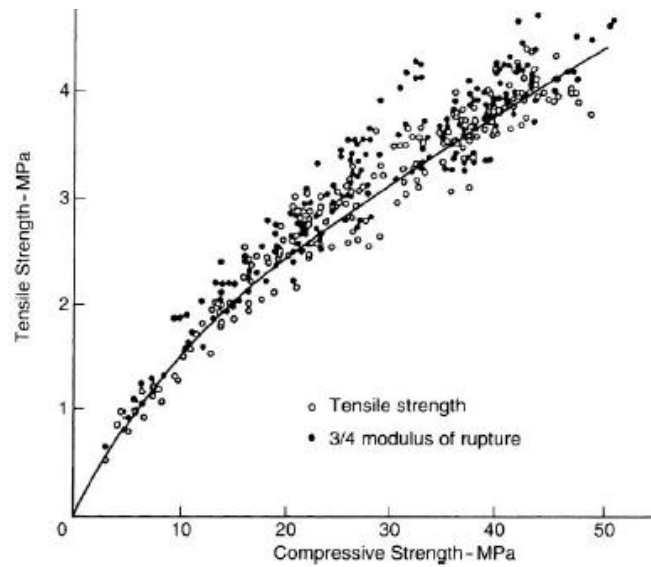
Figure I.12: Plot of the modulus of rupture against compressive strength of concrete [62].

The CERIB recommends that a coefficient of 0.6 be used to obtain the pure tensile strength:

$$f_t = 0.6 \, f_{cf} \qquad (4)$$

d. Parameters affecting the flexural strength

1. Effect of specimen dimensions

According to ASTM C 78 and ASTM C 293, the tested specimen must have a span three times its tested depth. Standard beam dimensions are generally 150 mm $\times$ 150 mm $\times$ 500 mm, with testing conducted on a 456 mm span. However, beam dimensions can vary depending on the maximum size of the coarse aggregate. The minimum dimension of the specimen must be at least three times the nominal maximum size of the coarse aggregate, and the width-to-depth ratio in its molded state should not exceed 1.5.

The effect of span length on flexural strength for a constant beam cross-section remains unclear. Kellerman [63] reported a decrease in strength with increasing span length for both center-point and two-point loading. In contrast, Reagel and Willis [64] found no significant impact of span length on strength under two-point loading conditions.

2. Effect of specimen size

It is commonly agreed that increasing the size of the tested specimen results in a decrease in flexural strength for both center-point and two-point loading methods [61,63–65]. Moreover, studies have indicated that larger specimen sizes lead to reduced variability in test results [65].

3. Effect of loading rate

Research indicates that the flexural strength of concrete increases with higher loading rates during testing. This is because concrete exhibits greater resistance to deformation at faster loading rates, resulting in higher measured strengths. Additionally, higher loading rates tend to reduce the variability in test results, enhancing the reliability of the data. This effect has been observed across various types of concrete, including plain and steel-fiber-reinforced concrete, although the degree of strength increase can vary depending on the specific concrete mix and test conditions [66,67].

4. Effect of moisture condition

The moisture condition of concrete specimens significantly influences the results of flexural strength tests. Research indicates that specimens tested in a dry state exhibit considerably lower apparent flexural strength compared to those tested in a saturated state [10,68–70]. This reduction in strength, which can be as high as 33% [69], is attributed to the tensile stresses induced by rapid surface drying. These stresses can lead to surface cracking or act as preloading conditions, both of which lead to lower failure loads. Consequently, to ensure accurate assessment of in-place concrete strength, it is recommended that flexural strength specimens be cured under similar conditions to the actual concrete structure and tested in a saturated state.

5. Effect of center-point versus two-point loading

The main difference between center-point loading and two-point loading tests is the location of load application (as shown in Figure I.13). In center-point loading, the load is applied at the specimen midspan. In two-point loading, the load is applied at the third points along the test span. For the first case, only the cross-section at midspan is subjected to maximum moment and maximum extreme fiber stress. However, in two-point loading, the middle third of the beam span is subjected to maximum bending moment, and thus maximum extreme fiber stress. In addition, this method better represents real-world conditions where loads are more evenly distributed, making it preferable for structural applications like pavements and slabs. The probability of having weak concrete in a region of highest stress is lower with the center-point loading compared with the two-point loading. As a result, flexural strengths obtained from center-point loading are higher than those obtained from two-point loading with differences of up to 15 % [61,63,65].
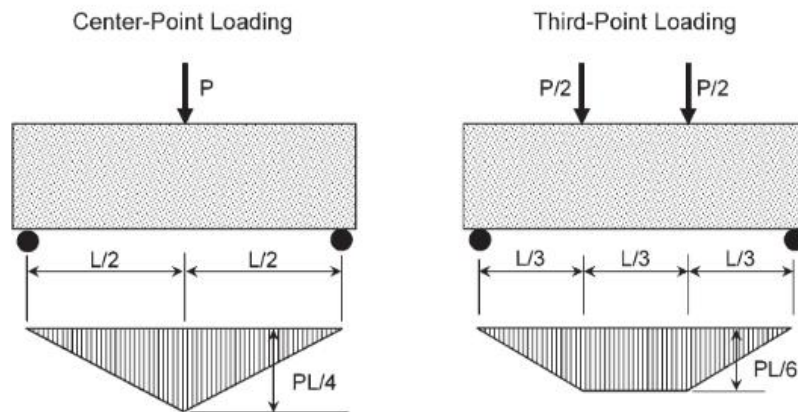
Figure I.13: Bending moment diagrams: center-point vs. two-point loading [71].

I.7.3. Direct tension test

The most accurate, fundamental, and straightforward way of measuring the tensile strength of concrete is still by directly applying the uniaxial tensile stress [72,73]. However, there are currently no standardized test procedures for determining the direct tensile strength of concrete. Besides, the direct tensile test is rarely used anywhere other than in research fields because of the experimental difficulties involved in inducing pure axial tension within a specimen without introducing localized stress concentrations [18].

There are several challenges when performing the direct tensile test, including ensuring a uniform distribution of stress in the whole cross-section, predetermining the crack position, capturing the propagation of the cracks, etc...

I.7.3.1. Specimen geometries in direct tensile test

According to the literature, various geometries have been employed to assess the tensile properties of concrete (shown in Table I.1), each with its advantages and challenges. Common geometries include cylindrical specimens, dog-bone shaped specimens, and prismatic forms with prefabricated notches, which are the most frequently used [74]. RILEM CPC7 [75] recommends a direct tensile test procedure for concrete utilizing cylindrical and prismatic specimens; however, specific details regarding the dimensions of the specimen and the end plates used to transfer the applied tensile loads are not provided. The measured tensile strength and fracture behavior are significantly affected by the dimensions and shapes of the specimens [76]. Kesner et al. [77] conducted a comparison between two uniaxial direct tensile tests and concluded that cylindrical specimens exhibit lower tensile strength and strain capacity compared to dog-bone specimens.

Table I.1: Specimen geometries and fixed method [74].

Shape and gripping method	Specimen size (middle part) (mm)			Grip/Attachment	Reference
	Length	**Width**	**Depth**		
	305 (205)	76.2	12.7	Side glued/pinned	Li et al. [78]
	300 (100)	100	100	Top glued/anchored	Liang [79]
	254 (1)	76 (50.6)	12.7	Top glued	Roth et al. [80]
	460 (120)	150 (100)	100	Anchored/pinned	Xu et al. [81]
	550 (260)	130 (100)	100	Anchored/pinned	CECS 13:2009 [82]
	740 (240)	200 (100)	35	Side glued/pinned	Benson et al. [83]
	475 (125)	125 (50)	25	Anchored/pinned	Nguyen et al. [84]
	240 (80)	40 (24)	40	Fixed	Jun and Mechtcherine [85]
	150 (40)	75 (45)	45	Anchored/pinned	Li and Liu [86]
	147 (76)	41 (25)	25	Anchored/pinned	Wille et al. [87]

I.7.3.2. Existing gripping modes for direct tensile tests

The direct application of a pure tensile force, free from eccentricity, presents considerable challenges. Consequently, extensive research efforts have been dedicated to investigating and refining the methodologies for conducting accurate direct tensile tests.

Depending on the method adopted for clamping the specimen ends to the test machine, direct tensile test methods used by various investigators can be classified into four groups as follows [88,89]:

1. Tensile testing by rings on truncated cones

This method involves using rings placed around truncated cylindrical specimens tapered outwards at their ends with end caps tapered internally to apply tensile forces [90]. The primary advantage of this technique is its ability to produce uniform tensile stress distribution across the specimen. In this method, the concrete specimen is shaped like a truncated cone and is surrounded by metal rings (Figure I.14.a). Tensile forces are then applied through these rings inducing tensile stress within the concrete by using a simple lever as illustrated in (Figure I.14.b). This configuration helps in distributing the tensile stress uniformly, reducing the chances of premature failure due to stress concentrations. The use of truncated cones ensures that the specimen has a consistent cross-sectional area where the stress is applied, further enhancing the reliability of the test results.
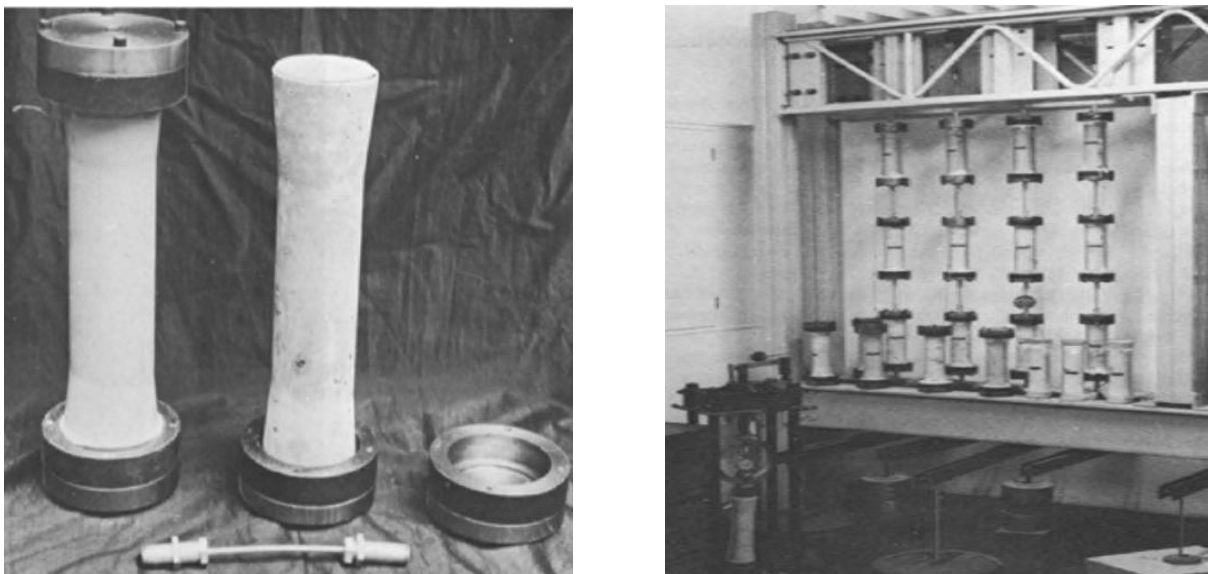
Figure I.14: a) The tensile specimen; b) The loading frame used for the test [90].

2. Tensile testing by lateral gripping

The Tensile testing by lateral gripping method is another technique used to determine the tensile strength of concrete [91,92]. In this technique, a specialized rig equipped with gripping mechanisms is designed to securely hold the specimens in place during testing which are affixed to their sides rather than at their ends as shown in Figure I.15. Specifically, the specimen is positioned between the lateral grips, which exert a uniform tensile force along its length. By gripping the specimen laterally, the tensile forces are applied directly along the axis of the specimen, which helps in achieving a pure tensile stress state. This configuration ensures that the applied load is evenly distributed across the specimen, minimizing the risk of stress concentration or premature failure at the grip interface. Notably, lateral gripping offers advantages over traditional end-gripping methods by mitigating potential issues related to eccentric loading and specimen slippage.

Figure I.15: Tensile test using lateral gripping method [93].

3. Tensile testing by means of embedded steel bars

In this method, specimens undergo tension using embedded steel bars [94]. The experimental setup typically includes cylindrical or prismatic concrete specimens with steel bars embedded at their ends (as shown in Figure I.16). These steel bars serve as anchor points for applying tensile loads during testing. The specimens are securely cast around the steel bars to ensure proper alignment and bonding. During the test, a tensile force is applied to the embedded steel bars, inducing tensile stress in the surrounding concrete. This method allows for direct measurement of the tensile strength and deformation properties of concrete under tension.
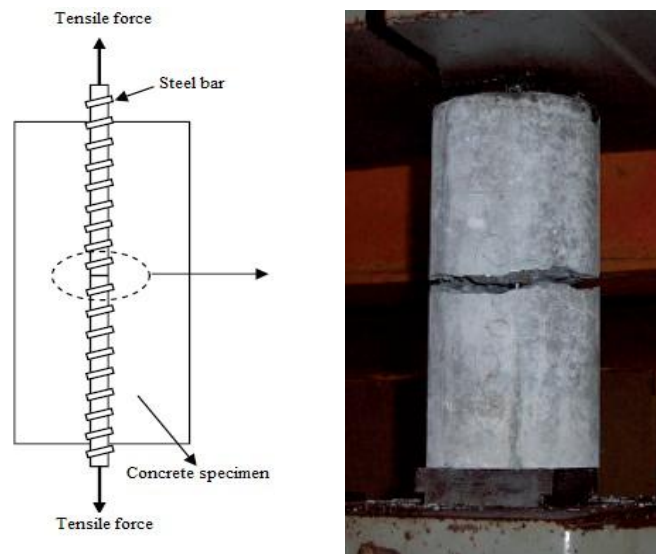
Figure I.16: Proposed direct tensile strength model [95].

Recently, several models have adopted the method of embedding studs into concrete at both ends to investigate its tensile strength [88,89,95–99] . Alhussainy et al. [99] introduced a novel procedure to analyze the stress-strain behavior of Self-Compacting Concrete (SCC) under direct uniaxial tension (see Figure I.17). Special steel claws were manufactured and installed at both ends of the SCC specimens. The test results showed that there was no slippage or fracture at the ends of any of the specimens.

Figure I.17: Test set-up for direct tension using embedded steel rods [99].

4. Tensile testing by gluing

Tensile testing by gluing encompasses a method where specimens are subjected to tension through adhesive bonding to ensure uniform stress distribution and reduce stress concentrations that can lead to premature failure [100]. This method is particularly advantageous for existing structures where creating specific specimen shapes for direct tensile testing might not be feasible [101]. The glued plates help in achieving better alignment and reducing eccentric loading, which are common issues in direct tensile tests.

In this approach, the tested specimens are attached to the loading machine using a double plate system and epoxy adhesive. To make the applied point load more evenly distributed, the US Bureau of Reclamation [102] proposes the use of a double plate system for cylindrical specimens. The outer plate is connected to the loading machine, while the inner plate is bonded to the concrete specimen with epoxy. The inner and outer plates are connected by bolts. Recently, this method was modified for cylindrical samples with a diameter of 101.6 mm and a height of 203.2 mm, as shown in Figure I.18, and showed acceptable results [103].
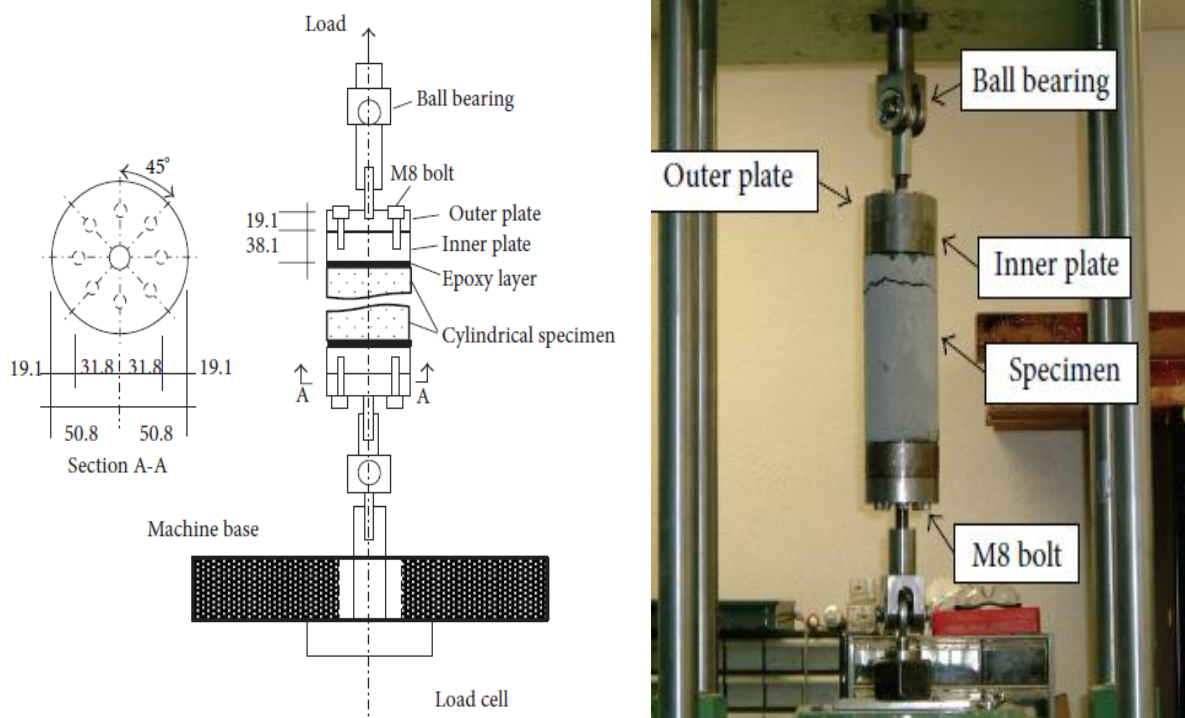
Figure I.18: Test setup for the direct tension test by gluing [104].

I.7.3.3.Limitations and difficulties associated with direct tensile tests

The above methods of gripping modes used in direct tensile tests present various challenges and limitations. These include:

a. Stress concentrations

Inadequate gripping often results in stress concentrations at the ends of the specimens, causing premature failure and unreliable tensile strength measurements.

b. Misalignment

Proper alignment of specimens is challenging, leading to eccentric loading and non-uniform stress distribution, which can affect the accuracy of results.

c. Gripping mode

The choice of gripping mechanism, whether mechanical clamps, adhesive bonding, or embedded ends, influences the stress distribution and can introduce errors if not properly managed. In addition, Excessive stress concentration at the specimen interfaces can cause fractures at these points, leading to invalid test results. Yan [105] outlines the stress distribution for various common connections and specimen shapes, as shown in Figure I.19.
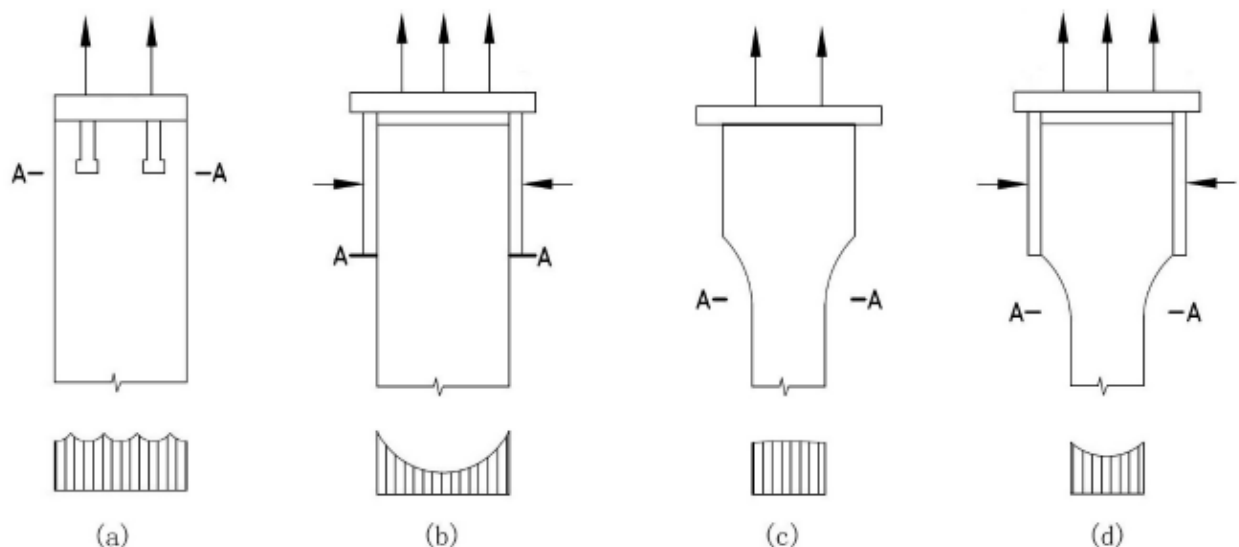
Figure I.19: The stress distribution of several common connections and specimen shapes [105].

d. Specimen damage

Gripping can cause damage to the specimen during setup, which affects the integrity and subsequent test results.

e. Slippage

Ensuring that the specimen does not slip within the grips is critical, as slippage can lead to inaccurate measurements and inconsistent test results.

f. Loading eccentricity

Achieving perfectly centered tensile loading is difficult, and any deviation can lead to erroneous data due to additional bending stresses.

g. Complex setup

The need for precise and often complex setups increases the difficulty and time required for testing, impacting efficiency and consistency [106].

I.7.3.4. Other approaches for evaluating the tensile strength of concrete

1. The Seesaw method

In this study, a novel method for evaluating the tensile strength of concrete was introduced using a seesaw device [107], as depicted in the test setup shown in Figure I.20. Concrete specimens with internal holes of specific dimensions were designed to facilitate the tensile tests (Figure I.21). The load was applied using a universal compression loading machine at a controlled rate of 0.02 MPa/s.

Figure I.20: The proposed test setup [107].

Figure I.21: Fabricated specimen [107].

The experimental results showed that the tensile strength values obtained from the seesaw method were approximately 25% lower compared to traditional splitting tests. Despite these lower values, the seesaw device demonstrated consistent and repeatable results with high accuracy. This consistency suggests that the seesaw method is a reliable alternative for measuring the tensile strength of concrete.

Complementing the experimental findings, two-dimensional finite element analysis was conducted using FRANC2D/L software. This analysis provided further insights into the stress distribution and failure mechanisms within the concrete specimens. As illustrated in Figure I.22, the numerical model revealed stress concentrations around the sides of the internal hole, with tensile stress concentration increasing as the hole diameter increased. Additionally, tensile cracks were observed to initiate and propagate along the horizontal plane experiencing maximum tensile stress.
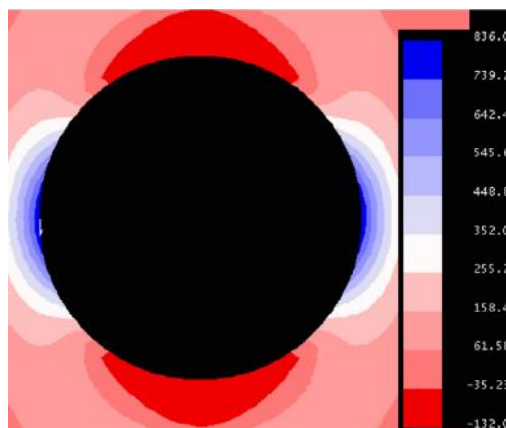
Figure I.22: Stress distribution in the concrete sample [107].

2. The Strut-and-Tie Methodology by Liao et al

The proposed method in this study is based on the strut-and-tie methodology as a novel approach for evaluating the tensile strength of concrete [93]. This method offers several advantages over traditional methods. It does not require special molds for casting the specimen, making preparation and handling easier. As shown in Figure I.23, the same loading equipment and testing setup used in flexural tests can be utilized, simplifying the process.

(a) (b)
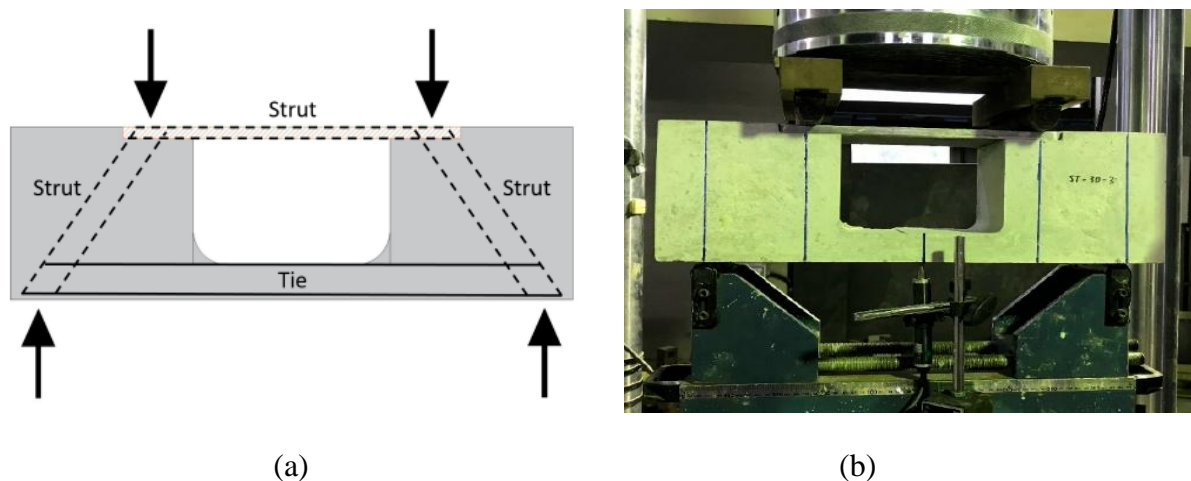
Figure I.23: The strut-and-tie method: a) force mechanism; b) test setup [93].

The study found that the optimal width of the opening in the strut-and-tie beam is 175 mm, ensuring uniform distribution of tensile stresses on both the upper and lower surfaces of the concrete tie member. The thickness of the tie member was set at 30 mm, based on the maximum size of aggregate used in the concrete. The geometry of the strut-and-tie beam specimen is shown in Figure I.24. The results indicate that this method has a high level of accuracy, with findings very close to those obtained from direct tension tests, showing only about a 9% variation. Additionally, the variation in test results using the strut-and-tie method is significantly lower than indirect tensile methods, with the variation in tensile test results about 40% and 70% in the splitting tensile test and flexural test, respectively.
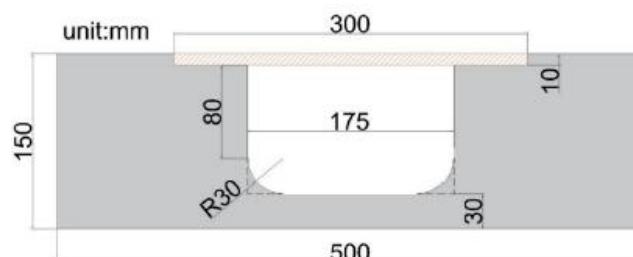
Figure I.24: The geometry of the proposed strut-and-tie beam [93].

3. A novel Strut-and-Tie Method by Sa'ad Fahad Resan et al

In the study "New approach of concrete tensile strength test" by Sa'ad Fahad Resan et al., a novel method for testing the tensile strength of concrete is introduced [108]. This approach addresses the limitations of traditional methods, which often face challenges such as load eccentricity, non-uniform stress or strain, and stress concentration at the specimen ends. The proposed model transforms the biaxial stress state into a controlled loading alignment and specific gauge length, resulting in a pure tensile stress state similar to a strut-tie model. The test setup and the failure mode of specimens using the proposed method are shown in Figure I.25 and Figure I.26.
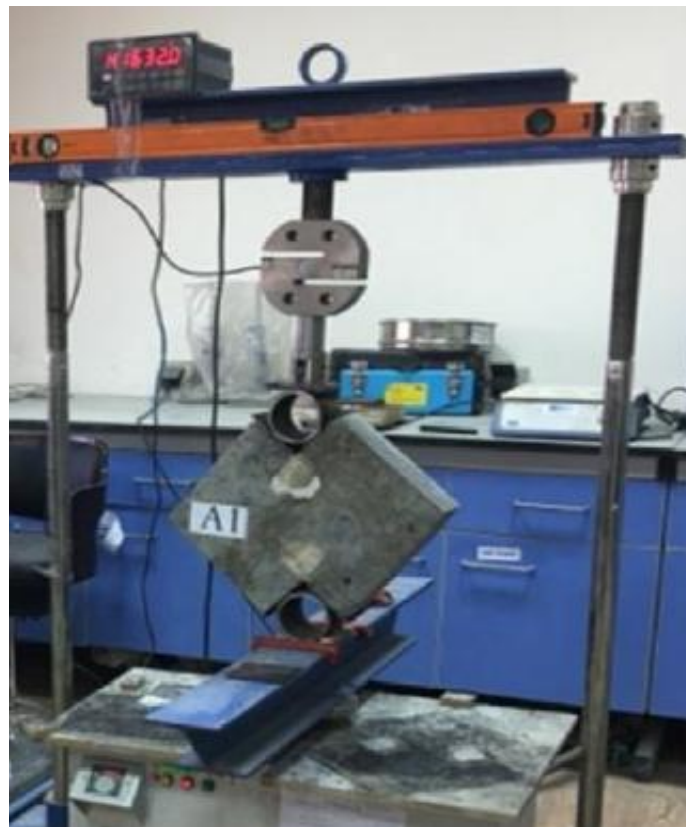
Figure I.25: Test setting of the proposed approach [108].

Figure I.26: Typical failure mode [108].

The experimental program conducted involved manufacturing and testing concrete specimens with different aggregate sizes and curing ages. The results showed that the tensile strength determined by the new method was higher than that of the Brazilian test (with f_t/f_s ratios ranging from 1.06 to 1.64) and lower than that of the flexural test (with f_t/f_r ratios ranging from 0.56 to 0.92). The new method demonstrated less variation in results compared to the Brazilian test. Additionally, this method simplifies the determination of the tensile stress-strain curve and mitigates the drawbacks associated with traditional tensile testing methods.

I.8. Tensile strength relationships

At present, there is no established standard test method for measuring the direct tensile strength of concrete. Indications of tensile strength are achieved through the splitting and flexural test methods. It is known that splitting tensile and flexural strength are different from direct tension samples, and the results obtained from indirect tensile test methods are particular only to the employed method which cannot be used interchangeably. For example, the failure in flexural tests is controlled by the strength of the outermost fiber of the beam. By contrast, the splitting tension test failure can be initiated anywhere in the portion of the diametrical plane that is in tension. Consequently, the tensile strength of concrete was found to be extremely sensitive to many parameters such as the size and shape of the specimens, the testing techniques used, and so on.

According to previous research results [88,109–111], it was found that the splitting tensile strength of concrete is generally 35–50% lower than the flexural tensile strength, whereas it is 5–12% greater than the direct tensile strength.

Due to the simplicity of conducting compressive strength tests, empirical correlation equations have been developed to estimate the tensile strength from the compressive strength [112–114]. Raphael [62] examined a large number of tensile strength results taken from different tensile test methods and concluded that both the direct tensile and splitting tensile strengths are about 10% of the corresponding compressive strength, while the flexural strength is about 15% of the compressive strength.

It has been noted that the compressive and tensile strengths are closely related. However, this relationship is influenced by many factors, including the type of tension test, testing age, curing conditions, concrete strength grade, and coarse aggregate properties [10]. Different empirical relations between compressive strength and tensile strength measured by different tension testing methods are discussed in the literature [10,115–120].

The empirical formula relating tensile strength to compressive strength, as suggested by researchers (see Table I.2), is as follows:

$$f_t = k(f_c)^n \tag{5}$$

Where:

f_t: the tensile strength, in Mpa;

f_c: the compressive strength of concrete cylinder, in Mpa;

k, n: regression coefficients.

Different values of the experimental coefficients (k) and (n) were recommended by various researchers, as shown in Table I.2.

Table I.2: Values of the proposed experimental coefficients (k) and (n).

Source	Tensile test method	k	n
Ahmad and Sahah [121]	Flexural strength	0.44	0.50
Xu and Shi [122]	Flexural strength	0.39	0.59
Perumal [123]	Flexural strength	0.259	0.843
Abbas et al [124]	Flexural strength	0.25	0.81
Oluokun [125]	Splitting tension	0.294	0.69
Nihal [126]	Splitting tension	0.387	0.63
Ahmad and Sahah [121]	Splitting tension	0.462	0.55
Choi and Yuan [114]	Splitting tension	0.60	0.50
Xu and Shi [122]	Splitting tension	0.21	0.83
Perumal [123]	Splitting tension	0.188	0.84
Abbas et al [124]	Splitting tension	0.508	0.498
Gardner [127]	Splitting tension	0.47	0.59
Raphael [62]	Splitting tension	0.313	0.667
Zheng [88]	Direct tension	0.47	0.50
Philips [128]	Direct tension	0.45	0.50
Lin [95]	Direct tension	0.52	0.50
Kim [103]	Direct tension	0.34	0.50
Li [129]	Direct tension	0.34	0.50

Furthermore, various regulations have proposed empirical equations for estimating tensile strength based on compressive strength. The following equations, determined by CEB-FIP MC-90 [130], are based on the assumption that tensile strength has a linear relationship with the two-thirds (2/3) power of the corresponding compressive strength, as follows:

$$f_{t,min} = 0.95 \left(\frac{f_c}{10}\right)^{2/3} \tag{6}$$

$$f_{t,max} = 1.85 \left(\frac{f_c}{10}\right)^{2/3} \tag{7}$$

Where:

$f_{t,min}$ and $f_{t,max}$: the upper and lower values of the characteristic tensile strength, in MPa.

f_c: the characteristic compressive strength, in MPa.

The mean value of the tensile strength is given by the relationship:

$$f_{t,mean} = 1.40 \left(\frac{f_c}{10}\right)^{2/3} \tag{8}$$

According to the American Concrete Institute (ACI-318) [131], the tensile strength of concrete is proportional to the square root of its compressive strength, and is expressed as follows:

$$f_t = 0.56\sqrt{f_c} \tag{9}$$

Recent researches suggest that the coefficients in ACI 318-2014 [132] depend on the general level of the compressive strength, overestimating the tensile strength for low-strength concrete and underestimating it for high-strength concrete [133]. Additionally, research findings indicate that the ratio of tensile strength to compressive strength in concrete is not constant; instead, it decreases as the compressive strength of the concrete increases [125,134–136]. Consequently, the 0.5 power relation used in ACI 318-2014 does not align well with the test results.

Other regulations have suggested different relationships for estimating the tensile strength based on compressive strength. Equations 10 and 11 show the tensile strength according to BAEL91 modified 99 [137] and Eurocode 2 [138] standards, respectively.

$$f_{tj} = 0.6 + 0.06 f_{cj} \tag{10}$$

$$f_{ctm} = 0.30\, f_{ck}^{\left(\frac{2}{3}\right)} \; (Strength\ classes\ \leq C50/60) \tag{11}$$

With:

f_{tj} and f_{ctm}: the average tensile strength, in MPa;

f_{cj} and f_{ck}: the average compressive strength, in MPa.

I.9.   Conclusion

In conclusion, this chapter has highlighted the importance of understanding the different strength properties of concrete and the factors affecting them. The discussion on the behavior of concrete under various stress states, including uniaxial compression, uniaxial tension, and shear stress, provides a comprehensive overview of how concrete responds to different loading conditions. The chapter also emphasizes the need for accurate testing methods to determine the tensile strength of concrete and how these methods can impact the observed results.

Chapter II

Development and Analysis of a Tensile Testing Device

Chapter II: Development and Analysis of a Tensile Testing Device

II.1. Introduction

This chapter focuses on the design and development of a mechanical device for conducting direct tensile tests on cylindrical concrete specimens. Key design considerations include ensuring device rigidity and developing effective specimen gripping mechanisms. Through detailed analysis and validation, this study aims to enhance the capability to evaluate tensile properties in modern cementitious materials.

II.2. Design

II.2.1. Design requirements

Direct tensile tests on concrete are less common compared to compression or flexural tests. However, in certain situations, direct tensile tests are essential to evaluate specific properties of concrete or for applications where assessing the tensile strength is crucial to ensure the serviceability and durability of structures.

It is essential to highlight that the development of innovative cementitious materials through the addition of fibers, has significantly increased interest in tensile testing. This trend has emerged in response to the quest for innovative solutions offering enhanced strength and durability across a range of applications. Consequently, there has been a need to design testing devices specifically adapted to these new materials, capable of providing precise and reliable measurements of their tensile properties, such as the tensile stress-strain behavior, post-peak response, tensile modulus of elasticity, and tensile strength.

To address this need and optimize the use of existing equipment, we have developed a mechanical device that can be inserted into the universal compression testing machine (Annexe 1) [139]. This device converts the compressive force of the press into a tensile force on the specimen. The primary technological challenges that must be overcome include:

- The limited distance between the plates of the compression loading machine, which is 350 mm;
- The length of the standardized specimen to be inserted into the device, which is not less than 200 mm;

-   The rigidity of the device to ensure that its deformation under compression remains negligible compared to that of the specimen;
-   Selecting an effective method for gripping the specimen within the device.

II.2.2. Design concept

The present testing device is an innovative test tool designed for measuring the direct tensile strength of cylindrical concrete specimens. The primary design requirement of the device is to transform the load applied by the universal compression testing machine into a tensile load on the concrete samples. The obvious advantage of the developed device is that the compression machine can be used for load application, which is practically available in all civil engineering laboratories worldwide.

II.2.3. Design Summary

To overcome the abovementioned challenges, we developed a testing device based on our Conventional Compressive Testing Machine UTEST (see Annexe 2). The sketch of the device is shown in Figure II.1.
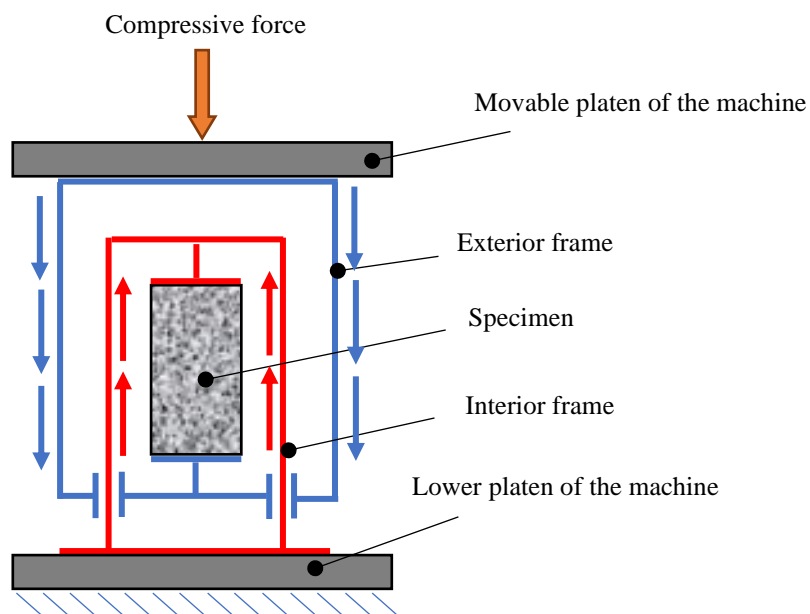
Figure II.1: Sketch describing the kinematics of the device.

The device consists of two rigid frames, one exterior and another one interior, which can slide relative to each other in an opposite direction under a compressive load (see Figure II.1). A compressive force on the two frames generates an inverse force (tension) on the specimen, which

is fixed to the jaws. Specific parts, such as the jaws, guiding axes, and the upper and lower steel plates of the frames, were constructed from hardened steel and machined using numerical control. Standard parts, such as screws and nuts, were commercially purchased. The total height of the device (upper frame and lower frame) must be less than 350 mm.

II.2.4. Detail design

II.2.4.1. Guiding axes dimensions

To ensure sufficient rigidity of the device frames, each frame must withstand a compressive force ten times greater than that applied to the specimen. Assuming the cylindrical specimens with a diameter D_{sp} must withstand a maximum tensile stress σ_t^{max}, the force that the frame must withstand is:

$$F_{frame} = 10\left(\sigma_t^{max}.\frac{\pi D_{sp}^2}{4}\right)$$

With: $\sigma_{sp}^{max} = 5\ MPa$; $D_{sp} = 100\ mm$;

We have: $\boldsymbol{F_{frame} = 393\ kN}$
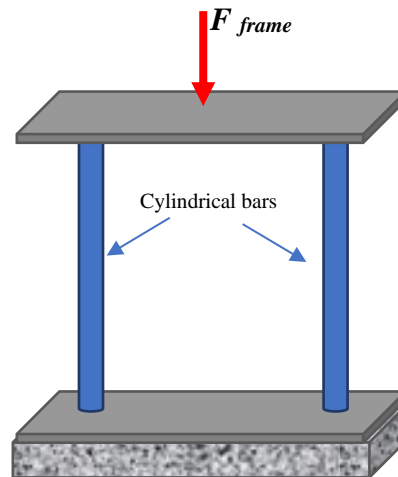
Figure II.2: Outer frame of the device.

The frame elements that need to withstand this force are two cylindrical bars made of construction steel (Figure II.2), with a yield strength of $\sigma_e = 300 MPa$.

Each bar must withstand a force of:

$$\frac{F_{frame}}{2} = \sigma_e . \frac{\pi d_b^2}{4}$$

Where:

d_b: The diameter of the cylindrical bars of the two frames (inner and outer).

This gives the minimum diameter for each bar as:

$$d_b^{min} = \sqrt{2 \frac{F_{frame}}{\pi \sigma_e}} = 28.9 \; mm$$

For our device, we have included an additional safety margin with a bar diameter equal to:

$$d_b = 32 \; mm$$

With this bar diameter of 32 mm, the frame can withstand a maximum compressive force of:

$$F_{frame}^{max} = 2 \left(\sigma_e \frac{\pi d_b^2}{4} \right) = 482.6 \; kN$$

Considering a maximum service load half lower:

$$F_{frame}^{ser} = 241.3 kN$$

The maximum tensile stress in the specimen is :

$$\sigma_t^{max} = \frac{4 \; F_{frame}^{ser}}{\pi d_{sp}^2} = 30.7 \; MPa$$

II.2.4.2. Displacement and deformation analysis

The mechanical properties of the material constituting the frame are illustrated in Table II.1:

Table II.1: Mechanical properties of construction Steel C35E.

Characteristics	Construction Steel C35E
Density (Kg/m³)	7850
Young's Modulus E (MPa)	2.0×10^5
Poisson's Ratio	0.3
Yield Strength (MPa)	300

For the displacement of the frame ends, considering a total height of the frame of 300mm ($H_{frame} = 300\ mm$), and assuming the frame consists of a cylindrical bar with stiffness:

$$k_{frame} = \frac{E_s . A_{frame}}{H_{frame}}$$

Where:

E_s: The Young's modulus of the material constituting the frame;

A_{frame}: The total cross-sectional area of the two lateral cylindrical bars.

In this case, the maximum displacement of the frame under the maximum service load is:

$$u_{frame}^{max} = \frac{F_{frame}^{ser}}{k_{frame}} = \frac{F_{frame}^{ser} . H_{frame}}{E_s . A_{frame}} = 0.450\ mm$$

With a maximum longitudinal deformation of the frame of:

$$\varepsilon_{frame}^{max} = \frac{u_{frame}^{max}}{H_{frame}} = 0.150\%$$

The two frames are arranged in series, and their equivalent stiffness is:

$$k_{eq} = k_{frame}/2$$

This allows for the calculation of the total displacement of the device under the compressive force of the compression loading machine:

$$u_{disp}^{max} = 2\frac{F_{frame}^{ser}}{k_{frame}} = 2\frac{F_{frame}^{ser} . H_{frame}}{E_s . A_{frame}} = 0.900\ mm$$

The displacement of the specimen with a material having Young's modulus of $E_{sp} = 32 . 10^3\ MPa$ is:

$$u_{sp}^{max} = \frac{F_{frame}^{ser}}{k_{sp}} = \frac{F_{frame}^{ser} . H_{sp}}{E_{sp} . A_{sp}} = 0.192\ mm$$

With a maximum longitudinal deformation of the specimen of:

$$\varepsilon_{sp}^{max} = \frac{u_{sp}^{max}}{H_{sp}} = 0.096\%$$

This deformation value is sufficient to cause tensile failure in cementitious materials with an ultimate stress lower than 25 MPa.

II.3. Verification of the rigidity of the device by numerical simulation

To verify the preliminary analytical calculations, the design elements (device components – specimen) were analyzed with a finite element modeling software using the commercial software ANSYS®. The entire assembly, including the frame and specimen, was fixed at the lower base while a progressive displacement was applied to the upper part. The applied displacement was set to 20% of the maximum displacement tolerated by the device, which is sufficient to produce tensile stress in the specimen exceeding 6.8 MPa.

The specimen is assumed to be fully attached to the jaws, which significantly simplifies the simulation aimed at validating the rigidity of the frames. Figure II.3 provides a perspective view of the designed device with the mounted specimen. Assembly screws are omitted from the illustration to maintain clarity.
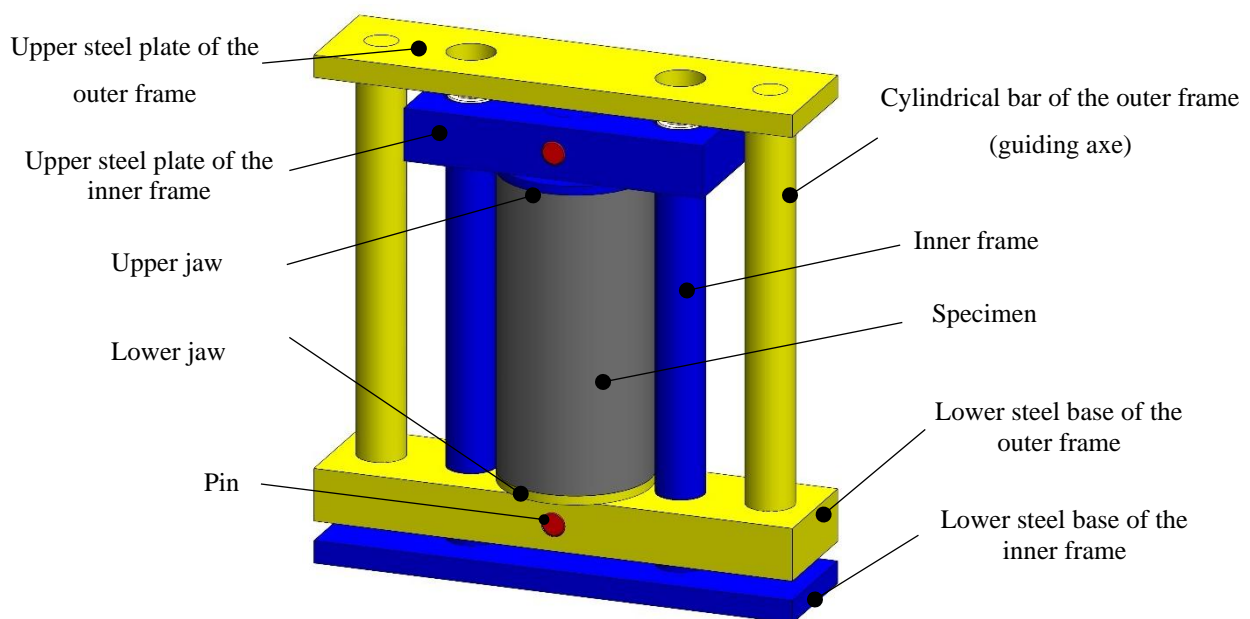
Figure II.3: Perspective view of the device with mounted specimen.

Figure II.4 illustrates the mesh used in the finite element analysis. We employed a combination of tetrahedral and hexahedral elements with a finite element size of 4 mm, resulting in 142064 elements and 380811 nodes. A contact condition, with a low friction coefficient, was

implemented between the cylindrical bars (guiding axes) of the inner frame and the guide holes in the steel plate of the outer frame.
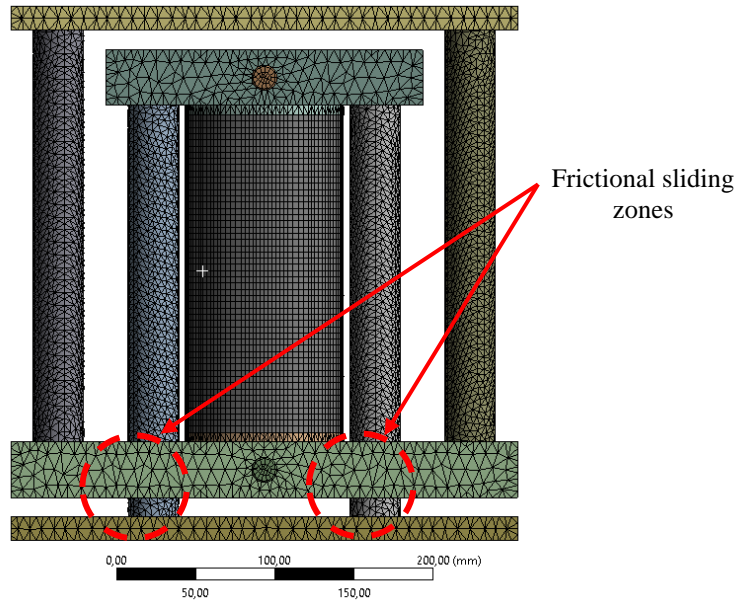
Figure II.4: Representation of the device after meshing.

The output of the analysis is displayed in Table II.2 and depicted in Figure II.5 and Figure II.6.

Table II.2: Simulation results obtained from Ansys analysis.

Analysis results	Device	Specimen
Maximum Equivalent Stress (MPa)	33.9	6.62
Maximum Equivalent Strain (%)	0.0171	0.022
Maximum Displacement in the loading direction (mm)	0.050	0.136×10^{-2}
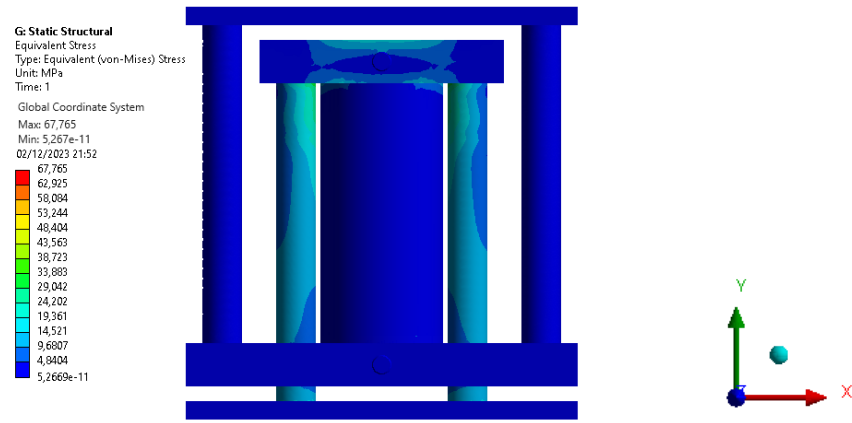
(a)
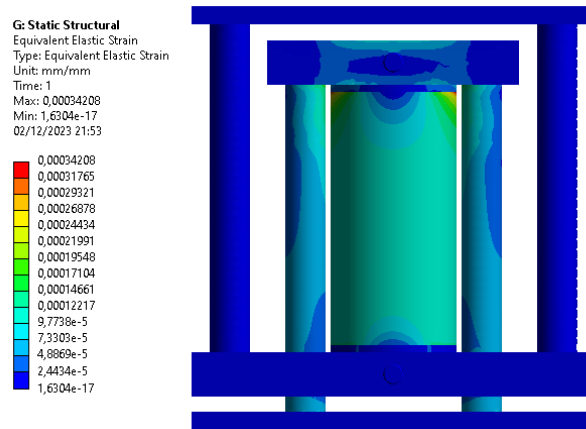
(b)
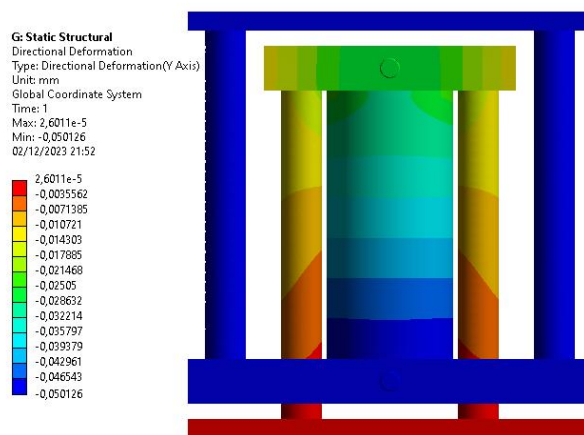
(c)

Figure II.5: Stress and strain distribution in the device: a) Equivalent Von-Mises Stress in MPa; b) Equivalent strain in mm/mm; c) Displacement in the loading direction.
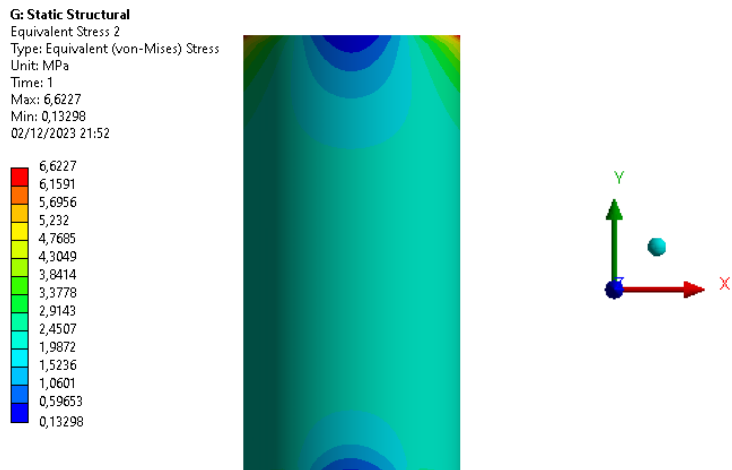
(a)
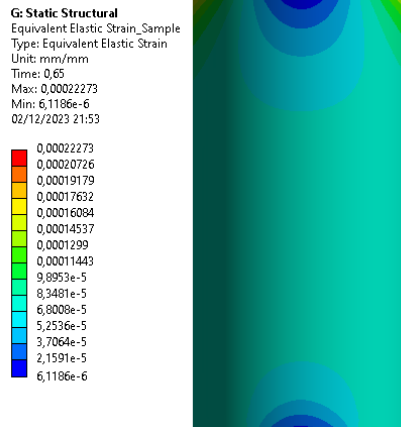
(b)
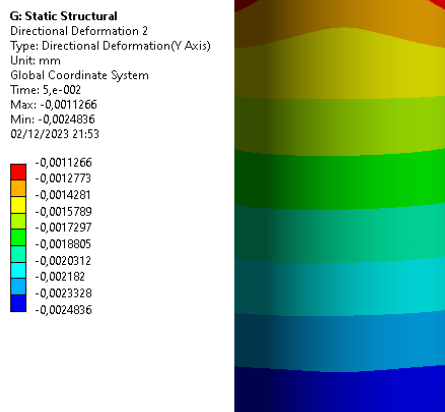
(c)

Figure II.6: Stress and deformation distribution in the specimen: a) Equivalent Von-Mises stress in MPa; b) Equivalent strain in mm/mm; c) Displacement in the loading direction.

II.4. Assembly of the testing device

The design of the device was performed using the commercial software SolidWorks® 2018. Detailed drawings are provided in the Annexe 3. The frames are assembled using four screws, allowing for a modular and adjustable setup according to needs. The main characteristics of the device are given below:
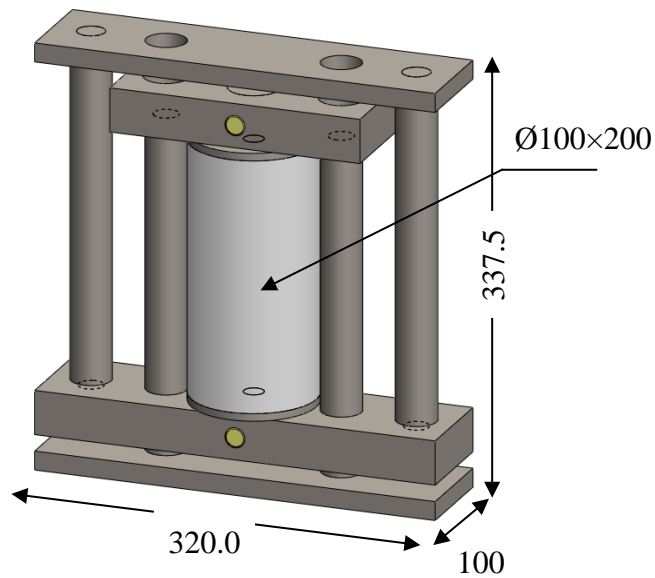
Figure II.7: Schematic view of the designed device.

- **Dimensions**:
    - Height: 337.5 mm;
    - Length: 320.0 mm;
    - Width: 100.0 mm;
- **Weight**: 24.54 kg (28.14 kg with specimen).
- **Materials**: Construction steel (XC35).
- **Maximum supported load**: 240 kN.
- **Specimen size**:
    - Length: 200 mm;
    - Diameter 100 mm.

II.5. The adopted methods for clamping the specimen to the device

To attach the specimen to the jaws of the device, two gripping methods were considered. The first involved using epoxy adhesive, while the second used embedded steel bars. Unfortunately, the use of epoxy did not yield the desired results, as failure consistently occurred at the interface between the adhesive and the specimen (detailed insights are provided in Chapter III). As for the second method, we proposed and tested three types of grips. For two of them, we observed a high concentration of stresses at the end of the embedded grips, resulting in failure at those points rather than in the middle of the specimen, as intended. Below, we present the results of numerical simulations conducted for these proposed grips.

II.5.1. Welded threaded steel rod grips

This type of grip involves using a steel threaded rod, 16 mm in diameter and 50 mm long, secured to the jaw by threading, onto which three rods of 5 mm in diameter and approximately 30 mm long are welded (Figure II.8).

Figure II.8: Welded threaded steel rod grips.

For the numerical simulation, only half of the specimen was considered, and a stress of 3.5 MPa was applied to the upper face of the jaw.

Figure II.9 illustrates the distribution of equivalent stress in the specimen. The red areas indicate locations with a high-stress concentration.

(a)   (b)
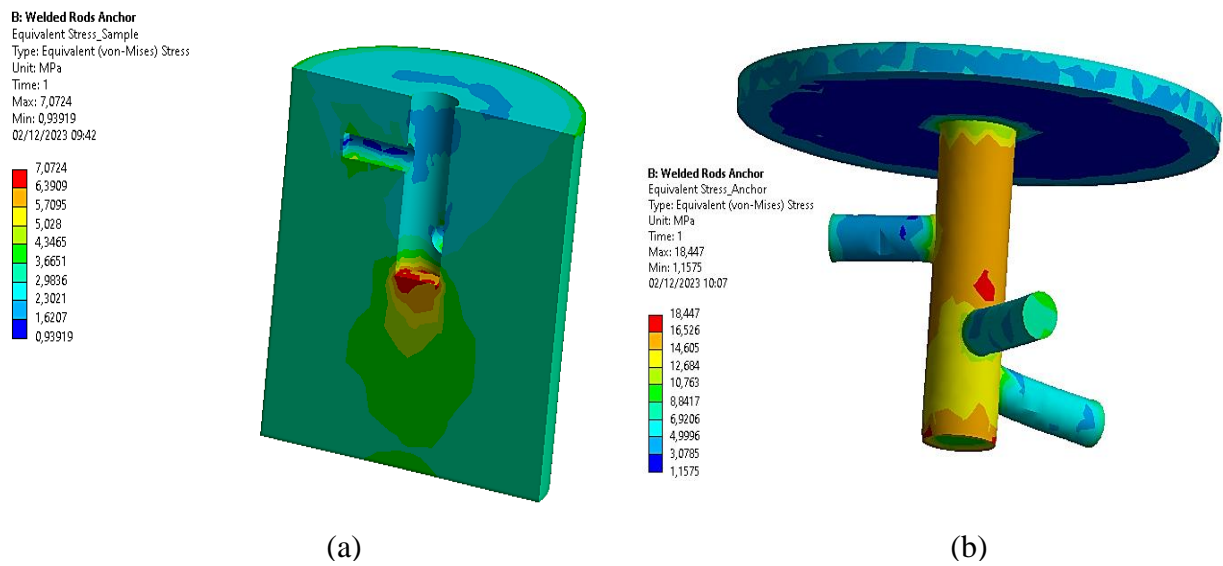
Figure II.9: Distribution of equivalent stress: a) in the specimen, b) and in the welded steel rod grip.

II.5.2. Threaded steel rod grip with nuts

This type of grip involves using a threaded steel rod, 16 mm in diameter and 50 mm long, screwed into the jaw, onto which three nuts are mounted (Figure II.10).
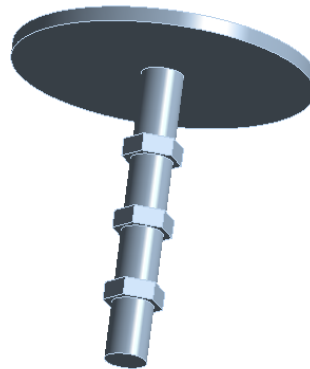
Figure II.10: Threaded steel rod grip with nuts.

For the numerical simulation, we considered only half of the specimen and applied a stress of 3.5 MPa to the upper face of the jaw. Figure II.11 illustrates the distribution of equivalent stress within the assembly (specimen and grip). The red areas indicate locations with high-stress concentration.

(a)   (b)
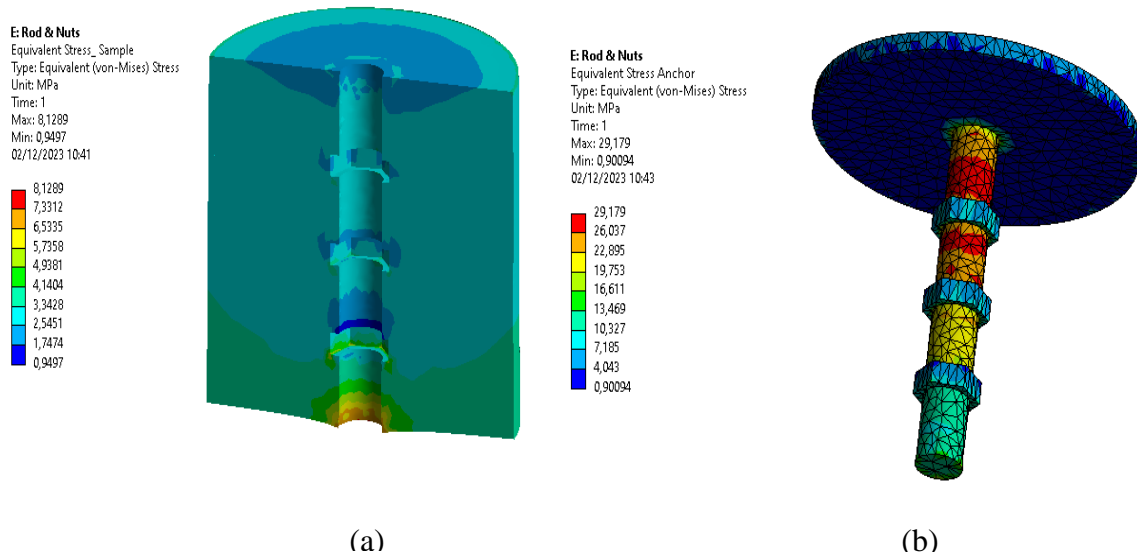
Figure II.11: Distribution of equivalent stress: a) in the specimen, b) and in the proposed gripping method.

II.5.3. Threaded steel rod grip

This type of grip involves using a threaded steel rod secured to the jaw, 16 mm in diameter and 110 mm long (Figure II.12). For the numerical simulation, we considered only half of the specimen and applied a stress of 3.5 MPa to the upper face of the jaw.

Figure II.12: Threaded steel rod grip.

Figure II.13 illustrates the distribution of equivalent stress within the specimen and at the grip. The red areas indicate locations with high-stress concentration.

It should be noted that this type of grip was selected for the experimental study because it exhibits a concentrated stress zone located specifically in the middle of the specimen.

<div align="center">(a)   (b)</div>
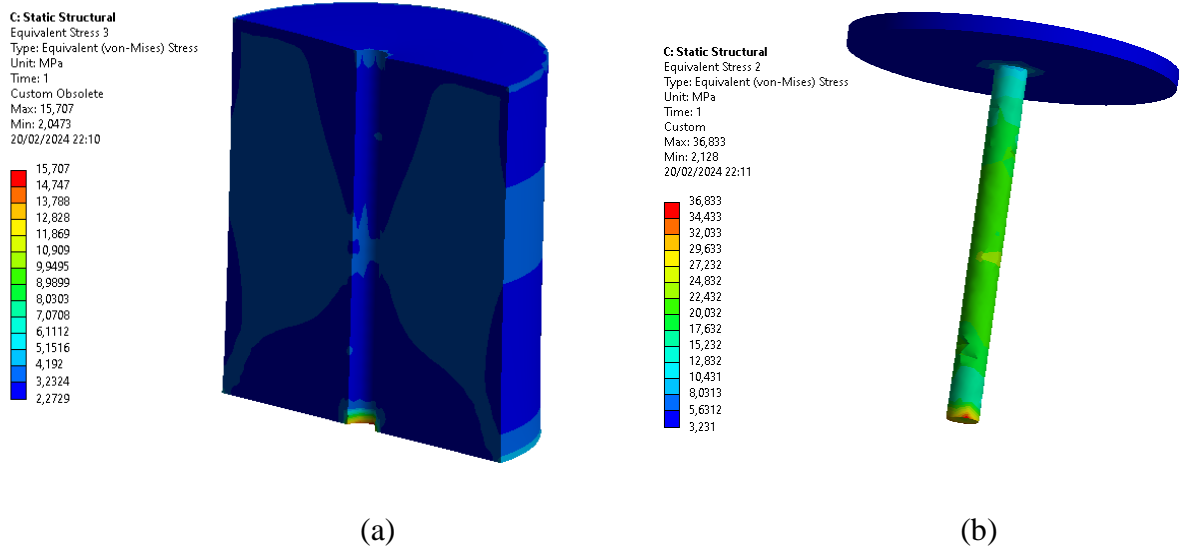
Figure II.13: Distribution of equivalent stress: a) in the specimen, b) and in the long-threaded rod grip.

II.6. Conclusion

This chapter detailed the design, development, and validation of a testing device for direct tensile tests of concrete specimens. Through rigorous analytical calculations and finite element simulations using ANSYS®, the capability of the device to convert compressive loads from a universal compression testing machine into tensile forces on the specimen was thoroughly validated. Further experimental studies will focus on evaluating the effectiveness of the testing device and the proposed gripping methods.

Chapter III

Experimental Procedure for Assessing the Proposed Testing Device

Chapter III: Experimental Procedure for Assessing the Proposed Testing Device

III.1. Introduction

This chapter presents an experimental program to evaluate the reliability of a new testing device using various gripping methods for direct tensile testing. The experimental work investigates three standardized test methods to validate and compared the results obtained: compressive strength test, flexural test, and splitting tensile test, using three types of concrete: Ordinary Concrete (OC) with a target compressive strength of 25 MPa, Self-Compacting Concrete (SCC), and Steel Fiber Reinforced Concrete (SFRC).

III.2. Materials

- **Cement**

Ordinary Portland cement type II (CEM II/B 42.5N) produced at the Lafarge cement plant (Wilaya of M'sila, Algeria) was employed in the present study to prepare the concrete mixes, which complied with standard EN197-1

- **Fine aggregate**

Natural sand having a maximum size of 4 mm was employed as fine aggregate.

- **Coarse aggregate**

Two classes of natural coarse aggregates (gravel 3-8 mm, gravel 8-16 mm) were used. The physical properties of the aggregates used are given in Table III.1.

Table III.1: Physical characteristics of aggregates.

Characteristics	Sand	Gravel 3/8	Gravel 8/16
Absolute density (g/cm^3)	2.66	2.62	2.66
Apparent density (g/cm^3)	1.44	1.21	1.32
Sand equivalent (%)	80	-	-
Fineness modulus	2.25	-	-

- **Steel fibers**

The hooked ended steel fibers were used for the steel fiber reinforced concrete (SFRC). The steel fiber was 50 mm long and 0.62 mm in diameter with a maximum tensile strength of 1270 MPa. The mechanical and physical properties of the steel fibers used are summarized in Table III.2 and shown in Figure III.1.

Table III.2: Mechanical properties of fibers used.

Type of fiber	Diameter d (mm)	Length L (mm)	Aspect ratio (L/d)	Density	Tensile strength (MPa)	Elastic Modulus (GPa)
Steel Fiber	0.62	50	80.64	7.8	1270	200
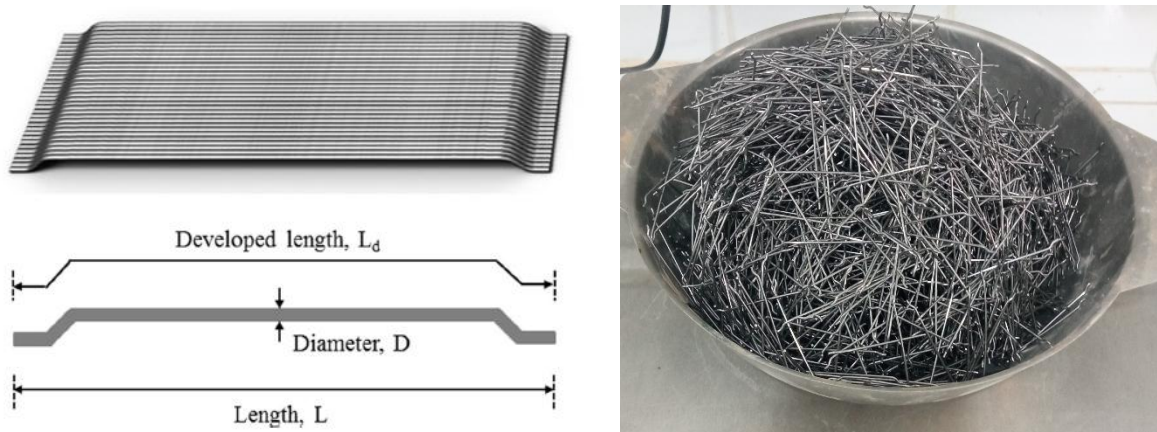
Figure III.1: Physical appearance of fibers.

- **Admixture**

The superplasticizer Medaflow 30 manufactured by Granitex-NP, was used in the self-compacting concrete (SCC) mixture as a high range water reducing agent.

- **Water**

Potable water was used in the mix design, which was also used for curing.

III.3. Mixture compositions

III.3.1. Ordinary concrete

The "Dreux-Gorisse" formulation method was used for the concrete composition [140]. The targeted concrete has a compressive strength of 25 MPa with a slump of 8 cm which gives a plastic concrete. The mix proportions of the ordinary concrete designed for this study are given in Table III.3.

Table III.3: Mix proportions of the ordinary concrete.

Material	Quantity
Cement	350 kg/m^3
Sand	526 kg/m^3
Gravel 3/8	269 kg/m^3
Gravel 8/16	1016 kg/m^3
Water	175 kg/m^3
Water/cement ratio	0.5

III.3.2. Self-compacting concrete

The general method suggested by Okamura [141] was adopted to formulate the SCC mixture. The mix proportions are presented in Table III.4. The results of the fresh property tests, including slump flow, V-funnel, segregation resistance, and L-box tests, are depicted in the Figure III.2 and summarized in the Table III.5.

Table III.4: Mix proportions of the self-compacting concrete.

Material	Quantity
Cement	519.23 kg/m^3
Sand	976.44 kg/m^3
Gravel 3/8	204.08 kg/m^3
Gravel 8/16	408.17 kg/m^3
Water	247.78 kg/m^3
Superplasticizer	5.71 kg/m^3

Table III.5: Fresh state properties of the SCC mix.

Slump flow (mm)	T_{500} (s)	V-funnel (s)	L-Box (%)	Sieve stability (%)
755	1.56	5.04	0.8	6.74

(a)

(b)

(c)

(d)

Figure III.2: Methods for assessing the fresh properties of the SCC mixture: (a) Slump flow test; (b) V-funnel test; (c) Segregation resistance; (d) L-box test.

III.3.3. Steel fiber reinforced concrete

To investigate the tensile strength of steel fiber reinforced concrete (SFRC) using the proposed test method, four different steel fiber volume fractions were added to a reference ordinary concrete mix: 0.5%, 0.75%, 1.25%, and 1.5%, corresponding to 39 kg, 58.5 kg, 97.5 kg, and 117 kg of steel fibers per cubic meter of concrete, respectively. The workability of both the ordinary and SFRC mixes was evaluated using the standard slump test, with slump values ranging between 70 and 90 mm. The mix proportions for the concrete mixes are presented in Table III.6 .

Table III.6: Mix proportions of the steel fiber reinforced concrete.

Concrete type	Cement (kg/m^3)	Sand (kg/m^3)	Gravel 3/8 (kg/m^3)	Gravel 8/16 (kg/m^3)	Water (kg/m^3)	Steel fiber (kg/m^3)	Fiber volume (%)
Mix-0	350	526	269	1016	175	0	0.00
Mix-0.5	350	526	269	1016	175	39	0.50
Mix-0.75	350	526	269	1016	175	58.5	0.75
Mix-1.25	350	526	269	1016	175	97.5	1.25
Mix-1.50	350	526	269	1016	175	117	1.50

III.4. Specimen preparation

A total of twelve specimens were cast and tested for each concrete mix and testing age. Nine cylindrical specimens (100 mm in diameter and 200 mm in height) were cast for compressive strength, splitting tensile strength, and direct tensile tests. Additionally, three prism specimens (70 mm × 70 mm in cross section and 280 mm in length) were cast for the flexural strength test. The samples were stored in the laboratory for 24 hours. Afterward, the specimens were demolded and placed in a water tank for curing until the testing day (Figure III.3). It should be noted that the specimen sizes were selected according to standard EN 206-1 [142] for compressive strength and splitting tensile tests, and EN 12390/1 [143] for flexural strength test.

(a)   (b)

(c)

Figure III.3: Specimen prepartion and curing condition: a) Fabricated specimens; b) Specimens after demolding; c) Specimens in water tank.

To successfully avoid the drawbacks that could occur during the direct tensile test by the specimens, such as misalignment, slippage, load eccentricity, and bending moments [7], a particular new mold was designed to prepare the specimens for the proposed direct tensile test (see Figure III.4). This mold consists of four separable parts, i.e., a supporting base, a supporting head, screwing rods, and a plastic mold. The diameter and height of the mold are 100 mm and 200 mm, respectively. The parts are connected through a pair of screwing rods (Annexe 4).
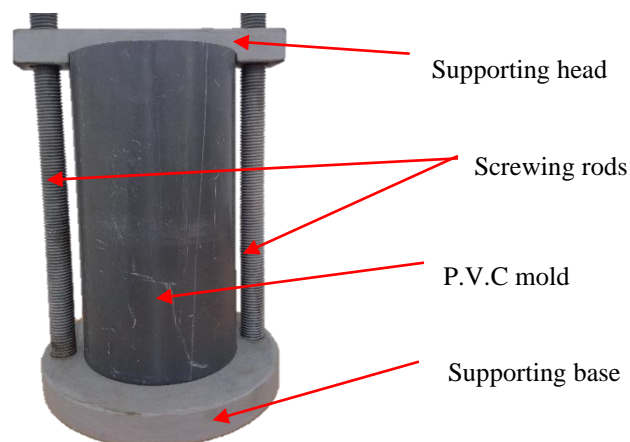
Figure III.4: Mold designed for the proposed direct tensile test setup.

As shown in the Figure III.5, to facilitate the alignment and centralization of the grips within the specimen, three holes were tapped in the middle and at the ends of the upper and lower steel parts of the mold. These tapped holes eliminated the need for washers and nuts to secure the grips. Then, a long-threaded rod (230 mm in length) was used, allowing for easy control of the alignment of the grips in the mold before casting.
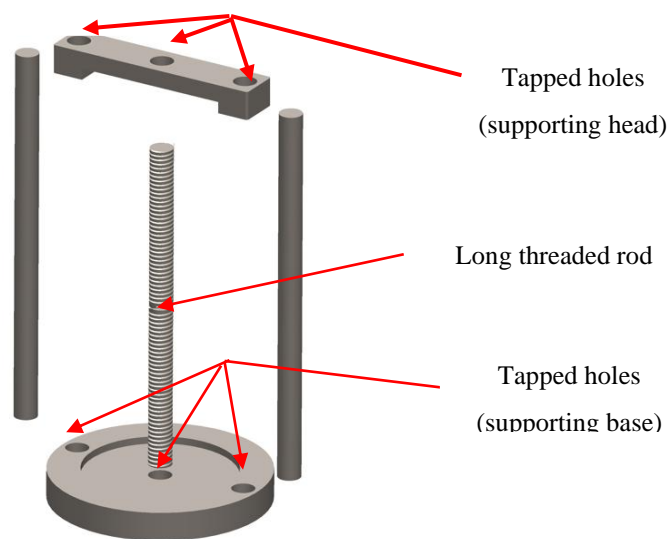
Figure III.5: The mold before adjustment.

Based on the numerical results for tensile stress distribution discussed in Chapter II, an experimental investigation was conducted using various direct tension test setups to grip the specimens. The setups included the use of epoxy adhesive (Annexe 6), welded threaded steel rod grips, threaded steel rod grips with nuts, and standard threaded steel rod grips (more details are shown in the Figure III.6).

(a)   (b)

(c)   (d)
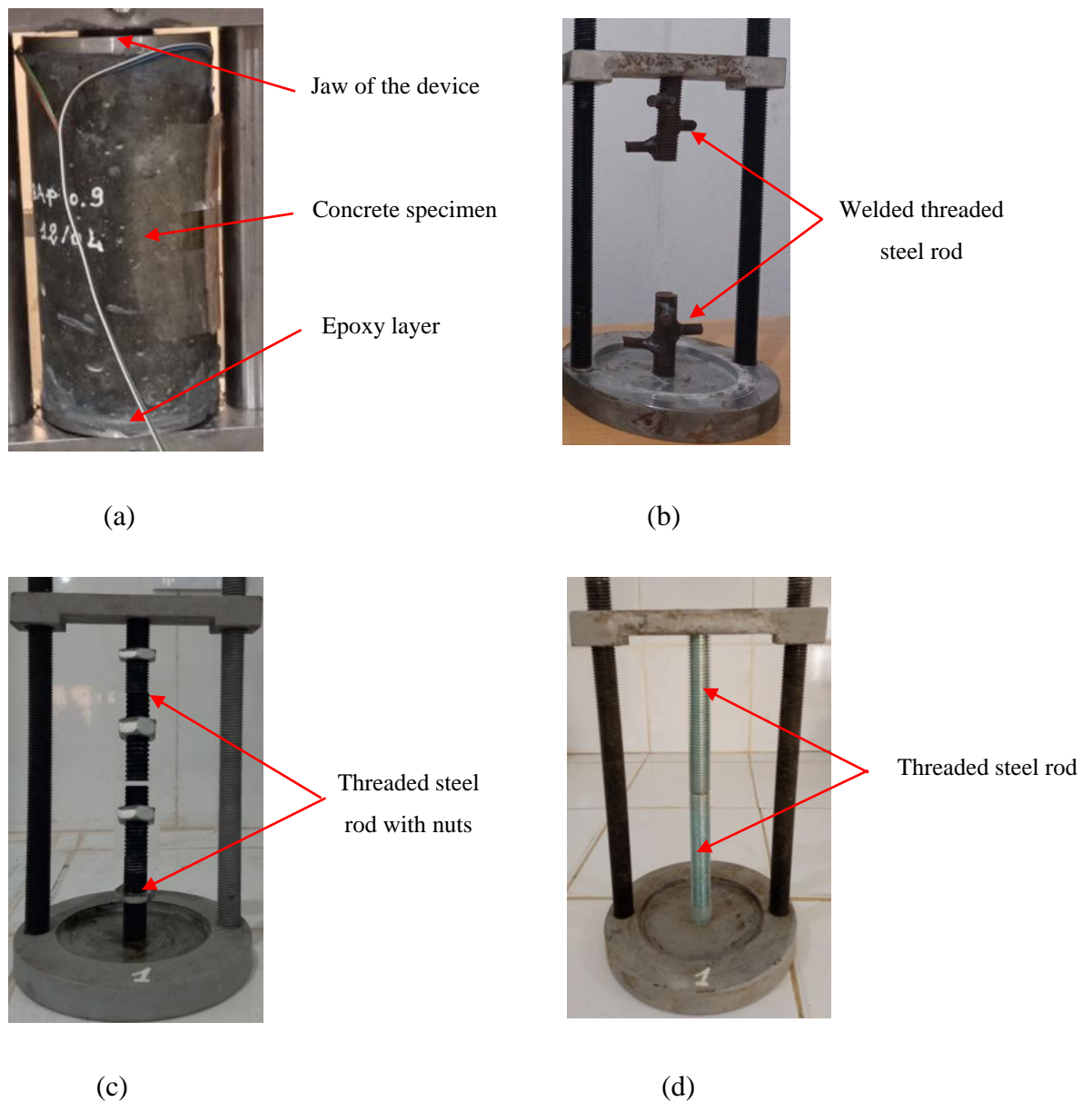
Figure III.6: Gripping methods used for the direct tensile test: (a) epoxy adhesive; (b) welded threaded steel rod grips; (c) threaded steel rod grips with nuts; (d) threaded steel rod grips.

III.5. Test procedure (testing methods)

III.5.1. Compressive strength test

The compressive strength of the concrete was determined according to EN 12390-3 [144] by testing three cylinders of 100 mm in diameter and 200 mm in height, for each concrete mix and testing age. The tests were conducted using a UTEST universal compression testing machine (Figure III.7) with a capacity of 2000 kN, applying the load at a constant rate as specified by EN standards.

Figure III.7: Compressive strength test.

III.5.2. Splitting tensile test

The tensile splitting strength tests were performed on cylinders of standard size (200 mm in length and 100 mm in diameter) in accordance with EN 12390-6 [145]. To ensure even distribution of the load along the entire length of the specimen, the specimen was aligned in the loading machine using the aligning jig shown in Figure III.8. The load was applied continuously and uniformly at a rate of 0.04 MPa/s until the specimen failed.

Figure III.8: Splitting tensile strength test.

III.5.3. Flexural tensile test

The flexural strength test (modulus of rupture) was conducted using the UTEST testing machine in accordance with EN 12390-5 [146]. For each concrete mix, three prism samples (70 mm × 70 mm in cross-section and 280 mm in length) were tested under three-point loading on a 210 mm span (Figure III.9). The loading rate was controlled at 0.04 MPa/s during the test.

Figure III.9: Flexural strength test**.**

III.5.4. Direct tensile test (proposed test method)

III.5.4.1. Technical details of the proposed device

The direct tensile strength of the concrete was determined using the device and testing method developed in this study. The testing device consists of two rigid frames (one exterior and one interior) made from hardened steel. These frames are designed to slide relative to each other in opposite directions under a compression load. The mechanism for load conversion and application to the concrete specimen is detailed in Chapter II. Each frame includes an upper rectangular steel plate, a lower rectangular steel base, and two parallel guiding axes.

The obvious advantage of the developed device is that the compression test machine can be used for load application, which is practically available in all civil engineering laboratories worldwide.

III.5.4.2. Device Assembly

Figure III.10 shows all the components of the device. Figure III.11 provides an exploded view of the device, illustrating the various parts of the assembly.

The following steps outline the procedure for setting up the testing device :

1. Insert the parallel guiding axes (part N°. 01) into the lower steel bases (part N°.02 and part N°.08) ensuring they are firmly fixed. These axes will guide the movement of the upper frame ;
2. Install the interior frame onto the exterior frame by aligning and connecting them using the guiding axes ;
3. Place the upper rectangular steel plates (part N°. 07 and part N°04) onto the guiding axes ;
4. Use the four screws (part N°. 05) to assemble all components together, securing the upper and lower frames in place ;
5. Install the pair of jaws (part N°. 03) in the inner frame. These jaws are designed to securely hold the concrete specimen through threaded steel rods embedded in both ends of the specimen ;
6. Use the pair of steel pins (part N°. 06) to attach the jaws to the steel bases of the device, ensuring the accurate positioning of the concrete specimen in the device.
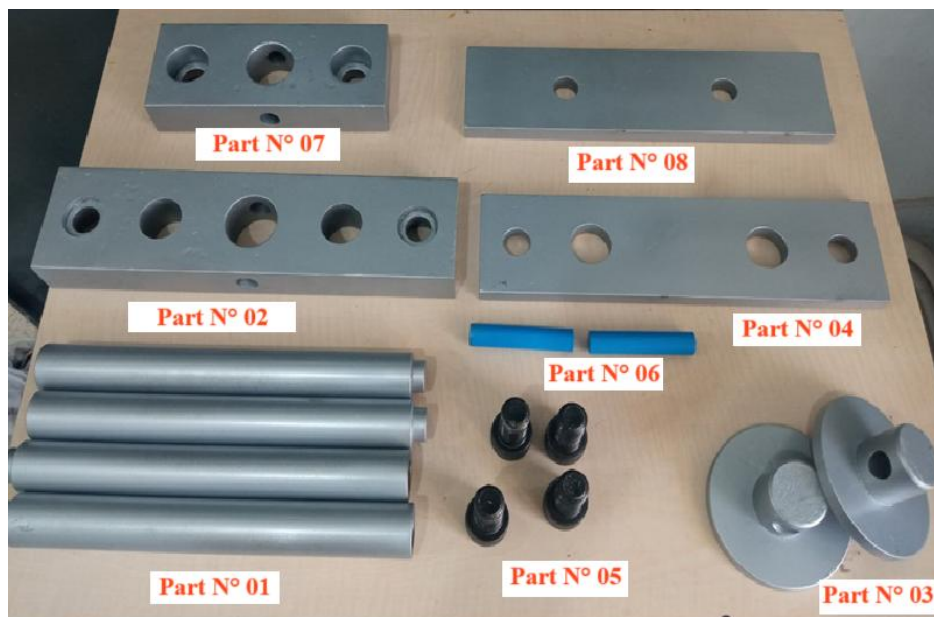
Figure III.10: Different components of the device.
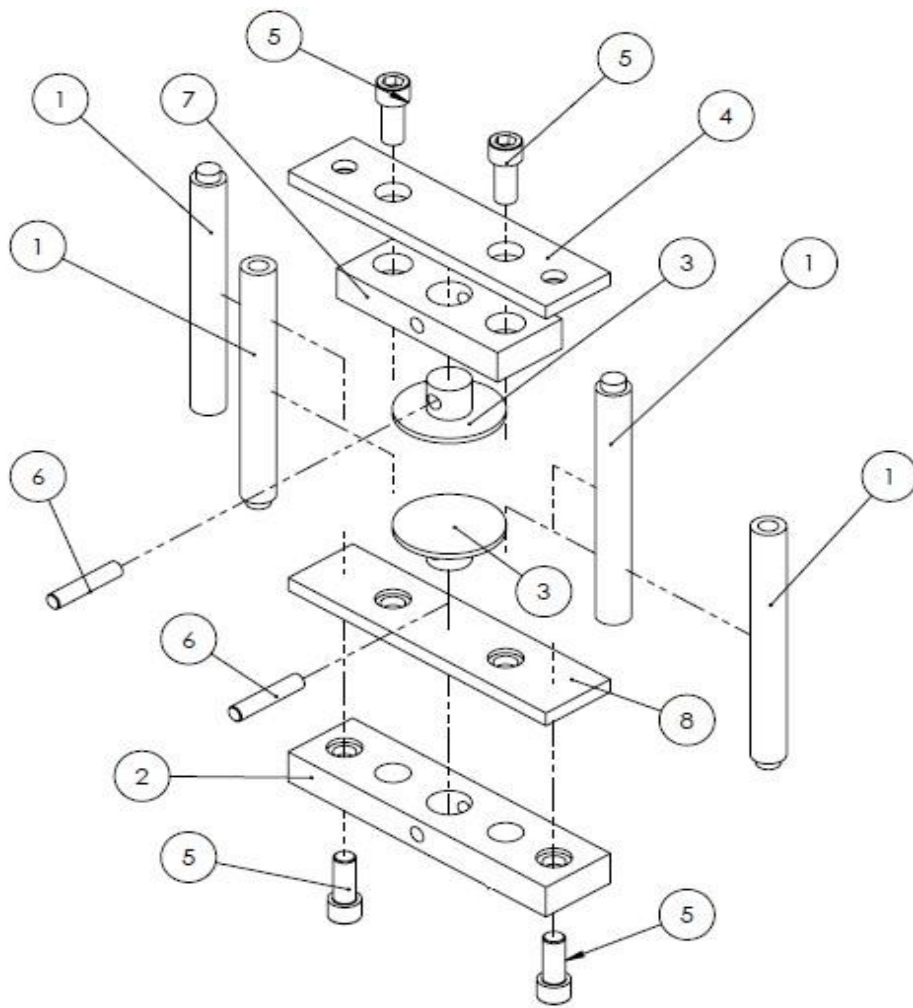
Figure III.11: Exploded view of the device.

III.5.4.3. Testing equipment and procedures

The same hydraulic testing machine used for compression and splitting strength tests is also used to perform the direct tensile test. In this setup (shown in Figure III.12), the assembly (device – tested specimen) is placed inside the compression testing machine, which applies force from the bottom upward. The upward force exerted by the bottom platen of the machine pushes the inner frame of the device upward. This action generates a downward force on the upper steel plate of the exterior frame of the device (as illustrated in Figure III.13), and then the concrete specimen is subjected to equal and opposite tensile forces.
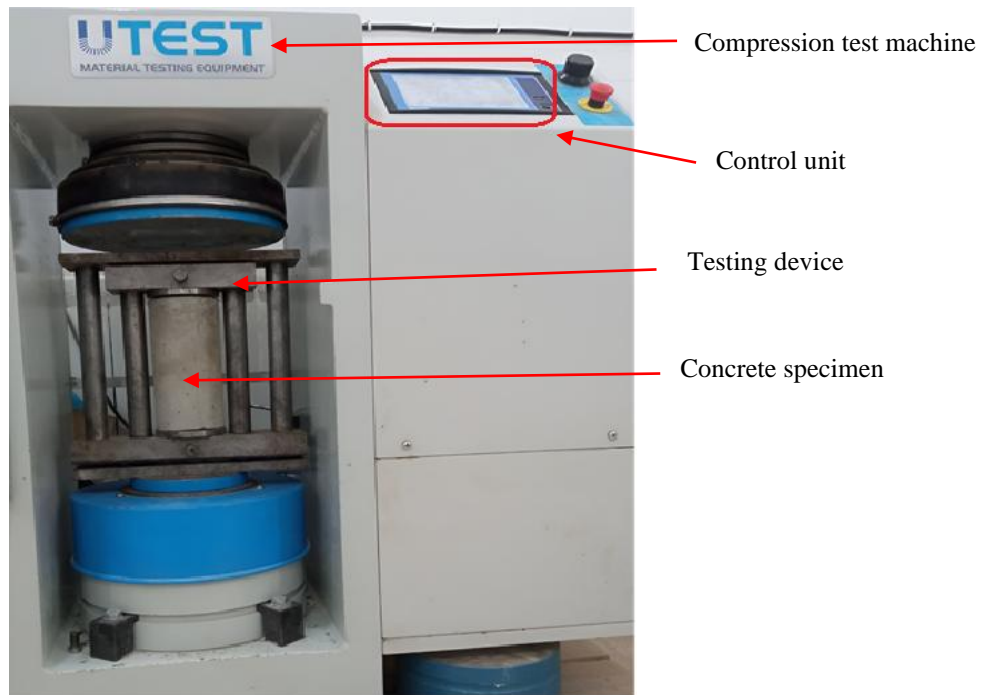
Figure III.12: The direct tensile test setup.
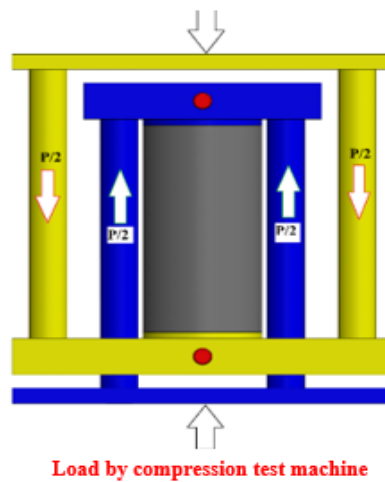
Figure III.13: Representation of the load transmission in the device.

The test is conducted at a constant loading rate of 0.04 MPa/s, which falls within the recommended range for splitting and flexural test procedures according to EN 12390-6 [147] and EN 12390-5 [146], respectively. The compressive load is applied continuously, without shock, and is controlled automatically using the control unit (Figure III.14).

The tensile stress is calculated by dividing the maximum load indicated by the compression machine by the net cross-sectional area of the specimen.
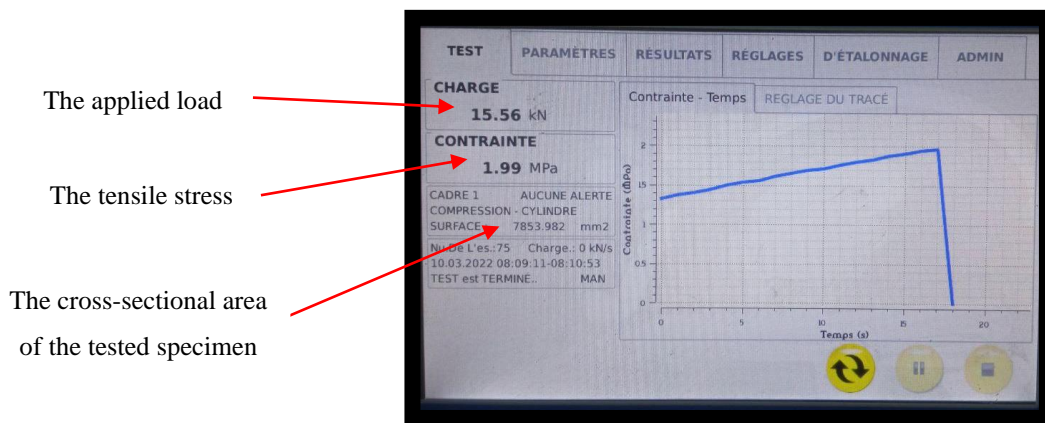
Figure III.14: The control unit of the compression machine.

III.5.4.4. Preliminary results

Based on the determination of the most suitable test setup from different proposed gripping methods mentioned above, a batch of ordinary concrete (Table III.3) was cast for preliminary tests. The compressive strength of the tested concrete specimens at 28 days ranged from 26 to 28 MPa. For each test, three repeated experiments were conducted to verify the tensile strength obtained using the proposed device. Various failure modes were observed for each gripping method. The findings were as follows:

- Specimens tested using epoxy adhesive and welded threaded steel rod grips, the cracking location was frequently concentrated at the top half of the specimen, as depicted in Figure III.15.a and Figure III.15.b.

- The specimens tested using embedded steel rod grips and threaded steel rod grips with nuts showed failure occurring in the middle part of the specimen (Figure III.15.c and Figure III.15.d). Moreover, the specimens tested with embedded steel rods exhibited failure sections perpendicular to the direction of the applied load. This perpendicular failure suggests a more uniform stress distribution and a true tensile failure, indicating that this method is effective in accurately capturing the tensile strength of the concrete.

(a)   (b)

(c)   (d)
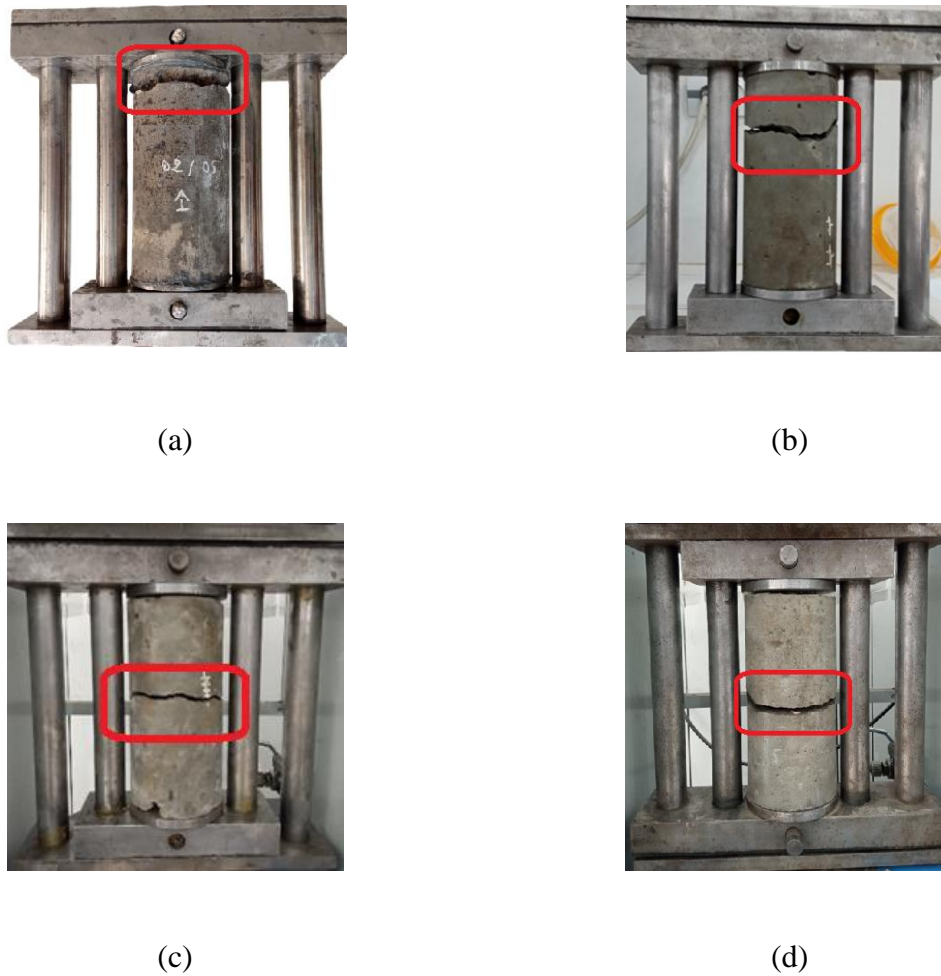
Figure III.15: Failure modes of proposed gripping modes using: (a) epoxy adhesive; (b) welded threaded steel rod grip; (c) threaded steel rod grips with nuts; (d) embedded threaded steel rod.

III.6. Conclusion

Based on the experimental results, the embedded threaded steel rod gripping method was chosen for the direct tensile tests conducted in this study. This method was selected due to its simplicity in specimen preparation process and its ability to deliver consistent and reliable results.

Chapter IV

Experimental Results and Discussion

Chapter IV: Experimental Results and Discussion

IV.1. Introduction

In this chapter, the experimental investigation into the mechanical properties of Ordinary Concrete (OC), Self-Compacting Concrete (SCC), and Steel Fiber Reinforced Concrete (SFRC) under various tensile and compressive testing methods is presented. The primary focus of the study is the evaluation of direct tensile strength using a novel testing method, alongside conventional methods for compressive, splitting tensile, and flexural strength. The results of these tests are critical for understanding the mechanical behavior of concrete under direct tension and help validate the effectiveness of the proposed testing technique.

IV.2. Failure modes

The typical failure mode of specimens subjected to the direct tensile test using the suggested testing technique (direct tensile testing with embedded steel bars) is illustrated in Figure IV.1. As expected, all tested specimens (over 66 samples) fractured successfully in the middle portion once they reached their peak load.

Figure IV.1: The concrete specimens after testing.

Previous studies, such as those by Lin et al. [148], Faez Alhusainy et al. [149], and Wee et al. [8], explored the tensile behavior of concrete under direct tension using embedded steel rods to clamp the ends of the specimens. Their experiments revealed a failure mode similar to that observed in the current study. This consistency indicates that the present tensile testing method is effective in transmitting stress along the length of the specimens, ensuring uniform stress distribution. Moreover, the absence of unexpected damage at the ends of the specimens suggests that misalignment and stress concentration were effectively avoided with this test method.

| (a) | (b) | (c) |
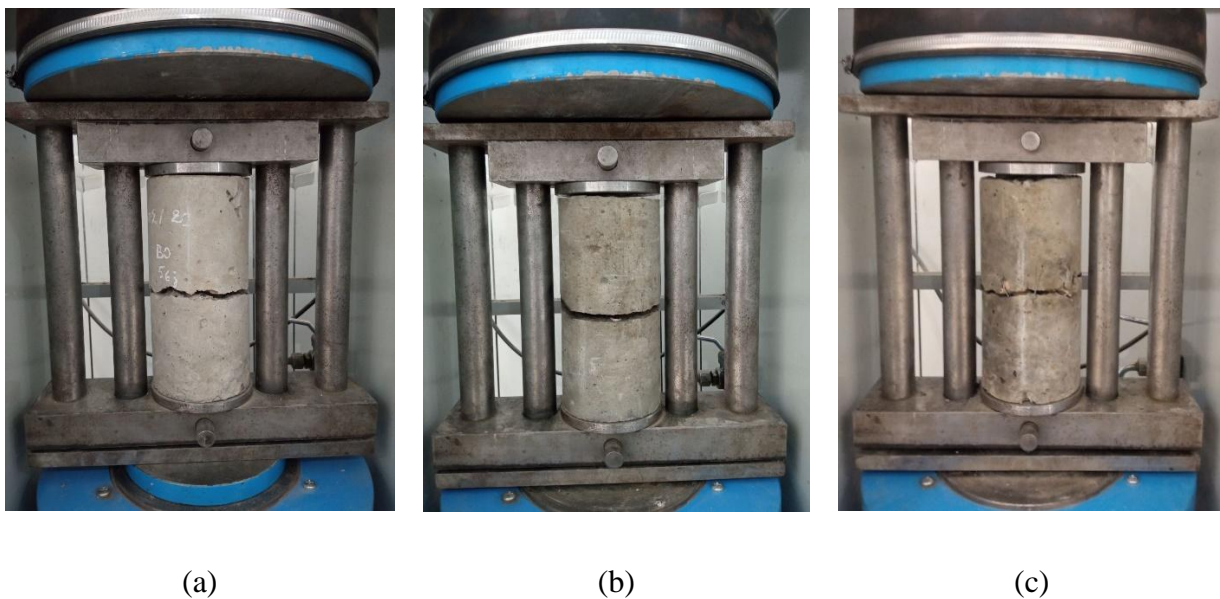
Figure IV.2: Failure mode of tested specimens: (a) OC, (b) SCC, (c) SFRC.

As shown in Figure IV.2, a single crack developed progressively until the failure of the tested specimens. This crack followed a linear path, with the applied load perpendicular to the fractured surface. Unlike the splitting test, the direct tensile test showed a sudden drop in load after reaching the peak, causing the sample to break into two parts. Each part was approximately 100 mm long and remained connected by the embedded bar due to strong bonding. Additionally, there was no slippage between the embedded steel bars and the concrete throughout the test, indicating a stable and secure connection (Figure IV.3).
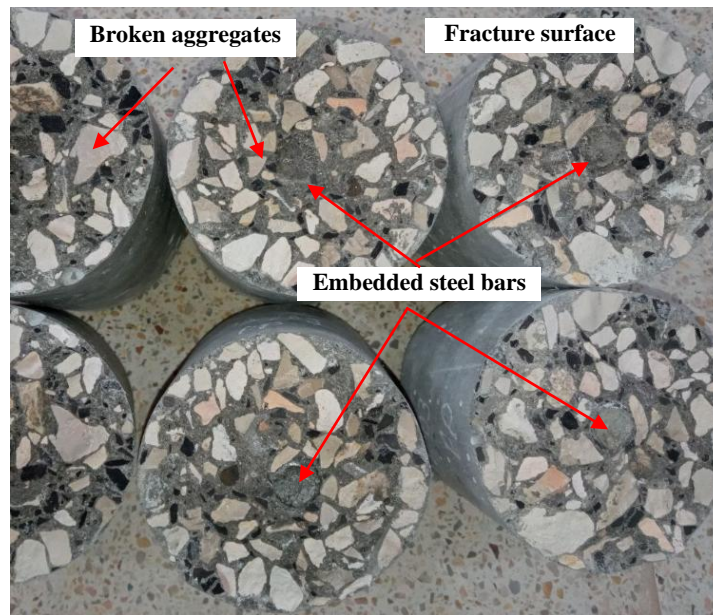
Figure IV.3: Fracture surface textures of ordinary concrete specimens.

IV.3. Strength results for Ordinary Concrete (OC)

IV.3.1. Test results

The direct tensile strength values obtained from experimental testing of Ordinary Concrete (OC) were thoroughly analyzed to validate the developed direct tensile testing method. The Table IV.1 below summarizes the average results, including compressive strength (f_{cu}), flexural strength (f_{fl}), splitting tensile strength (f_{sp}), and direct tensile strength (f_{dir}), across various curing conditions and testing ages.

The mechanical properties, including compressive, splitting, and flexural strengths were determined using standard concrete testing methods, while the direct tensile strength was measured using the novel testing method developed in this study.

The concrete specimens were subjected to two distinct curing conditions: submersion in a water tank and storage in a laboratory room at a temperature of $23 \pm 2°C$. Specimens were kept under these conditions until the designated testing ages of 3, 7, 14, 28, 56, and 90 days. The compressive strength curves as a function of testing age are shown in Figure IV.4.

Table IV.1: Test results.

Batch type[*]	Test age (days)	Compressive strength f_{cu} (MPa)	Direct tensile strength f_{dir} (MPa)	Splitting tensile strength f_{sp} (MPa)	Flexural strength f_{fl} (MPa)
I	3	14.98	1.55	1.85	4.07
	7	21.37	2.31	2.45	5.48
	14	24.71	2.55	2.98	6.22
	28	27.18	3.21	3.17	6.59
	56	28.38	3.34	3.34	6.92
	90	28.64	3.35	3.46	7.00
II	3	14.17	1.43	1.76	3.94
	7	20.54	2.00	2.24	4.48
	14	21.22	2.23	2.50	5.01
	28	22.68	2.33	2.61	5.71
	56	23.40	2.40	2.61	5.95
	90	23.50	2.40	2.64	6.30

[*]**Batch type I**: specimens cured in the water tank; **Batch type II**: specimens cured in the laboratory room.
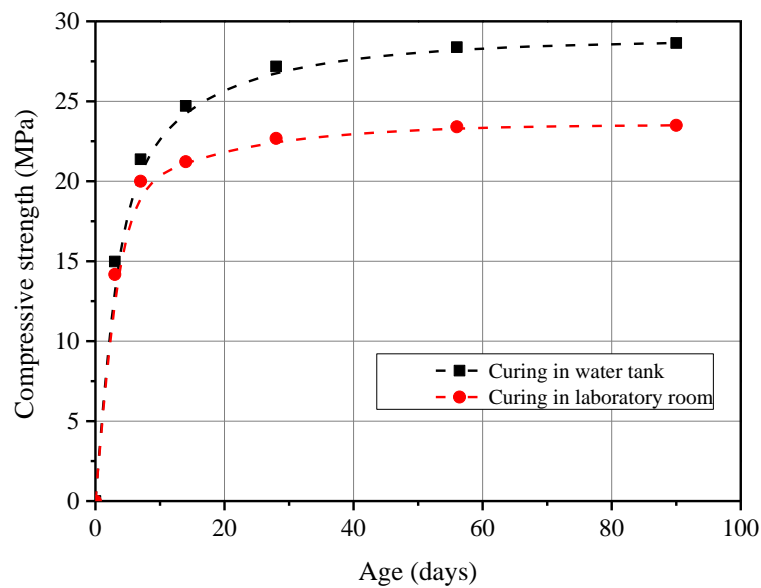
Figure IV.4: Typical compressive strength curves of ordinary concrete during 90 days.

As shown in Figure IV.4, the compressive strength of the OC cylinders monitored at 90 days of curing was found 28.64 MPa and 23.50 MPa for specimens cured in water tank and laboratory room, respectively. A similar trend was observed in both direct and indirect tension tests. For the same concrete mixture, both compressive and tensile strengths of specimens cured in water tank consistently exhibited higher values compared to those cured in the laboratory room due to the condition of curing in presence of water which influences the hydration reaction of the cement during the curing period. Typical tensile strength development curves of concrete samples for various curing conditions recorded from direct and indirect tensile tests are shown in the Figure IV.5 and Figure IV.6.
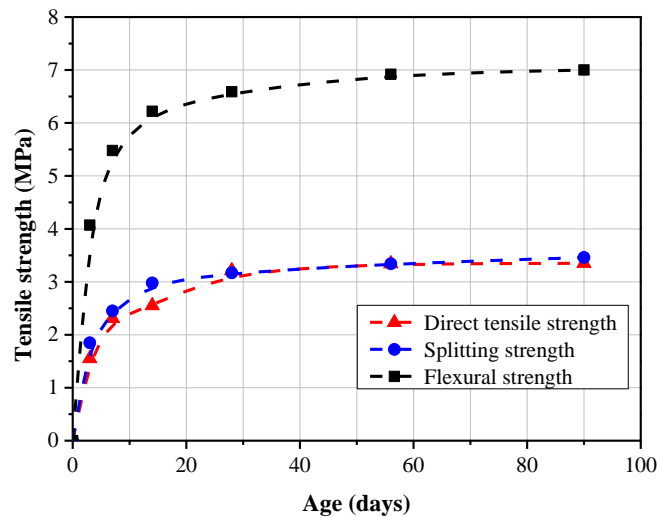
Figure IV.5: Tensile strength curves of ordinary concrete cured in the water tank.
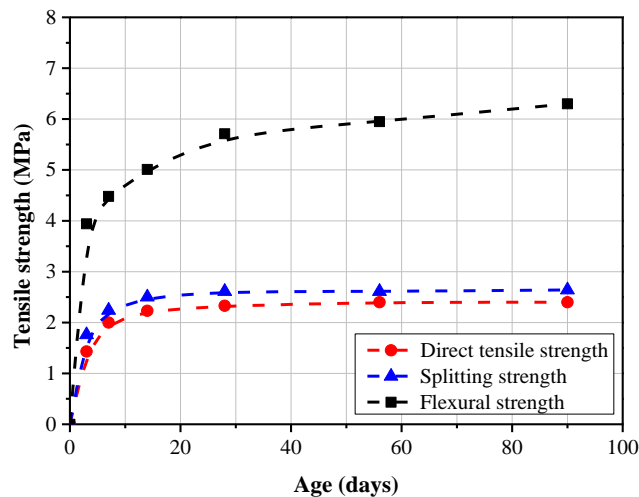
Figure IV.6: Tensile strength curves of ordinary concrete cured in the laboratory room.

Regardless of the testing method used, the tensile strength development of OC specimens varied depending on the curing conditions. After 90 days, the average direct tensile strength for specimens cured in water tank was 3.35 MPa, while those cured in laboratory room exhibited a lower average of 2.40 MPa. For the split tensile test, specimens cured in water tank had an average strength of 3.46 MPa, compared to 2.64 MPa for those cured in the laboratory room. Similarly, the flexural strength was measured at 7 MPa for specimens cured in water tank, versus 6.30 MPa for those cured in the laboratory room.

IV.3.2. Comparative analysis

To confirm the reliability of the testing device and the proposed testing method for the direct tensile test, a comparative analysis was conducted between the conventional test methods and the newly developed model. The comparison between the strengths obtained from various testing methods are detailed in Table IV.2.

Table IV.2: Result comparison.

Batch type*	Test age (days)	Ratio: %				
		$(f_{dir}/f_{cu})\times100$	$(f_{sp}/f_{cu})\times100$	$(f_{fl}/f_{cu})\times100$	$(f_{dir}/f_{sp})\times100$	$(f_{dir}/f_{fl})\times100$
I	3	10.35	12.35	27.17	83.78	38.08
	7	10.81	11.46	25.64	94.29	42.15
	14	10.32	12.06	25.17	85.57	41.00
	28	11.81	11.66	24.25	101.26	48.71
	56	11.77	11.77	24.38	100.00	48.27
	90	11.69	12.08	24.44	96.82	47.86
II	3	10.09	12.42	27.81	81.25	36.29
	7	9.74	10.91	21.81	89.29	44.64
	14	10.51	11.78	23.61	89.20	44.51
	28	10.27	11.51	25.18	89.27	40.81
	56	10.26	11.15	25.43	91.95	40.34
	90	10.21	11.23	26.81	90.91	38.10

*∗**Batch type I**: specimens cured in the water tank; **Batch type II**: specimens cured in the laboratory room.*

As illustrated in the Table IV.2, the results show that the direct tensile strength of specimens tested using the proposed method, under various curing conditions, maintains a relatively constant ratio to the compressive strength over 90 days. Specifically, the direct tensile strength of specimens cured in either a water tank or a laboratory environment is approximately 10-11% of the compressive strength. In comparison, the splitting tensile strength and flexural strength of these specimens are approximately 11-12% and 22-28% of the compressive strength, respectively. Figure IV.7 and Figure IV.8 show the variation in the ratio of direct tensile strength to conventional standard tests across different testing age.
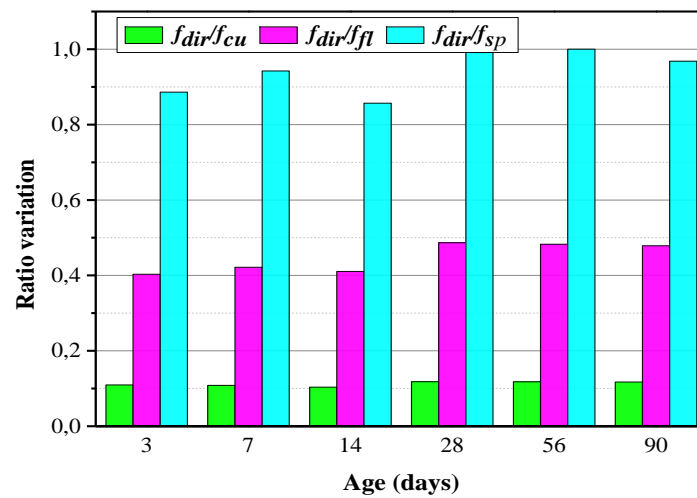
Figure IV.7: Variation of obtained direct tensile strengths of ordinary concrete specimens cured in the water tank with other testing methods.
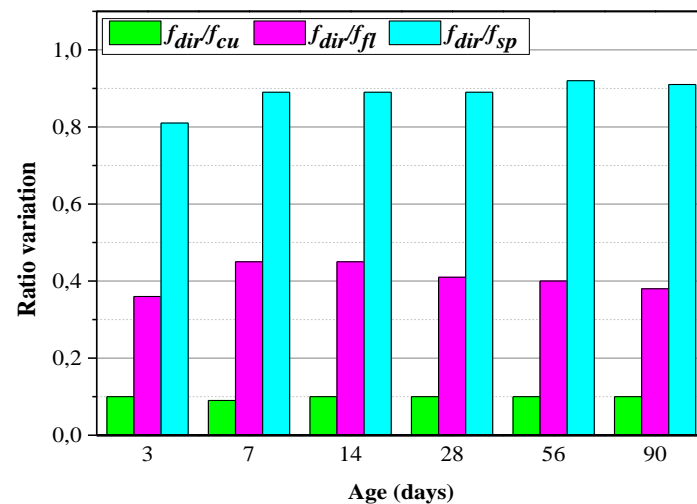
Figure IV.8: Variation of obtained direct tensile strengths of ordinary concrete specimens cured in the laboratory room with other testing methods.

The direct tensile strength obtained using the proposed method was approximately 7-12% and 60-66% lower than the splitting tensile strength and flexural strength, respectively. This finding aligns with previous research, which indicates that the true tensile strength of concrete is around 5-12% of its splitting strength [150–152] and about 65-70% of its flexural strength [148] [153,154].

The experimental data revealed considerable variability in the strength results obtained from direct and indirect tensile tests. Various studies have explained why tensile strength measured by indirect methods often tends to be higher than that obtained through direct methods [155]. One notable example is the flexural strength test of ordinary concrete (OC) beams using the center-point loading method, which frequently overestimates tensile strength. This overestimation arises due to the formula used for calculating strength, which is based on Hooke's law and assumes a linear elastic stress distribution along the cross-section up to the point of cracking. However, the actual stress distribution across the section is non-uniform and more accurately represented by a parabolic flexural stress-strain relationship. Consequently, under loading, the beam is simultaneously subjected to tensile and compressive stresses below and above the neutral axis, respectively. In this scenario, only the extreme bottom fiber is subjected to the maximum tensile stress.

Although the splitting tensile strength is relatively close to the direct tensile strength, the method used to determine this strength is based on the assumption that uniform horizontal tensile stress is distributed along the longitudinal cross-section, which may not accurately reflect the true tensile behavior of concrete. In practice, this standard method subjects the specimen to a combination of stresses : high compressive stresses develop at the friction zones near the ends of the cylinder due to contact with packing strips, while tensile stresses increase along the plane of the applied load. Moreover, the test's accuracy is significantly influenced by factors such as maximum aggregate size, which affects the stress distribution and failure behavior of the specimen under the Brazilian test conditions.

IV.3.3. Relationship between the mechanical properties of OC

IV.3.3.1. Relationship between tensile and compressive strengths of OC

This section of the study investigates the relationship between the tensile strengths and the corresponding compressive strength of ordinary concrete (OC) for various tensile test methods. Figure IV.9 and Figure IV.10 illustrate the relationships between tensile and compressive strengths of concrete specimens cured in a water tank and in laboratory conditions, respectively.
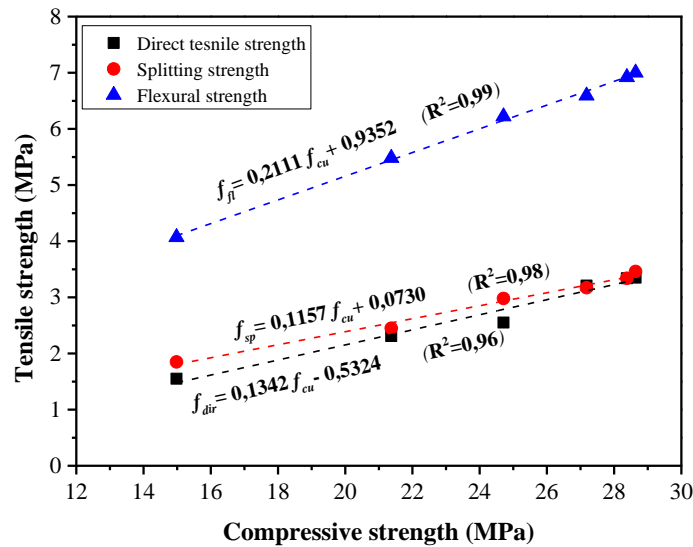
Figure IV.9: Relationship between tensile and compressive strengths from different test methods for OC (cured in water tank).
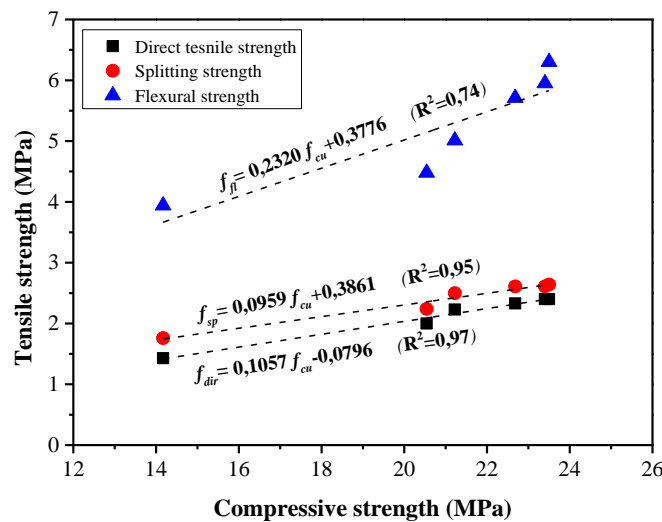
Figure IV.10: Relationship between tensile and compressive strengths from different test methods for OC (cured in laboratory room).

A linear relationship is observed between tensile and compressive strengths across both direct and indirect tensile tests, with R^2 values exceeding 0.95 for both curing conditions. However, the R^2 value for the relationship between flexural and compressive strength of concrete cured in laboratory conditions is 0.74, indicating greater variability and lower reliability in this correlation. This scatter in data points could result from factors not accounted for in the regression analysis, such as curing conditions, curing duration, and other variables. Therefore, the correlation between the results shows that it is possible to estimate the tensile strength from the compressive strength.

IV.3.3.2. Relationship between direct tensile and splitting strengths of OC

The relationship between direct tensile strength (f_{dir}) and splitting tensile strength (f_{sp}) of OC was analyzed using regression analysis for both curing conditions, as shown in Figure IV.11 and Figure IV.12. The coefficients of determination (R^2) for the proposed relationships are 0.94 and 0.99 for specimens cured in a water tank and in a laboratory room, respectively. These high R^2 values reflect a strong correlation between the two tensile strength measures, indicating that the proposed relationships are reliable and accurate for estimating direct tensile strength based on the splitting strength.
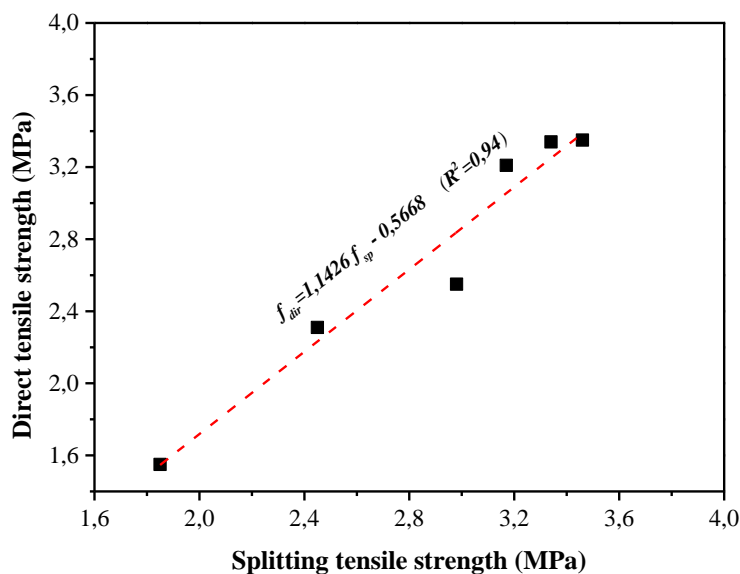
Figure IV.11: Relationship between direct tensile and splitting strengths of OC (cured in water tank).
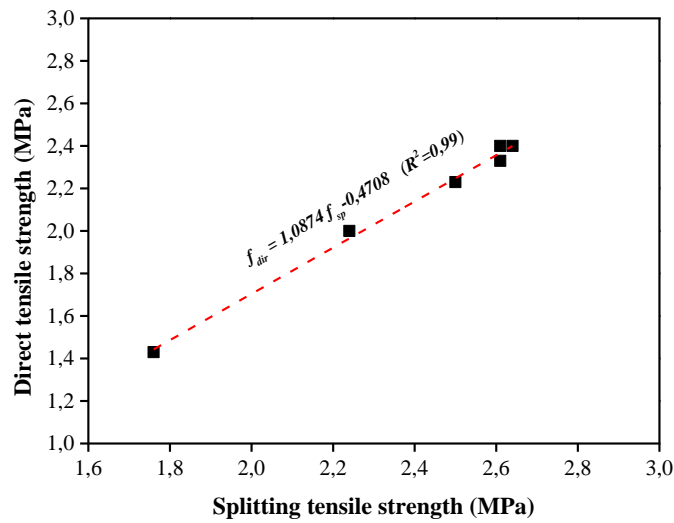
Figure IV.12: Relationship between direct tensile and splitting strengths of OC (cured in laboratory room).

IV.3.3.3. Relationship between direct tensile and flexural strengths of OC

Figure IV.13 and Figure IV.14 present the relationship between direct tensile strength and flexural strength of ordinary concrete (OC). Regression analysis reveals R^2 values of 0.94 and 0.78 for specimens cured in a water tank and in a laboratory room, respectively. While the high R^2 value for water-cured specimens suggests a reliable correlation, the lower R^2 for laboratory-cured specimens indicates a higher variability, reducing the reliability of the proposed relationship in that environment.
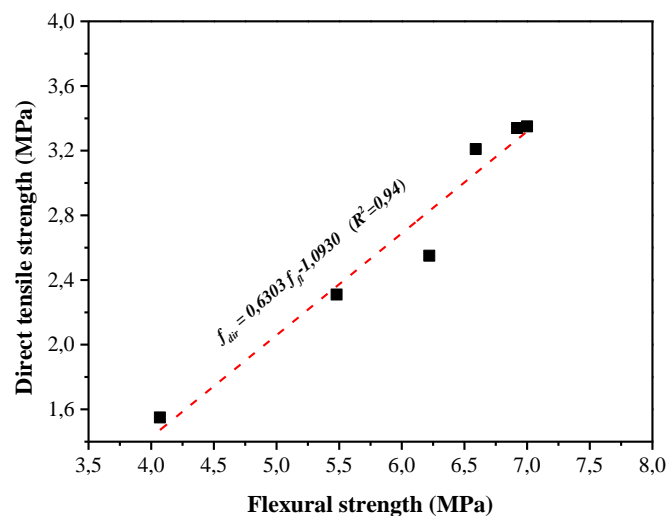
Figure IV.13: Relationship between direct tensile and flexural strengths of OC (cured in water tank).
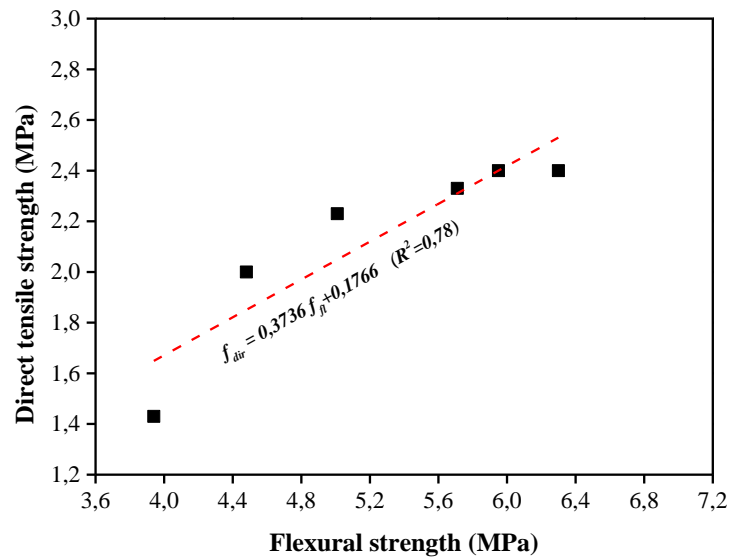
Figure IV.14: Relationship between direct tensile and flexural strengths of OC (cured in laboratory room).

IV.4. Strength Results for Self-compacting concrete (SCC)

IV.4.1. Comparative Analysis

Table IV.3 summarises the mechanical properties of the SCC obtained from the proposed direct tensile test and standard tests. Two batches of SCC specimens were prepared and tested at 7 and 28 days. The average strength was calculated for each test and used as the representative strength in all subsequent analyses. The results show a clear increase in all measured mechanical properties (compressive strength, direct tensile strength, splitting tensile strength, and flexural strength) as the concrete ages from 7 to 28 days. Compressive strength increased by approximately 17%, direct tensile strength by 38%, splitting tensile strength by 25%, and flexural strength demonstrated the most significant relative increase of over 51%.

It was observed that the direct tensile strength of SCC is lower than both the splitting tensile strength and flexural strength. Specifically, the average direct tensile strength was 2.21 MPa at 7 days and 3.06 MPa at 28 days, whereas the splitting tensile strength values were slightly higher. Flexural strength, which measures an indirect form of tensile strength, reached 5.36 MPa at 7 days and 8.13 MPa at 28 days, producing significantly higher results than the direct tensile tests.

Table IV.3: Tests results.

Test age (days)	Compressive strength f_{cu} (MPa)	Direct tensile strength f_{dir} (MPa)	Splitting tensile strength f_{sp} (MPa)	Flexural strength f_{fl} (MPa)
7	30.79	2.21	2.72	5.36
28	36.18	3.06	3.41	8.13

The lower value of the direct tensile strength compared to the splitting and flexural strengths aligns with observations reported by Alhusainy et al. [9] for self-compacting concrete. The predicted direct tensile strength value, according to ACI 318-11 [21] was only 0.3 MPa higher than the experimentally obtained value at the age of 28 days.

Table IV.4 provides a comparison of direct tensile strength, indirect tensile strength, and compressive strength as determined from the tests.

Table IV.4: Result comparison.

Test age (days)	Ratio: %				
	$(f_{dir}/f_{cu})\times100$	$(f_{sp}/f_{cu})\times100$	$(f_{fl}/f_{cu})\times100$	$(f_{dir}/f_{sp})\times100$	$(f_{dir}/f_{fl})\times100$
7	7.18	8.83	17.41	81.25	41.23
28	8.46	9.43	22.47	89.74	37.64
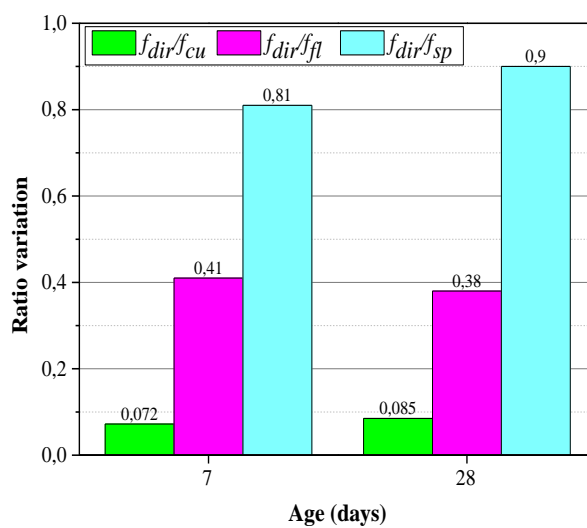
Figure IV.15: Variation of obtained direct tensile strengths of self compacting concrete specimens with other testing methods.

The results shown in the Figure IV.15 illustrate the variation in strength ratios of the proposed direct tensile test method across different testing ages compared to compressive and indirect tensile tests. The direct tensile to compressive strength ratio increases from 7.18% at 7 days to 8.46% at 28 days, indicating that continued hydration and improved bonding between the aggregate and mortar contribute to enhanced tensile strength over time.

Moreover, the ratio of direct tensile strength to splitting tensile strength shows a converging trend, increasing from 81.25% at 7 days to 89.74% at 28 days. This suggests that the proposed direct tensile test yields results that become more comparable to splitting tensile strength as the concrete gains strength over time.

Conversely, the direct tensile to flexural strength ratio shows a slight decrease from 41.23% at 7 days to 37.64% at 28 days, indicating that flexural strength develops more rapidly compared to direct tensile strength during this period.

IV.5. Strength results for Steel Fiber Reinforced Concrete (SFRC)

IV.5.1. Comparative analysis

All concrete mixes were tested for compressive strength, direct tensile strength, splitting tensile strength, and flexural strength after 7 and 28 days of curing. The results of the hardened concrete properties are summarized in Table IV.5.

Table IV.5: Test results.

Concrete type	Compressive strength f_{cu} (MPa)		Direct tensile strength f_{dir} (MPa)		Splitting tensile strength f_{sp} (MPa)		Flexural strength f_{fl} (MPa)	
	7 days	28 days	7 days	28 days	7 days	28 days	7 days	28 days
Mix-0	20.53	28.14	1.91	3.02	2.45	3.13	4.48	5.51
Mix-0.5	20.97	29.23	1.98	3.12	2.95	3.69	5.50	6.11
Mix-0.75	21.18	30.41	2.04	3.22	3.05	4.50	6.05	6.81
Mix-1.25	23.92	32.48	2.20	3.32	3.75	4.82	6.38	7.81
Mix-1.50	22.62	31.89	2.23	3.38	4.09	4.86	7.36	8.12

IV.5.1.1. Compressive strength

As shown in the Table IV.5, the compressive strength of the five concrete mixes ranged from 20 MPa to 24 MPa at 7 days, and from 28 MPa to 32 MPa at 28 days. The results indicate a consistent increase in compressive strength as the volume fraction of steel fibers increased. Specifically, at 7 days, the compressive strength showed improvements ranging from 2.14% to 16.53% compared to the reference mix with the inclusion of steel fibers.

Similarly, at 28 days, the compressive strength followed the same trend, showing greater enhancement as the steel fiber content increased. The improvement in compressive strength for SFRC compared to the reference concrete ranged from 3.87% at 0.5% fiber content to a maximum of 15.42% at 1.25% fiber content. However, at 1.5% fiber volume, the compressive strength slightly decreased to 13.33%, which, while still significant compared to the reference mix, is slightly lower than the peak strength at 1.25%. This slight reduction may be attributed to issues such as reduced workability and the increase of air content in concrete with increase of steel fiber content, which can affect the overall strength development. The compressive strength results are graphically illustrated in Figure IV.16.
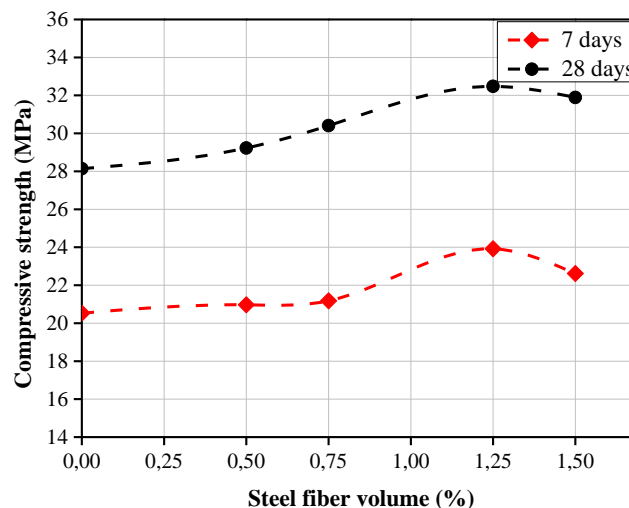
Figure IV.16: Variation in compressive strength of SFRC.

IV.5.1.2. Comparison of tensile test methods

The comparison of tensile strength results from different test methods (direct tensile, splitting tensile, and flexural tests) reveals significant variations. Across all concrete mixtures and

curing times, direct tensile tests consistently yield the lowest tensile strength values, while flexural tests provide the highest, as shown in Figure IV.17 and Figure IV.18.

The splitting tensile test consistently overestimates the tensile strength compared to the direct tensile test, with this overestimation becoming more pronounced with curing time as the fiber content in the concrete increase. For example, in Mix-1.50, the splitting tensile strength at 28 days is 4.86 MPa, about 43.8% higher than the direct tensile strength of 3.38 MPa. This trend is consistent across all mixes, likely due to the ductile behavior of steel fiber reinforced concrete (SFRC), which creates a larger compressive zone under the applied load in splitting test.

The flexural strength tests yield significantly higher tensile strength values compared to other methods. For instance, Mix-1.50 shows a flexural strength of 8.12 MPa, approximately 140% higher than the direct tensile strength. This significant additional increase in flexural strength of SFRC is primarily due to the fibers' ability to resist tensile forces during bending. Under flexural stress, the steel fibers delay failure by either rupturing or pulling out at relatively higher tensile stresses. This action enhances the concrete's load-bearing capacity and helps prevent early crack formation. Additionally, the fibers improve stress distribution and add ductility, allowing the concrete to absorb more energy and resist cracking for longer periods, which greatly enhances its performance under bending stress.
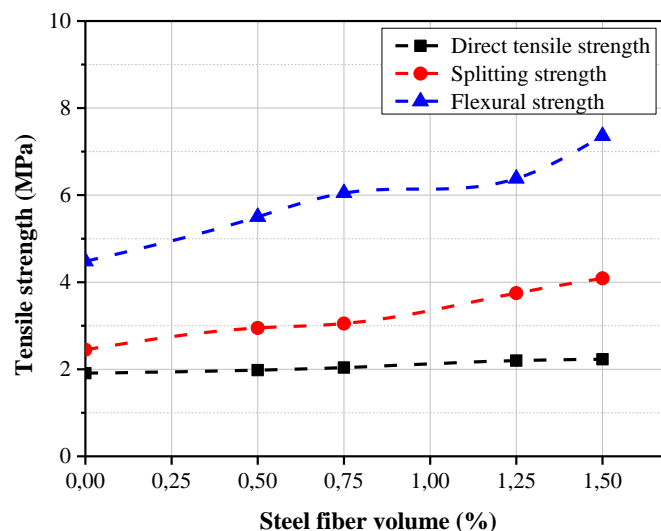
Figure IV.17: Variation in 7 days tensile strengths of SFRC determined by various test methods.
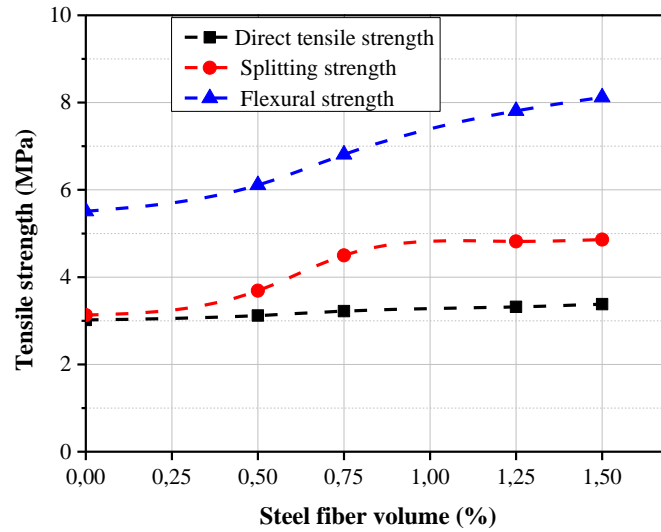
Figure IV.18: Variation in 28 days tensile strengths of SFRC determined by various test methods.

IV.5.2. Relationship between the mechanical properties of SFRC

IV.5.2.1. Relationship between tensile and compressive strengths of SFRC

As shown in the Figure IV.19, a regression analysis was conducted on the experimental data points of SFRC at 28 days, including both direct and indirect tensile strengths in relation to the corresponding compressive strength. Through this analysis, the following relationships were obtained:

$$f_{dir} = 0.078 f_{cu} + 0.8357 \qquad (1)$$

$$f_{sp} = 0.406 f_{cu} - 8.1670 \qquad (2)$$

$$f_{fl} = 0.5975 f_{cu} - 11.3122 \qquad (3)$$

Where :

f_{dir}, f_{sp}, f_{fl} and f_{cu} are the direct tensile strength, splitting tesnile strength, flexural tensile strength and compressive strength, respectively.

The coefficients of determination (R^2) for these proposed relationships are 0.91, 0.91, and 0.93 for direct tensile, splitting tensile, and flexural strengths, respectively, indicating strong correlations between these variables.
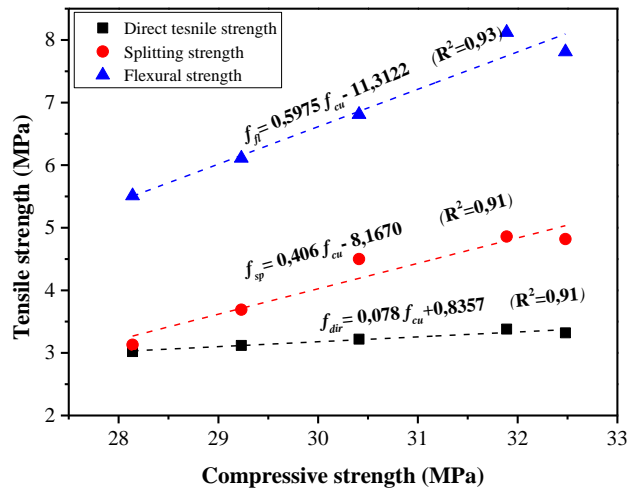
Figure IV.19: Relationship between tensile strength and compressive strength of SFRC.

IV.5.2.2. Relationship between direct tensile and splitting tensile strength of SFRC

In Figure IV.20, as previously described, the experimental data points of direct tensile strength (f_{dir}) and splitting tensile strength (f_{sp}) of SFRC at 28 days are plotted. Through regression analysis, the following empirical relationship was established:

$$f_{dir} = 0.1868f_{sp} + 2.4271 \qquad (4)$$

The corresponding R^2 of this proposed relation is 0.93, indicating a strong correlation between these two variables.
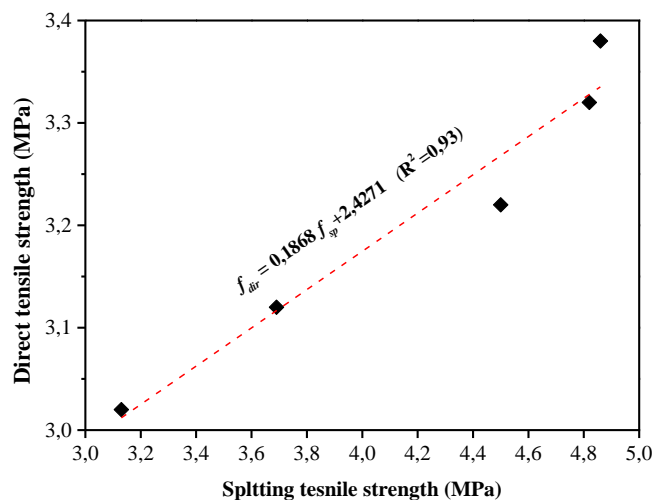
Figure IV.20: Relationship between direct tensile strength and splitting tensile strength of SFRC.

IV.5.2.3. Relationship between direct tensile and flexural tensile strength of SFRC

The correlation between the direct tensile strength (f_{dir}) and flexural strength (f_{fl}) of SFRC was also analyzed using regression analysis, as illustrated in Figure IV.21. The resulting empirical relationship can be expressed as follows:

$$f_{dir} = 0.1316f_{fl} + 2.3072 \tag{5}$$

The R^2 value for this proposed relationship is 0.98, indicating a strong correlation between these two mechanical properties.
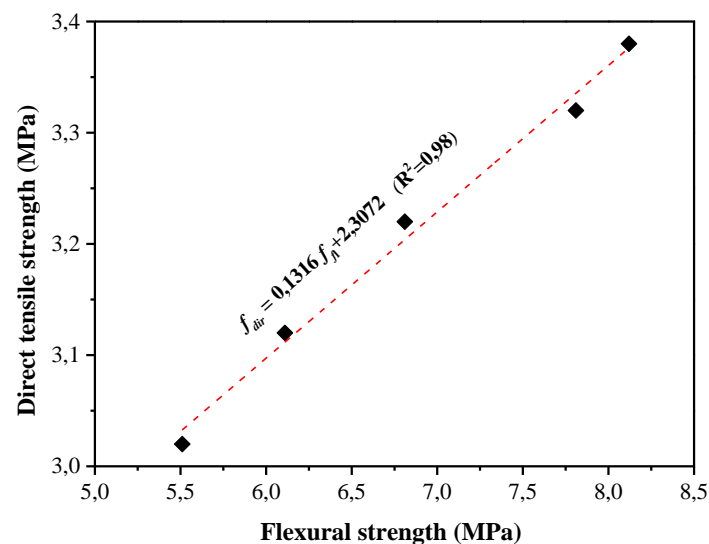
Figure IV.21: Relationship between direct tensile strength and flexural strength of SFRC.

IV.6. Conclusion

This chapter presents a detailed analysis of the mechanical properties of Ordinary Concrete (OC), Self-Compacting Concrete (SCC) and Steel Fiber Reinforced Concrete (SFRC) using various testing methods, with a particular focus on direct tensile strength as measured by the novel test method. The experimental results indicate that the direct tensile strength values were consistently lower than those obtained from splitting and flexural tensile tests, emphasizing the significance of the proposed method in assessing the tensile behavior of concrete. It is important to note that the relationships established between different strength parameters are confined to the

scope of this investigation. As previously mentioned, this study is part of ongoing research on the development of direct tensile strength measurement.

Conclusions and Prospects

Conclusions and Prospects

This research aimed to develop a novel method for accurately determining the tensile strength of concrete through direct tensile testing. A new testing device was designed and validated to address the limitations of traditional indirect methods, such as the splitting and flexural tensile tests, which tend to overestimate tensile strength. The proposed device, along with a novel specimen preparation technique, was shown to effectively measure the tensile strength of concrete, with results closely aligning with its actual tensile strength and earlier findings. The following conclusions can be drawn:

1. Three different types of tensile tests for concrete were studied, and a new method was proposed for evaluating the tensile strength of concrete. This new method was successfully developed, and the test results indicated that the proposed method produces reliable results.

2. The main advantages of the proposed device over other testing techniques are as follows: the use of the same testing machine that is typically employed for compressive and splitting tensile tests, easy to setup, use of a standardized-shaped specimen, and less-expensive.

3. Experimental and numerical methods were used to support the designed device and proposed test setup.

4. The mold proposed for preparing the specimen for the tension test overcomes the difficulties in centralizing and aligning the embedded bars within the specimen.

5. The gripping method used for the concrete samples enhances the bond strength between the embedded bars and the concrete, and minimizes stress concentrations at the ends of the embedded bars.

6. The proposed method consistently produced predictable tensile failure modes, with cracks forming at expected locations, which concentrated in the central part of the specimen.

7. The accuracy of the results was confirmed by comparing them with those obtained from indirect testing methods, as well as with earlier research findings.

8. Direct tensile strength values obtained from the three types of concrete (ordinary concrete, self-compacting concrete and steel fiber reinforced concrete) were consistently lower than those obtained from flexural tensile tests and closer to those from splitting tensile tests.

9. The study established clear relationships between compressive, direct tensile, splitting tensile, and flexural strengths, providing valuable data for future concrete strength estimations.

Perspectives

- Further research is required to apply the developed testing device and procedure to determine the direct tensile strength of various types of concrete, including lightweight and high-performance concretes.

- Further research should explore the applicability of this testing device for steel fiber-reinforced concrete with higher fiber contents, especially to assess its potential for capturing hardening behavior.

- Investigate the influence of unit weight on the cracking strength and cracking location in concrete specimens under uniaxial tension using the developed testing method and epoxy adhesive for specimen attachment.

- Evaluate the impact of strain rate on the direct tensile strength of concrete using the proposed testing method.

- Study the size effect of test specimens on the direct tensile strength of concrete to establish any scaling laws or corrections applicable to the test results.

Bibliographic References

Bibliographic References

[1]   P.J.M. Monteiro, S.A. Miller, A. Horvath, Towards sustainable concrete, Nat Mater 16 (2017) 698–699.

[2]   H. Liu, Q. Zhang, C. Gu, H. Su, V.C. Li, Influence of micro-cracking on the permeability of engineered cementitious composites, Cem Concr Compos 72 (2016) 104–113.

[3]   W. Liao, P. Chen, C. Hung, S.K. Wagh, An Innovative Test Method for Tensile Strength of Concrete by Applying the Strut-and-Tie Methodology, (2020).

[4]   T. Akazawa, New test method for evaluating internal stress due to compression of concrete (the splitting tension test)(part 1), J Jpn Soc Civ Eng 29 (1943) 777–787.

[5]   F. Carneiro, A new method to determine the tensile strength of concrete, in: Proceedings of the 5th Meeting of the Brazilian Association for Technical Rules, 1943: pp. 126–129.

[6]   W. Zheng, A.K.H. Kwan, P.K.K. Lee, Direct tension test of concrete, Materials Journal 98 (2001) 63–71.

[7]   J.G.M. Van Mier, M.R.A. Van Vliet, Uniaxial tension test for the determination of fracture parameters of concrete: state of the art, Eng Fract Mech 69 (2002) 235–247.

[8]   T.H. Wee, H.R. Lu, S. Swaddiwudhipong, Tensile strain capacity of concrete under various states of stress, Magazine of Concrete Research 52 (2000) 185–193.

[9]   Y. Dai, Y. Li, X. Xu, Q. Zhu, Y. Yin, S. Ge, A. Huang, L. Pan, Characterization of tensile failure behaviour of magnesia refractory materials by a modified dog-bone shape direct tensile method and splitting tests, Ceram Int 46 (2020) 6517–6525.

[10]   A.M. Neville, Properties of Concrete: Fourth and Final Edition, Wiley, 1996.

[11]   P. Mehta, P.J.M. Monteiro, Concrete: Microstructure, Properties, and Materials, McGraw-Hill Education, 2005.

[12]   J. Weiss, Elastic properties, creep, and relaxation, in: Significance of Tests and Properties of Concrete and Concrete-Making Materials, ASTM International, 2006.

[13]   J.G.M. Van Mier, Strain-softening of concrete under multiaxial loading conditions, (1984).

[14]   H. Mihashi, F.H. Wittmann, Stochastic approach to study the influence of rate of loading on strength of concrete, Stevin-Laboratory of the Department of Civil Engineering of the Delft …, 1980.

[15]   F.H. Wittmann, Creep and shrinkage mechanisms, Creep and Shrinkage in Concrete Structures (1982) 129–161.

[16]   R. Park, T. Paulay, Reinforced Concrete Structures, Wiley, 1991.

[17]   J. Haavisto, A. Husso, A. Laaksonen, Compressive strength of core specimens drilled from concrete test cylinders, Structural Concrete 22 (2021) E683–E695.

[18]   J. Weiss, Elastic properties, creep, and relaxation, in: Significance of Tests and Properties of Concrete and Concrete-Making Materials, ASTM International, 2006.

[19]   W. Bai, X. Lu, J. Guan, S. Huang, C. Yuan, C. Xu, Stress–strain behavior of FRC in uniaxial tension based on mesoscopic damage model, Crystals (Basel) 11 (2021) 689.

[20]   F.L. Zongjin Li T. Y. Paul Chang, and Yiu-Wing Mai, Uniaxial Tensile Behavior of Concrete Reinforced with Randomly Distributed Short Fibers, ACI Mater J 95 (n.d.). https://doi.org/10.14359/399.

[21]   R.C.K. Wong, S.K.Y. Ma, R.H.C. Wong, K.T. Chau, Shear strength components of concrete under direct shearing, Cem Concr Res 37 (2007) 1248–1256.

[22]   H. Kupfer, H.K. Hilsdorf, H. Rusch, Behavior of concrete under biaxial stresses, in: Journal Proceedings, 1969: pp. 656–666.

[23]   N.J. Carino, The behavior of a model of plain concrete subject to compression-tension and tension-tension biaxial stresses., (1975).

[24]   S. Mindess, J.F. Young, D. Darwin, Concrete Prentice-Hall, Englewood Cliffs, NJ 481 (1981) 939.

[25]   S. Timoshenko, History of strength of materials: with a brief account of the history of theory of elasticity and theory of structures, Courier Corporation, 1983.

[26]   E. Siviero, B. Simoncelli, Early experimental investigations to establish the tensile strength of concrete, CEB Comité Euro International Du Béton, Bulletin (1997) 17–36.

[27]   C.C. Garcia-Fernandez, C. Gonzalez-Nicieza, M.I. Alvarez-Fernandez, R.A. Gutierrez-Moizant, Analytical and experimental study of failure onset during a Brazilian test, International Journal of Rock Mechanics and Mining Sciences 103 (2018) 254–265.

[28] C. Astm, 1609: standard test method for flexural performance of fiber-reinforced concrete (using beam with third-point loading), ASTM Vol. 0.4 2 (2005).

[29] M. Mellor, I. Hawkes, Measurement of tensile strength by diametral compression of discs and annuli, Eng Geol 5 (1971) 173–225.

[30] M.I. Khan, Direct tensile strength measurement of concrete, Applied Mechanics and Materials 117 (2012) 9–14.

[31] I. Löfgren, H. Stang, J.F. Olesen, The WST method, a fracture mechanics test method for FRC, Mater Struct 41 (2008) 197–211.

[32] A. Abrishambaf, J.A.O. Barros, V.M.C.F. Cunha, Tensile stress–crack width law for steel fibre reinforced self-compacting concrete obtained from indirect (splitting) tensile tests, Cem Concr Compos 57 (2015) 153–165.

[33] Z.Y. Liao, J.B. Zhu, C.A. Tang, Numerical investigation of rock tensile strength determined by direct tension, Brazilian and three-point bending tests, International Journal of Rock Mechanics and Mining Sciences 115 (2019) 21–32.

[34] F.L.L.B. Carneiro, Tensile strength of concretes, Rilem Bull. 13 (1953) 103–107.

[35] T. Akazawa, Tension Test Methods for Concretes, International Union of Testing and Research Laboratories for-Materials and Structures (RILEM), Paris, Bulletin 16 (1953) 11–23.

[36] P.K. Mehta, P. Monteiro, Concrete: microstructure, properties, and materials, (No Title) (2006).

[37] B.S. EN, 12390-1 (2012). Testing hardened concrete. Shape, dimensions and other requirements for specimens and moulds, British Standards Institute, London. United Kingdom (n.d.).

[38] M. Standard, MS EN 12390-2: 2012: Testing hardened concrete-Part 2: Making and curing specimens for strength tests (Second revision), (2012).

[39] S. Nilsson, The tensile strength of concrete determined by splitting tests on cubes, Rilem Bulletin 11 (1961) 63–67.

[40] L. Jin, W. Yu, X. Du, Size Effect on Static Splitting Tensile Strength of Concrete : Experimental and Numerical Studies, 32 (2020) 1–14. https://doi.org/10.1061/(ASCE)MT.1943-5533.0003382.

[41] S.P. Timoshenko, J.N. Goodier, H.N. Abramson, Theory of Elasticity (3rd ed.), J Appl Mech 37 (1970) 888. https://doi.org/10.1115/1.3408648.

[42] X. Régal, Caractérisation du comportement en traction du béton sous fortes sollicitations : essais de flexion trois points aux barres de Hopkinson, (2016).

[43] C. Rocco, G. V Guinea, J. Planas, M. Elices, Mechanism of rupture in splitting test, Materials Journal 96 (1999) 52–60.

[44] V.J. García, C.O. Márquez, A.R. Zúñiga-Suárez, B.C. Zuñiga-Torres, L.J. Villalta-Granda, Brazilian test of concrete specimens subjected to different loading geometries: Review and new insights, Int J Concr Struct Mater 11 (2017) 343–363.

[45] P.J.F. Wright, Comments on an indirect tensile test on concrete cylinders, Magazine of Concrete Research 7 (1955) 87–96.

[46] E. Denneman, E.P. Kearsley, A.T. Visser, Splitting tensile test for fibre reinforced concrete, Mater Struct 44 (2011) 1441–1449.

[47] V.M. Malhotra, Are 4 x 8 inch concrete cylinders as good as 6 x 12 inch cylinders for quality control of concrete?, in: Journal Proceedings, 1976: pp. 33–36.

[48] C. Rocco, G. V Guinea, J. Planas, M. Elices, Size effect and boundary conditions in the Brazilian test: Experimental verification, Mater Struct 32 (1999) 210–217.

[49] S. Carmona, Effect of specimen size and loading conditions on indirect tensile test results, Materiales de Construcción 59 (2009) 7–18.

[50] W. Li-cheng, X. Li-kun, S. Yu-pu, Mesoscale modeling on size effect of splitting tensile strength and flexural compressive strength of concrete, 工程力学 31 (2014) 69–76.

[51] N. Zhang, Size effect and failure characteristics on splitting tensile strength of concrete, DA Lian: Da Lian University of Technology (2016).

[52] F.P. Zhou, R. V Balendran, A.P. Jeary, Size effect on flexural, splitting tensile, and torsional strengths of high-strength concrete, Cem Concr Res 28 (1998) 1725–1736.

[53] T. Hasegawa, T. Shioya, T. Okada, Size effect on splitting tensile strength of concrete, in: Proceedings Japan Concrete Institute 7th Conference, 1985: pp. 309–312.

[54] Z.P. Bazant, M.T. Kazemi, T. Hasegawa, J. Mazars, Size effect in Brazilian split-cylinder tests. Measurements and fracture analysis, ACI Mater J 88 (1991) 325–332.

[55] C. Rocco, G. V Guinea, J. Planas, M. Elices, Size effect and boundary conditions in the Brazilian test: theoretical analysis, Mater Struct 32 (1999) 437–444.

[56] F.M.B. and J.G. MacGregor, Effect of Moisture Condition on Concrete Core Strengths, ACI Mater J 91 (n.d.). https://doi.org/10.14359/4328.

[57] Y. Wu, Z. Qi, M. Niu, Y. Yao, Z. Luo, K. Zhang, Effect of Moisture Condition of Brick–Concrete Recycled Coarse Aggregate on the Properties of Concrete, Materials 15 (2022) 7204.

[58] X. Chen, L. Sun, W. Zhao, Y. Zheng, Effect of loading rate on tensile and failure behavior of concrete, Sensors 20 (2020) 5994.

[59] B. Standard, B.S. EN, EN 12390-5 (2009)–Testing hardened concrete, Flexural Strength of Test Specimens (n.d.).

[60] P.K. Mehta, P. Monteiro, Concrete: microstructure, properties, and materials, (No Title) (2006).

[61] P.J.F. Wright, F. Garwood, The effect of the method of test on the flexural strength of concrete, Magazine of Concrete Research 4 (1952) 67–76.

[62] J.M. Raphael, Tensile strength of concrete, in: Journal Proceedings, 1984: pp. 158–165.

[63] W.F. Kellermann, Effect of Size of Specimen, Size of Aggregate and Method of Loading Upon the Uniformity of Flexural Strength Results, Public Roads 13 (1933) 177–184.

[64] F. V Reagel, T.F. Willis, The effect of dimensions of test specimens on the flexural strength of concrete, Public Roads 12 (1931) 37–46.

[65] P.M. Carrasquillo, R.L. Carrasquillo, Improved concrete quality control procedures including third point loading, (1987).

[66] D. McHenry, J.J. Shideler, Review of Data on Effect of Speed in Mechanical Testing of Concrete, Symposium on Speed of Testing of Non-Metallic Materials STP185-EB (1956) 0. https://doi.org/10.1520/STP46845S.

[67] P. Yuan, X. Ren, Y. Xie, Experimental Study on the Flexural Properties of Steel-Fibre-Reinforced Concrete Specimens with Different Heights, Sustainability 16 (2024) 1900.

[68] C.D. Johnston, E.H. Sidwell, Influence of drying on strength of concrete specimens, in: Journal Proceedings, 1969: pp. 748–755.

[69] K.E.C. Nielsen, Effect of various factors on the flexural strength of concrete test beams, Magazine of Concrete Research 5 (1954) 105–114.

[70] S. Mindess, J.F. Young, D. Darwin, Concrete, PrenticeHall Inc, Englewood Cliffs, NJ (1981).

[71] J. Weiss, Elastic properties, creep, and relaxation, in: Significance of Tests and Properties of Concrete and Concrete-Making Materials, ASTM International, 2006.

[72] J.G.M. Van Mier, M.R.A. Van Vliet, Uniaxial tension test for the determination of fracture parameters of concrete: state of the art, Eng Fract Mech 69 (2002) 235–247.

[73] Y. Dai, Y. Li, X. Xu, Q. Zhu, Y. Yin, S. Ge, A. Huang, L. Pan, Characterization of tensile failure behaviour of magnesia refractory materials by a modified dog-bone shape direct tensile method and splitting tests, Ceram Int 46 (2020) 6517–6525.

[74] F. Liu, W. Ding, Y. Qiao, Experimental investigation on the tensile behavior of hybrid steel-PVA fiber reinforced concrete containing fly ash and slag powder, 241 (2020) 1–14.

[75] T.C. RILEM, CPC 7 Direct tension of concrete specimens, l975, RILEM Recommendations for the Testing and Use of Constructions Materials (1994) 23–24.

[76] K. Yu, L. Li, J. Yu, Y. Wang, J. Ye, Q. Xu, Direct tensile properties of engineered cementitious composites: A review, Constr Build Mater 165 (2018) 346–362.

[77] K.E. Kesner, S.L. Billington, K.S. Douglas, Cyclic response of highly ductile fiber-reinforced cement-based composites, Materials Journal 100 (2003) 381–390.

[78] V.C. Li, H. Wu, M. Maalej, D.K. Mishra, T. Hashida, Tensile behavior of cement-based composites with random discontinuous steel fibers, Journal of the American Ceramic Society 79 (1996) 74–78.

[79] N. Liang, The mechanics performance test of multi-scale polypropylene fiber concrete and the study of tension and compression damage constitutive model, Chongqing University (2014).

[80] M.J. Roth, C.D. Eamon, T.R. Slawson, T.D. Tonyan, A. Dubey, Ultra-High-Strength, Glass Fiber-Reinforced Concrete: Mechanical Behavior and Numerical Modeling., ACI Mater J 107 (2010).

[81] L. Xu, H. Xu, Y. Chi, Y. Zhang, Experimental study on tensile strength of steel-polypropylene hybrid fiber reinforced concrete, Adv Sci Lett 4 (2011) 911–916.

[82] Regulation of China Association for Engineering Construction Standardization, Standard test methods for fiber reinforced concrete (CECS 13:2009), Beijing, 2009.

[83] S.D.P. Benson, B.L. Karihaloo, CARDIFRC®–Development and mechanical properties. Part III: Uniaxial tensile response and other mechanical properties, Magazine of Concrete Research 57 (2005) 433–443.

[84] D.L. Nguyen, G.S. Ryu, K.T. Koh, D.J. Kim, Size and geometry dependent tensile behavior of ultra-high-performance fiber-reinforced concrete, Compos B Eng 58 (2014) 279–292.

[85] P. Jun, V. Mechtcherine, Behaviour of strain-hardening cement-based composites (SHCC) under monotonic and cyclic tensile loading: part 1–experimental investigations, Cem Concr Compos 32 (2010) 801–809.

[86] H. Li, G. Liu, Tensile properties of hybrid fiber-reinforced reactive powder concrete after exposure to elevated temperatures, Int J Concr Struct Mater 10 (2016) 29–37.

[87] K. Wille, S. El-Tawil, A.E. Naaman, Properties of strain hardening ultra high performance fiber reinforced concrete (UHP-FRC) under direct tensile loading, Cem Concr Compos 48 (2014) 53–66.

[88] W. Zheng, A.K.H. Kwan, P.K.K. Lee, Direct tension test of concrete, Materials Journal 98 (2001) 63–71.

[89] T.H. Wee, Ã.H.R.Ã. Lu, S.Ã. Swaddiwudhipong, Tensile strain capacity of concrete under various states of stress, (2000) 185–193.

[90] R.H. Elvery, W. Haroun, A direct tensile test for concrete under long- or short-term loading, Magazine of Concrete Research 20 (1968) 111–116. https://doi.org/10.1680/macr.1968.20.63.111.

[91] C.D. Johnston, Testing concrete in tension and in compression, Magazine of Concrete Research 20 (1968) 221–228.

[92] M.C. Baishya, R.L. Cook, M.T. Kelly, Testing of polymer injection material, Concrete International 19 (1997) 48–51.

[93] W. Liao, P. Chen, C. Hung, S.K. Wagh, An Innovative Test Method for Tensile Strength of Concrete by Applying the Strut-and-Tie Methodology, (2020).

[94] X. Nianxiang, L. Wenyan, Determining tensile properties of mass concrete by direct tensile test, Materials Journal 86 (1989) 214–219.

[95] W.-T. Lin, A. Cheng, R. Huang, T.-C. Cheng, A method for testing the strength of concrete using uniaxial direct tension, Journal of the Chinese Institute of Engineers 36 (2013) 295–303.

[96] M.I. Khan, Direct tensile strength measurement of concrete, Applied Mechanics and Materials 117–119 (2012) 9–14. https://doi.org/10.4028/www.scientific.net/AMM.117-119.9.

[97] S.-J. Choi, K.-H. Yang, J.-I. Sim, B.-J. Choi, Direct tensile strength of lightweight concrete with different specimen depths and aggregate sizes, Constr Build Mater 63 (2014) 132–141.

[98] S. Swaddiwudhipong, H.-R. Lu, T.-H. Wee, Direct tension test and tensile strain capacity of concrete at early age, Cem Concr Res 33 (2003) 2077–2084.

[99] F. Alhussainy, H.A. Hasan, S. Rogic, M.N. Sheikh, M.N.S. Hadi, Direct tensile testing of self-compacting concrete, Constr Build Mater 112 (2016) 903–906.

[100] M. UEDA, N. HASEBE, M. SATO, H. OKUDA, Fracture mechanism of plain concrete under uniaxial tension, Doboku Gakkai Ronbunshu 1993 (1993) 69–78.

[101] J. Nilimaa, R. Nilforoush, A direct tensile strength testing method for concrete from existing structures, CivilEng 4 (2023) 333–344.

[102] U. Standard, 4914–92,", Procedure for Direct Tensile Strength, Static Modulus of Elasticity, and Poisson's Ratio of Cylindrical Concrete Specimens in Tension," Concrete Manual, United States Department of Interior, Bureau of Reclamation, Denver, CO (1992).

[103] J.J. Kim, M. Reda Taha, Experimental and numerical evaluation of direct tension test for cylindrical concrete specimens, Advances in Civil Engineering 2014 (2014). https://doi.org/10.1155/2014/156926.

[104] J.J. Kim, M.R. Taha, Research Article Experimental and Numerical Evaluation of Direct Tension Test for Cylindrical Concrete Specimens, (n.d.).

[105] D.M. Yan, Experimental and theoretical study on the dynamic properties of concrete, Dalian University of Technology, China, 2006.

[106] F. Alhussainy, H.A. Hasan, M.N. Sheikh, M.N.S. Hadi, A New Method for Direct Tensile Testing of Concrete, J Test Eval 47 (2019) 704–718. https://doi.org/10.1520/JTE20170067.

[107] V. Sarfarazi, H. Haeri, P. Ebneabbasi, A.B. Shemirani, A. Hedayat, Determination of tensile strength of concrete using a novel apparatus, Constr Build Mater 166 (2018) 817–832.

[108] S.M. Chassib, S.K. Zemam, M.J. Madhi, New approach of concrete tensile strength test, Case Studies in Construction Materials 12 (2020) e00347.

[109] S. Popovics, Strength relationships for fly ash concrete, J. Am. Concr. Inst.;(United States) 79 (1982).

[110] S. Popovics, History of a mathematical model for strength development of Portland cement concrete, Materials Journal 95 (1998) 593–600.

[111] W. Khaliq, V.K.R. Kodur, Effect of High Temperature on Tensile Strength of Different Types of High-Strength Concrete., ACI Mater J 108 (2011).

[112] I. Narrow, E. Ullberg, Correlation between tensile splitting strength and flexural strength of concrete, in: Journal Proceedings, 1963: pp. 27–38.

[113] S. Bhanja, B. Sengupta, Influence of silica fume on the tensile strength of concrete, Cem Concr Res 35 (2005) 743–747.

[114] Y. Choi, R.L. Yuan, Experimental relationship between splitting tensile strength and compressive strength of GFRC and PFRC, Cem Concr Res 35 (2005) 1587–1591.

[115] W.H. Price, Factors influencing concrete strength, in: Journal Proceedings, 1951: pp. 417–432.

[116] H.F. Gonnerman, Compression, flexure and tension tests of plain concrete, Proc. ASTM, Part II 28 (1928) 527.

[117] S.A. Mirza, J.G. MacGregor, M. Hatzinikolas, Statistical descriptions of strength of concrete, Journal of the Structural Division 105 (1979) 1021–1037.

[118] C.E. Kesler, Statistical relation between cylinder modified cube and beam strength of plain concrete, TAM R 55 (1954).

[119] A.N. Johnson, Concrete in tension, in: Proc West Mark Ed Assoc Conf, American Society for Testing and Materials, 1926: pp. 441–450.

[120] S. Popovics, Strength and related properties of concrete: A quantitative approach, John Wiley & Sons, 1998.

[121] S.H. Ahmad, S.P. Shah, Structural properties of high strength concrete and its implications for precast prestressed concrete, PCI Journal 30 (1985) 92–119.

[122] B.W. Xu, H.S. Shi, Correlations among mechanical properties of steel fiber reinforced concrete, Constr Build Mater 23 (2009) 3468–3474.

[123] R. Perumal, Correlation of compressive strength and other engineering properties of high-performance steel fiber–reinforced concrete, Journal of Materials in Civil Engineering 27 (2015) 4014114.

[124] W. Abbass, M.I. Khan, S. Mourad, Evaluation of mechanical properties of steel fiber reinforced concrete with different strengths of concrete, Constr Build Mater 168 (2018) 556–569.

[125] F.A. Oluokun, E.G. Burdette, J.H. Deatherage, Splitting tensile strength and compressive strength relationships at early ages, Materials Journal 88 (1991) 115–121.

[126] N. Arıoglu, Z.C. Girgin, E. Arıoglu, Evaluation of ratio between splitting tensile strength and compressive strength for concretes up to 120 MPa and its application in strength criterion, ACI Mater J 103 (2006) 18–24.

[127] N.J. Gardner, Effect of Temperature on the Early-age Properties of Type I, Type II, and Type III/fly ash concretes with temperature, Materials Journal 87 (1990) 68–78.

[128] D. V Phillips, Z. Binsheng, Direct tension tests on notched and un-notched plain concrete specimens, Magazine of Concrete Research 45 (1993) 25–35.

[129] Q. Li, Y.L. Duan, G.L. Wang, Behaviour of large concrete specimens in uniaxial tension, Magazine of Concrete Research 54 (2002) 385–391.

[130] C. CEB-FIP, Model Code 1990 for Concrete Structures, Comit e Euro-International du B eton and F ed eration Internationale de la Pr econtrainte, (1993).

[131] 318 ACI Committee, Building code requirements for structural concrete (ACI 318-08) and commentary, in: American Concrete Institute, 2008.

[132] A.C. Institute, Building Code Requirements for Structural Concrete (ACI 318-14): An ACI Standard: Commentary on Building Code Requirements for Structural Concrete (ACI 318R-14), an ACI Report, in: American Concrete Institute, 2012.

[133] S. Ros, H. Shima, Relationship between splitting tensile strength and compressive strength of concrete at early age with different types of cements and curing temperature histories, Concr. Inst. Proc 35 (2013) 427–432.

[134] N.J. Carino, H.S. Lew, Re-examination of the relation between splitting tensile and compressive strength of normal weight concrete, in: Journal Proceedings, 1982: pp. 214–219.

[135] F. Oluokun, Prediction of concrete tensile strength from its compressive strength: an evaluation of existing relations for normal weight concrete, Materials Journal 88 (1991) 302–309.

[136] N.J. GARDNER, EFFECT OF TEMPERATURE ON THE EARLY-AGE PROPERTIES OF TYPE-I, TYPE-III, AND TYPE-I FLY-ASH CONCRETES-CLOSURE, ACI Mater J 87 (1990) 654–655.

[137] C. Eyrolles, BAEL Rules 91 revised 99: Technical rules for the design and calculation of reinforced concrete works and constructions following the limit states method, Eyrolles Editions, 2000.

[138] P. Code, Eurocode 2: design of concrete structures-part 1–1: general rules and rules for buildings, British Standard Institution, London 668 (2005) 659–668.

[139] O. Merabet, N. Amoura, M. Bentchikou, Dispositif mécanique, permettant la mesure de la résistance en traction de matériaux cimentaires, adapté aux presses à béton, Institut National Algérien de La propriété industrielle, N° 11988, 2023.

[140] G. Dreux, F. Gorisse, J. Simonnet, COMPOSITION DES BETONS: METHODE DREUX-GORISSE-BILAN DE CINQ ANNEES D'APPLICATION EN COTE D'IVOIRE, ANN ITBTP (1983).

[141] H. Okamura, K. Ozawa, M. Ouchi, Self-compacting concrete, Structural Concrete 1 (2000) 3–17.

[142] STN EN 206-1 (STN 73 2403) (2002) Concrete. Part 1: specification, performance, production and conformity. Slovak Institute for Technical Normalization, Bratislava, Publication No. 85349:72, (n.d.).

[143] B. Standard, Testing hardened concrete, Compressive Strength of Test Specimens, BS EN (2009) 12390–12393.

[144] B.S. En, 12390-3:(2009). Testing Hardened Concrete. Compressive Strength of Test Specimens, British Standard Institution, London 16 (2019).

[145] B.S. En, 12390-6:(2009). Testing Hardened Concrete. Tensile Splitting Strength of Test Specimens, British Standard Institution, London (2009).

[146] B. Standard, B.S. EN, EN 12390-5 (2009)–Testing hardened concrete, Flexural Strength of Test Specimens (n.d.).

[147] B.S. En, 12390-6:(2009). Testing Hardened Concrete. Tensile Splitting Strength of Test Specimens, British Standard Institution, London (2009).

[148] W.-T. Lin, A. Cheng, R. Huang, T.-C. Cheng, A method for testing the strength of concrete using uniaxial direct tension, Journal of the Chinese Institute of Engineers 36 (2013) 295–303.

[149] F. Alhussainy, H.A. Hasan, M.N. Sheikh, M.N.S. Hadi, A New Method for Direct Tensile Testing of Concrete, J Test Eval 47 (2019) 704–718. https://doi.org/10.1520/JTE20170067.

[150] S. Popovics, Strength relationships for fly ash concrete, in: Journal Proceedings, 1982: pp. 43–49.

[151] S. Popovics, History of a mathematical model for strength development of Portland cement concrete, Materials Journal 95 (1998) 593–600.

[152] W. Khaliq, V.K.R. Kodur, Effect of High Temperature on Tensile Strength of Different Types of High-Strength Concrete., ACI Mater J 108 (2011).

[153] C. Rocco, G. V Guinea, J. Planas, M. Elices, Review of the splitting-test standards from a fracture mechanics point of view, Cem Concr Res 31 (2001) 73–82.

[154] M.F.M. Zain, H.B. Mahmud, A. Ilham, M. Faizal, Prediction of splitting tensile strength of high-performance concrete, Cem Concr Res 32 (2002) 1251–1258.

[155] S. Wu, X. Chen, J. Zhou, Tensile strength of concrete under static and intermediate strain rates: Correlated results from different testing methods, Nuclear Engineering and Design 250 (2012) 173–183. https://doi.org/10.1016/j.nucengdes.2012.05.004.

Annexes

Annexe 1

بـــراءة إختـــراع
BREVET D'INVENTION

R2-FO-10

(22) Date de dépôt: 01/02/2022

(11) N° du brevet : 11988

(21) N° Dépôt: 220064

(54) Titre de l'invention:
Dispositif mécanique, permettant la mesure de la résistance en traction de matériaux cimentaires, adapté aux presses à béton..

(71) Déposant :
Laboratoire de Mécanique, Physique et Modélisation Mathématique (LMP2M)
Université de Médéa, Bloc des laboratoires de recherche, Pôle urbain - Médéa
26000 Algérie

(72) Inventeur :
MERABET Oussama-AMOURA Nasreddine-BENTCHIKOU Mohamed

(73) Titulaire :
Laboratoire de Mécanique, Physique et Modélisation Mathématique (LMP2M)
Université de Médéa, Bloc des laboratoires de recherche, Pôle urbain - Médéa
26000 Algérie

(74) Mandataire :

(30) Données relatives à la priorité:

BREVET D'INVENTION

Déposant

Laboratoire de Mécanique, Physique et Modélisation Mathématique

Bloc des laboratoires de recherche, Université Dr Yahia Farés de Médéa,

Pôle urbain – 26000, Médéa, Algérie.

Titre de l'invention

Dispositif mécanique, permettant la mesure de la résistance en traction de matériaux cimentaires, adapté aux presses à béton

Titre de l'invention

Dispositif mécanique, permettant la mesure de la résistance en traction de matériaux cimentaires, adapté aux presses à béton

Domaine Technique auquel se rapporte l'Invention

5   La présente invention se rapporte au domaine technique des essais mécaniques en génie civil, plus particulièrement, elle concerne les dispositifs permettant de mesurer la résistance en traction directe du béton sur des éprouvettes cylindriques.

But de l'invention

La détermination de la résistance en traction des matériaux cimentaire, tel le
10   béton, est majoritairement réalisée via des tests indirects tels la flexion trois ou quatre points ou par fendage (essai brésilien). Dans ces essais, l'estimation de la limite en traction du matériau est appréciée au moyen de formules dérivées de la théorie de l'élasticité. L'essai de traction direct est un test expérimental permettant de mesurer, de manière directe, la résistance à la traction et le module d'élasticité
15   du matériau cimentaire, mais sa mise en œuvre nécessite des machines de grandes tailles adaptées aux dimensions importantes des éprouvettes.

L'objectif de la présente invention est de fournir un dispositif à faible coût, adapté aux presses à béton, qui permet de réaliser l'essai de traction direct sur une éprouvette cylindrique et mesurer la résistance en traction du matériau.

20   Ce système mécanique de traction est destiné aux organismes, publics ou privés, équipés de presses à béton (universités, laboratoires de recherche en génie civil laboratoires privés spécialisés dans les essais du béton…) et travaillant sur de

nouveaux types de bétons afin de déterminer leurs caractéristiques mécaniques en traction.

La mise en Œuvre de l'invention

5   Le dispositif est composé de deux cadres rigides, l'un extérieur et l'autre intérieur, pouvant coulisser l'un par rapport à l'autre. Un effort de pression sur les deux cadres produit un effort inversé (une tension) sur l'éprouvette, fixée aux mâchoires. Les pièces spécifiques, comme les mâchoires, les axes de guidage, les traverses et les bases des cadres sont usinées à partir de brut d'acier par

10 commande numérique. Les pièces standards comme les boulons et les écrous sont achetés dans le commerce.

Etat de la technique antérieure

L'essai de traction directe est le plus préconisé pour caractériser le comportement d'un matériau sous un effort longitudinal de traction. Cependant, La résistance à la

15 traction sur des éprouvettes en béton reste l'une des caractéristiques des moins bien définies, notamment à cause de l'absence d'une technique expérimentale qui soit à la fois économique et fiable tout en restant parfaitement rigoureuse au point de vue mécanique.

Une recherche étendue sur le net avec les mots clé « Direct tensile test of

20 concrete», fait ressortir que les dispositifs d'essai de matériaux cimentaires ont été le sujet de plusieurs inventions brevetées dans divers pays.

Titre de l'invention	N° de Brevet	Date	Titulaire
Apparatus for testing material strength	US 3975950	24/08/1976	Karoly Erdei
A New Concrete Axial Tensile Test Device	CN 211955007 U	17/11/2020	Liaocheng University
A novel direct tensile test device for concrete sample	CN 210108832 U	21/02/2020	Hu Liangpeng
Apparatus for tensile test by compression	US 2015/0377755A1	31/12/2015	Hasan Semsi
Concrete tension-compression dual-function dynamic creep test device	CN 111735706	02/10/2020	Jiang Heng

Enoncé des figures

Figure 1 : Vue assemblée du dispositif d'essai avec les repères des différentes pièces.

5   Figure 2 : Vue éclatée du dispositif montrant les différentes pièces de l'ensemble.

Présentation de l'invention et mode de réalisation

Dans un mode de réalisation de l'invention, le dispositif proposé (Figure 1) est constitué d'un cadre extérieur et d'un cadre intérieur en acier. Chaque cadre comporte une base plate rectangulaire et une traverse, qui sont parallèles l'une à

10   l'autre. Les deux cadres du dispositif sont assemblées par des axes de guidage (1) de même taille. Ces derniers sont reliés verticalement, entre la base (2) et la traverse supérieure (4), pour le cadre extérieur, et la base (7) avec la traverse

inférieure (8) pour le cadre inférieur, par l'intermédiaire des boulons (5) (détail sur figure 2). Les boulons (5), passent à travers les trous des traverses, sont vissés dans les bases (2 et 7) avec les axes de guidage (1) pour être rigidement liés.

5 L'éprouvette utilisée pour le test est de forme cylindrique, selon la norme européenne NF EN 12390-1 (100 mm de diamètre sur 200 mm de hauteur). Cette dernière est fixée verticalement entre les deux bases (2) et (7) par l'intermédiaire des mâchoires (3) et des tiges filetées (9), ancrées dans l'éprouvette sur une profondeur de 50 mm. Les mâchoires (3) sont reliées aux bases (2) et (7) et à l'éprouvette au moyen des goupilles cylindriques (6).

10 Pour effectuer le test de traction, le dispositif proposé est monté sur une presse hydraulique qui exerce un effort de compression sur ce dernier. A ce moment, le dispositif réalise une inversion de la force appliquée par la presse hydraulique de telle sorte que l'éprouvette s'étire. La mesure de la force de traction est déterminée par le système d'acquisition de la presse hydraulique.

15 Dans un mode de réalisation de l'invention, l'éprouvette est équipée de jauges de contraintes permettant la mesure de la déformation longitudinale au moyen d'un pont de Wheatstone.

20

Revendications

1- Dispositif d'essai de traction directe permettant des essais sur des éprouvettes cylindriques faites d'un matériau cimentaire.

5

2- Dispositif selon la revendication 1, caractérisé en ce qu'il peut être monté sur une presse hydraulique et permet d'inverser la sollicitation de compression en effort de traction sur le corps de l'éprouvette.

3- Dispositif selon la revendication 1, caractérisé en ce qu'il présente un
10   encombrement réduit et peut être produit localement à coût réduit.

4- Dispositif selon la revendication 1, caractérisé en ce qu'il est conçu pour tester des éprouvettes en béton de forme cylindriques de 100 mm de diamètre sur 200 mm de hauteur.

15

20

Abrégé descriptif

La présente invention est un dispositif d'essai de traction directe sur éprouvettes en matériaux cimentaires. Les éprouvettes utilisées ont un diamètre de 100 mm et une hauteur de 200 mm. Ces dernières sont fixées aux mâchoires du dispositif à
5 l'aide de tiges filetées ancrés dans les éprouvettes sur une profondeur de 50 mm. Ce dispositif se compose de deux cadres, chacun comporte une base, une traverse et deux axes de guidage. Le dispositif selon l'invention se monte sur une presse à béton et réalise une inversion de la compression appliquée par la machine en tension appliquée sur le corps de l'éprouvette.
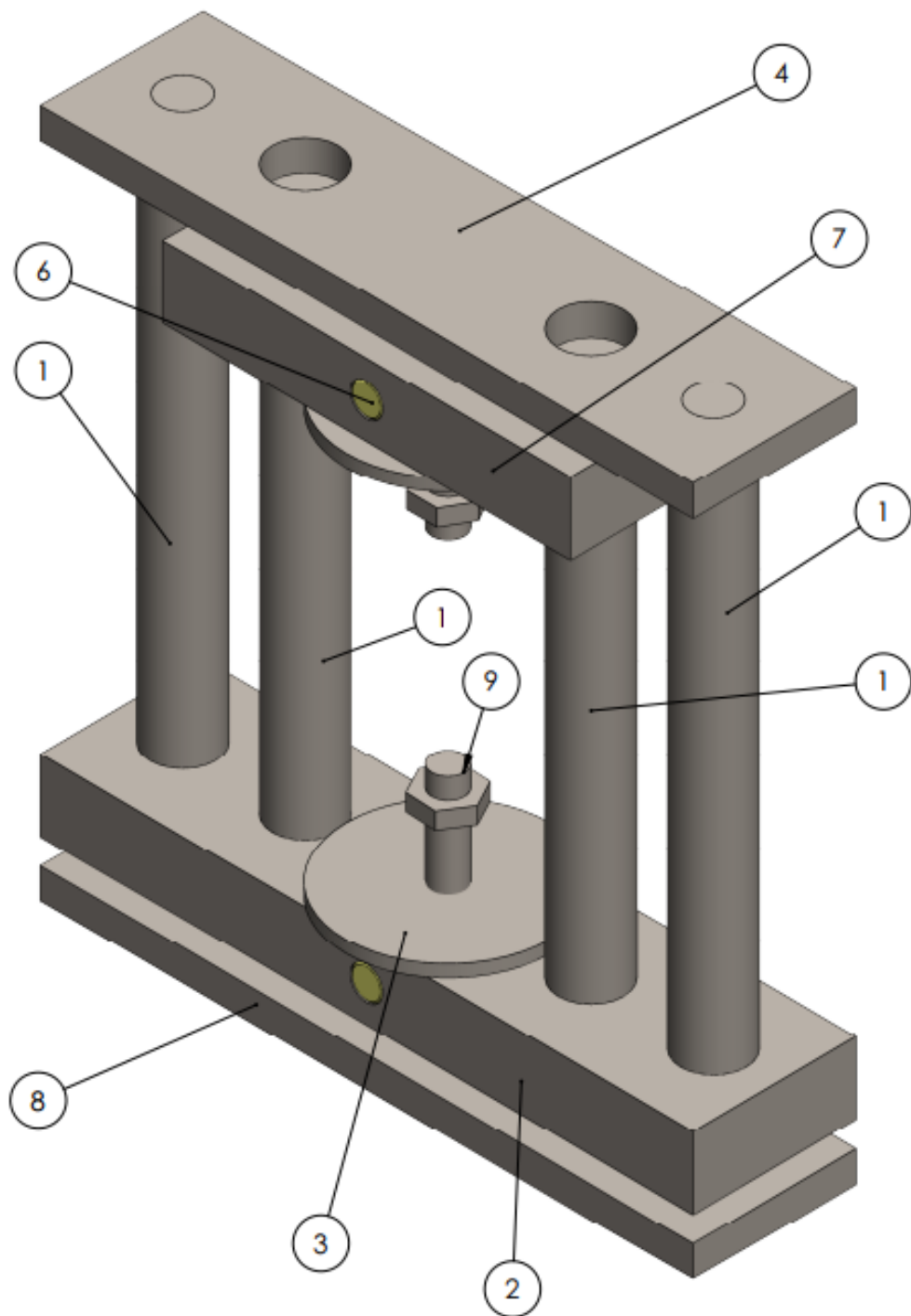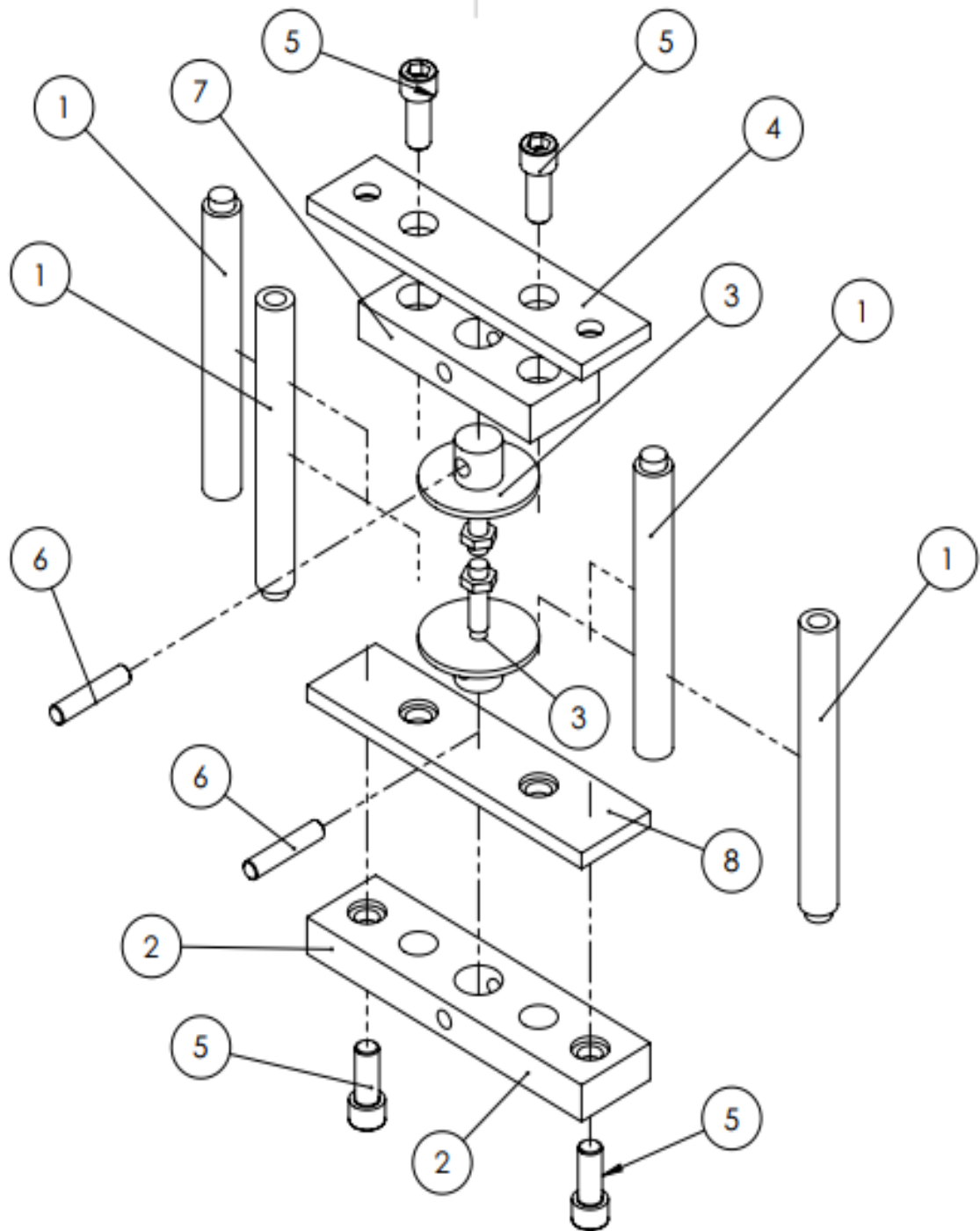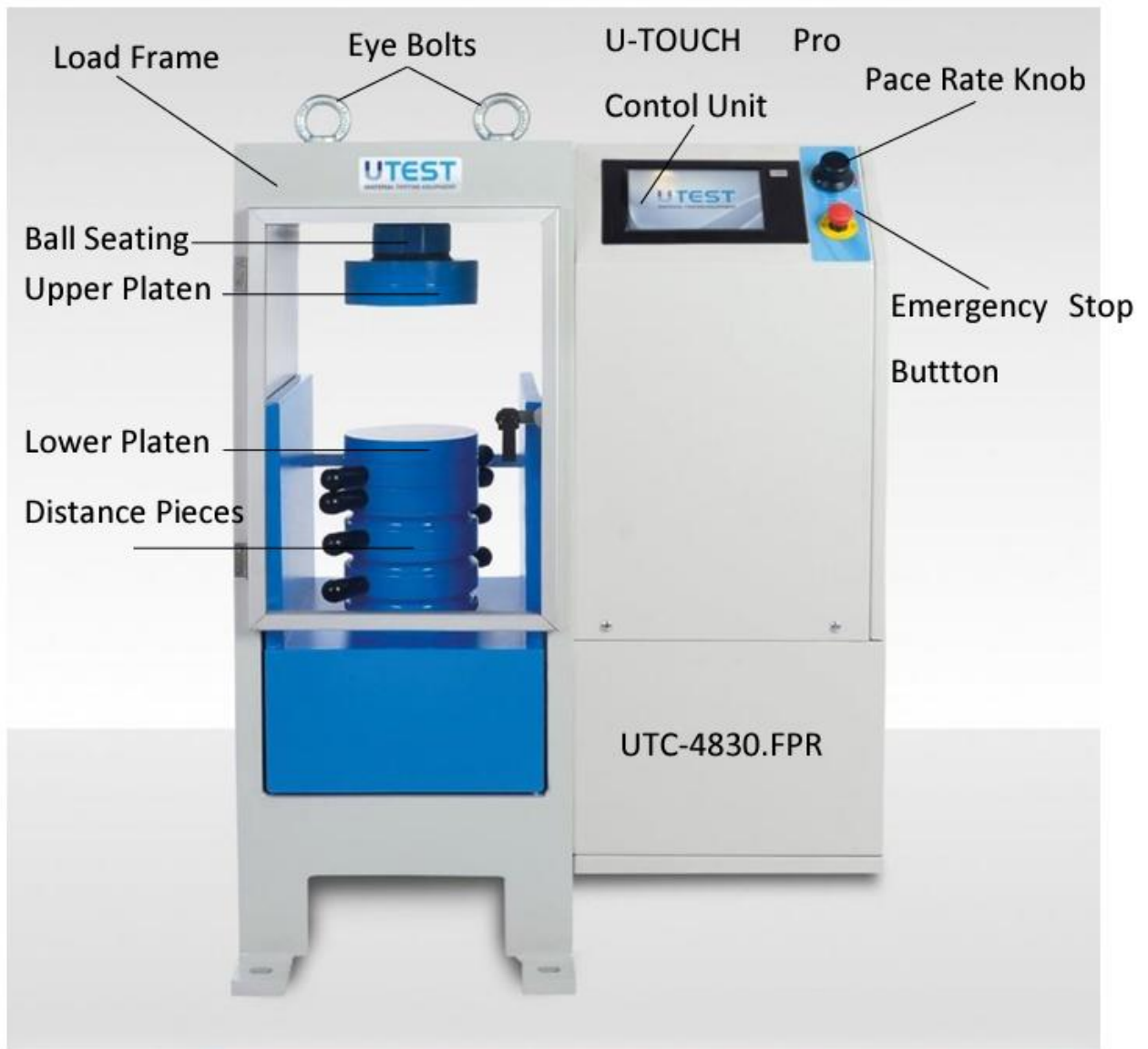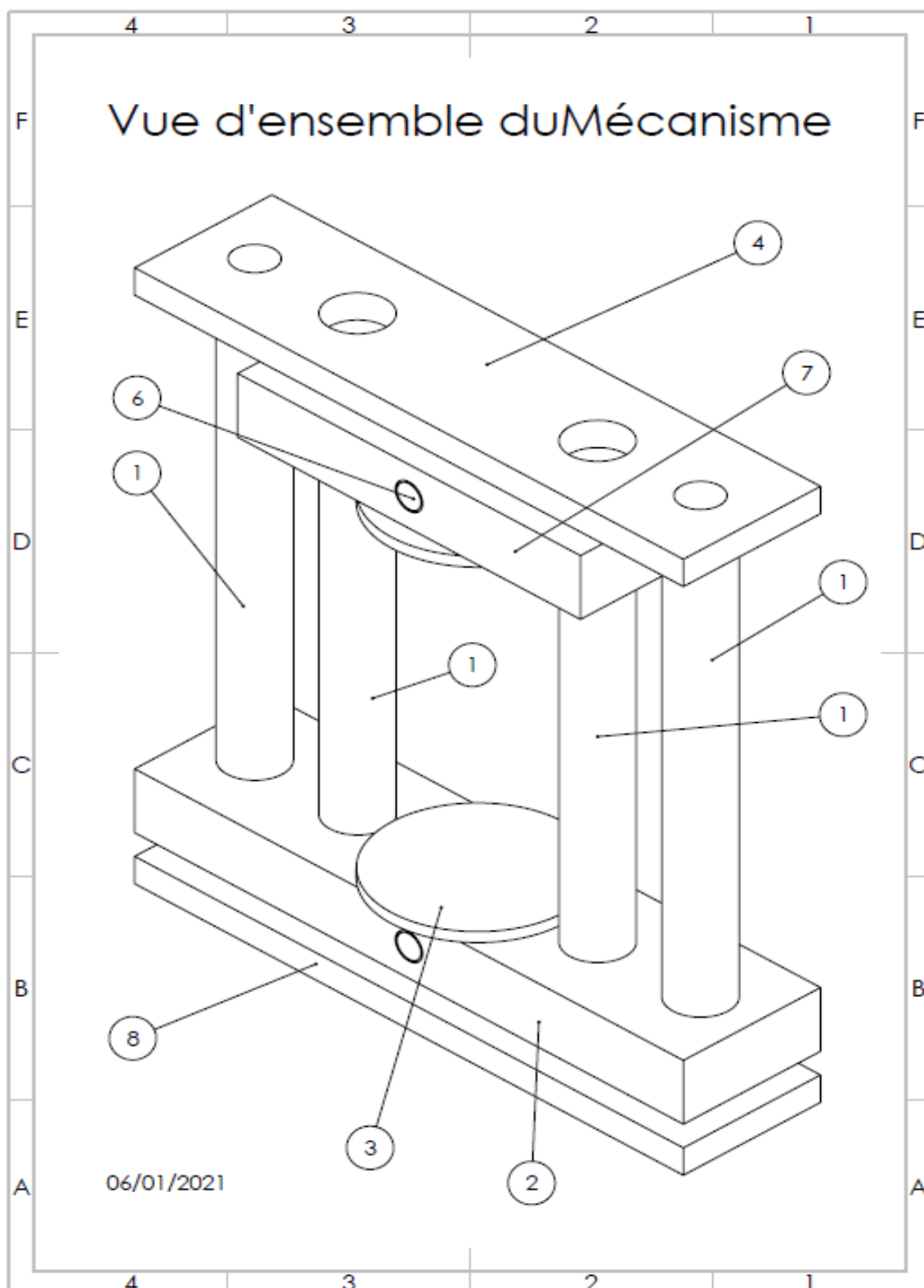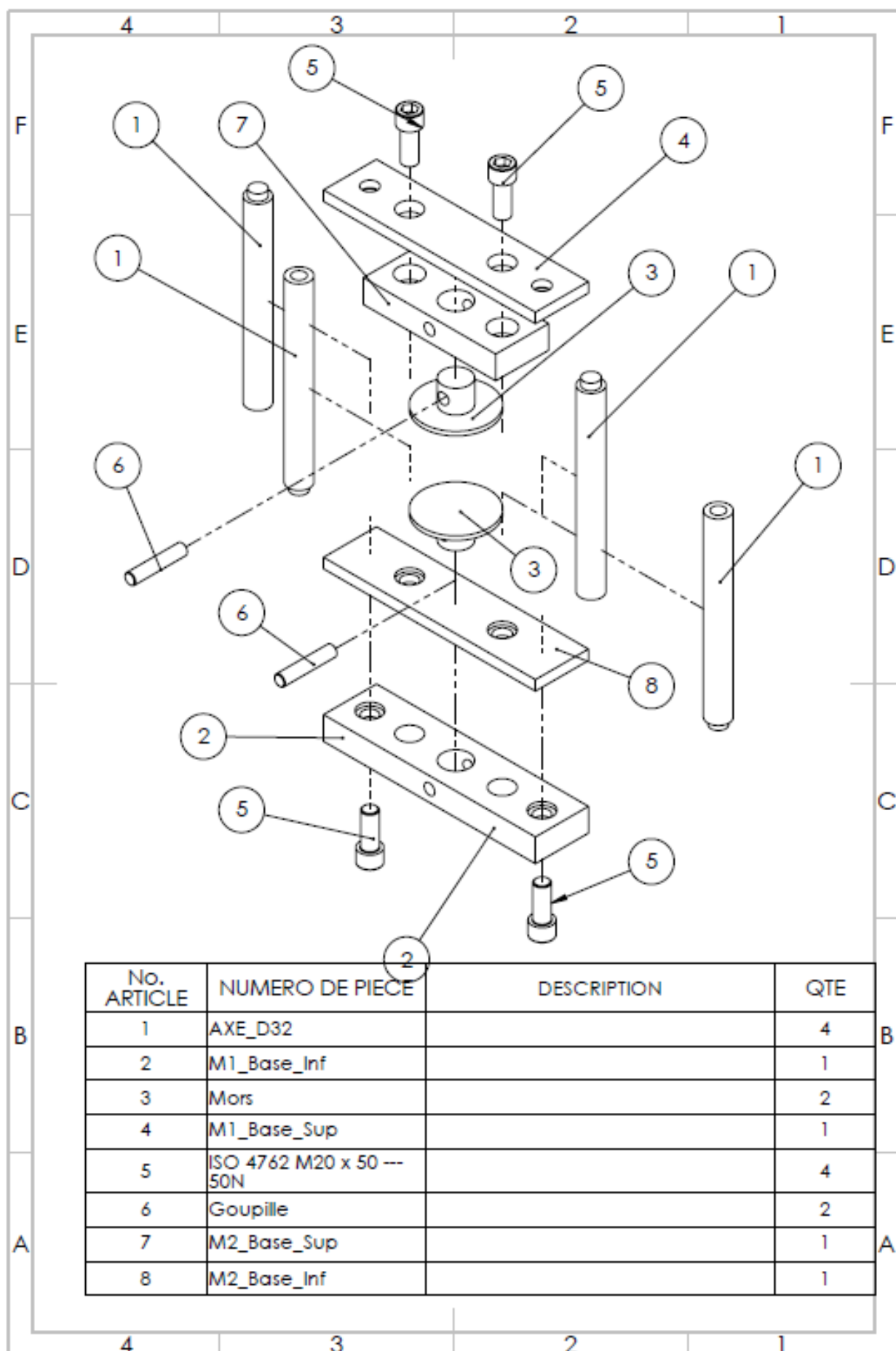
10

15

Figure 1

Figure 2

Annexe 2

Automatic compression testing machine

Annexe 3

Vue d'ensemble duMécanisme

06/01/2021

No. ARTICLE	NUMERO DE PIECE	DESCRIPTION	QTE
1	AXE_D32		4
2	M1_Base_Inf		1
3	Mors		2
4	M1_Base_Sup		1
5	ISO 4762 M20 x 50 --- 50N		4
6	Goupille		2
7	M2_Base_Sup		1
8	M2_Base_Inf		1

Annexe 4

Schematic drawing of the mold
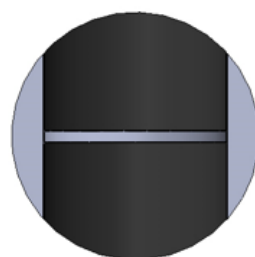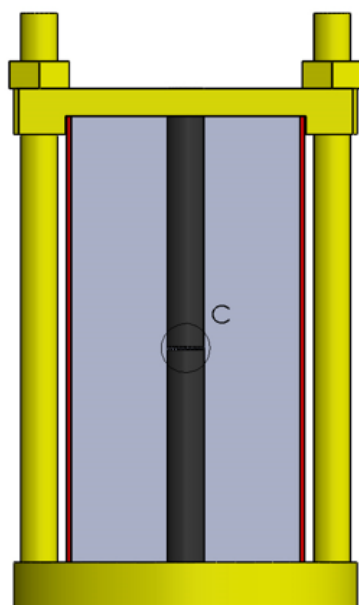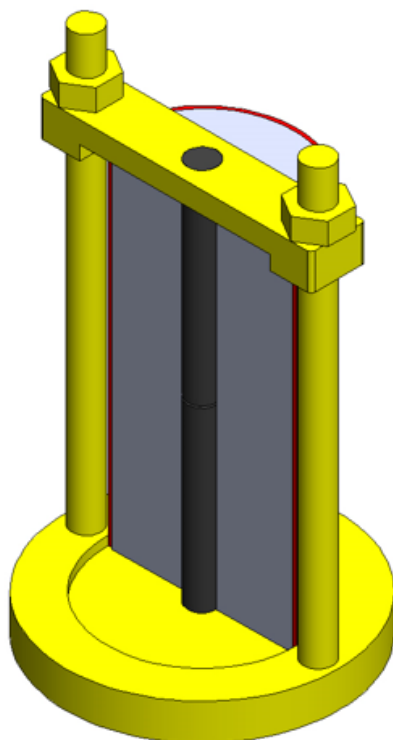
DETAILC

Annexe 6

Schematic drawing of the testing device

DETAIL D

Annexe 6

Epoxy Adhesive

EPOTEK FIX

PÂTE ÉPOXYDIQUE THIXOTROPE POUR COLLAGE STRUCTURAL ET RÉPARATION

TEKNA CHEM
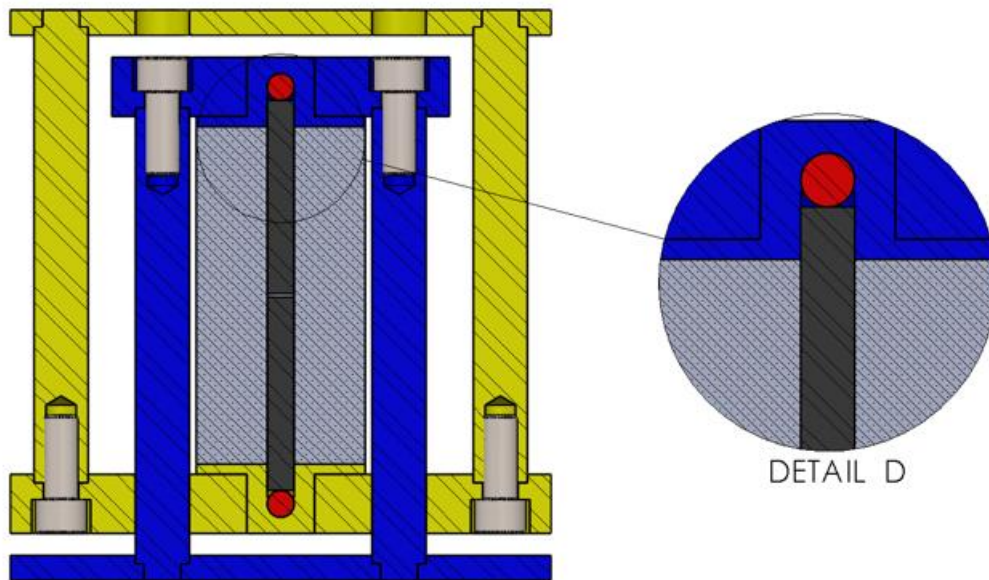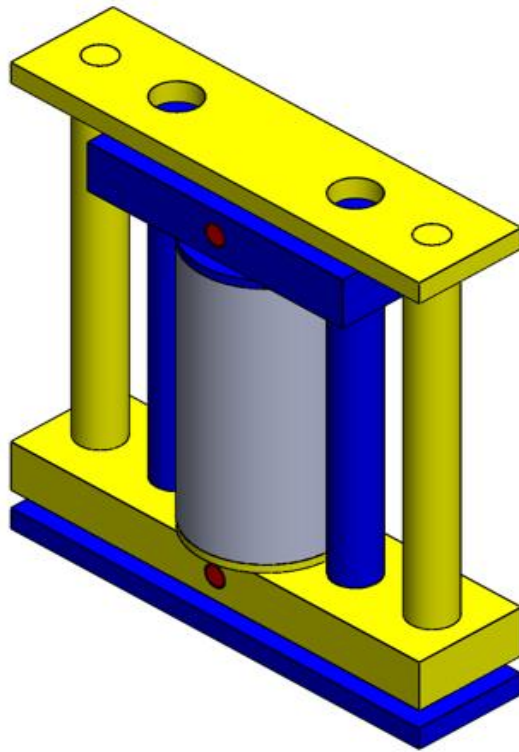
DESCRIPTION

EPOTEK FIX est une pâte époxydique bi-composant de type structurale, sans solvant, avec une adhésion élevée sur tous matériaux de construction.

EPOTEK FIX est un produit thixotrope à base de résine époxydique, spécialement formulé pour être utilisé en horizontal et en vertical.

EPOTEK FIX se présente en kit de 2 composants :

  - Composant **A : résine**.
  - Composant **B : durcisseur**.

DOMAINES D'APPLICATION

EPOTEK FIX est utilisé comme adhésif structural, en génie civil pour :

  - Les ancrages horizontaux et verticaux.

  - Le collage de structures en béton préfabriqué, même porteuses, pour consolider son unicité.

  - L'ancrage de machineries, boulons, plaques, monte- charges, etc.

  - La réparation et le renforcement structurel entre matériaux de différents types (acier et béton), « renforcement par collage de plaque ou fibre d'acier ».

  - Nivelage et surfaçage.

  - Réparation des lèvres de joints de dilatation.

PROPRIETES ET EFFETS

  - Pouvoir d'adhésion élevé sur tous types de support.

  - Possibilité d'obtenir des liens structurels entre béton et béton, béton et acier, béton et bois.

  - Résistances mécaniques élevées.

  - Sans retrait.

  - Très bonne résistance à l'eau, aux huiles minérales, à l'essence, aux solutions agressives acides et alcalines et aux solutions salines.

CARACTERISTIQUES

Couleur :..Grise
Densité :...1,6 Kg/L
Extrait sec :..100 %
Temps d'ouvrabilité :............................30 min à 20 °C
Durcissement total (à 20 °C) :................7 jours
Temps. Minimum d'application :...................10 °C
Résistance à la compression (UNI 4279) :......> 60 Mpa
Résistance à la flexion (UNI 7219) :............> 20 Mpa
Allongement à la rupture :............................2 %
Adhérence sur béton :..............................> 3 Mpa

MODE D'EMPLOI

Préparation du support :

Le support doit être parfaitement propre, dépoussiéré, et exempt de toutes graisses ou parties non adhérentes.

Préparation du produit :

  - Procéder au mélange, en versant le **composant B** dans le **composant A** en respectant le rapport du mélange.

  - Le mélange doit être fait avec spatule ou avec un agitateur électrique à bas rpm durant 4 à 5 minutes jusqu'à obtention d'une parfaite homogénéité des composants (jusqu'à obtenir une couleur homogène).

  - En pratique, nous conseillons l'utilisation de toute la quantité des **composants A et B**, vu que les poids sont pré-dosés pour éviter d'éventuelles erreurs de pesées fractionnées.

  - En cas d'utilisation fractionnée veiller à conserver la juste proportion en poids des 2 composants.

APPLICATION

  - L'**EPOTEK FIX** s'applique à la spatule ou tout autre matériel adéquat.

  - **EPOTEK FIX** doit être appliqué sur les 2 surfaces concernées et exercer une pression à l'aide de pinces.

CONSOMMATION

Environ 1,6 Kg/m²/mm d'épaisseur.

CONDITIONNEMENT ET STOCKAGE

Kits de (composant A + composant B) :

  - Kit de 02 Kilogrammes................................(1 Kg + 1 Kg)
  - Kit de 10 Kilogrammes................................(5 Kg + 5 Kg)
  - Kit de 20 Kilogrammes...........................(10 Kg + 10 Kg)
  - Kit de 40 Kilogrammes...........................(20 Kg + 20 Kg)

Dans son emballage d'origine fermé et stocké à des températures entre 10 et 35 °C, le produit se conserve une année.

REMARQUE

Si le produit est conservé à des températures inférieures à 10 °C, sa densité peut être modifiée. Dans ce cas, mettre les deux boîtes de l'**EPOTEK FIX** dans un bain marie afin de leur rendre leurs propriétés initiales.

PRECAUTIONS D'EMPLOI

Utiliser des gants, se protéger les yeux et la peau.

Se référer à la fiche de données de sécurité.

DOCUMENT DE REFERENCES

PV d'essais établi par le CNERIB.